Microbial and Biochemical Mechanisms Underlying Greenhouse Gas Mitigation in Agriculture

by

Seongmin Yang

B.S., Jeonbuk National University, 2017
M.S., Korea Advanced Institute of Science and Technology (KAIST), 2019

AN ABSTRACT OF A DISSERTATION

submitted in partial fulfillment of the requirements for the degree

DOCTOR OF PHILOSOPHY

Department of Civil Engineering
Carl R. Ice College of Engineering

KANSAS STATE UNIVERSITY
Manhattan, Kansas

2026

Abstract

Greenhouse gases (GHGs) such as carbon dioxide (CO_2), nitrous oxide (N_2O), and methane (CH_4) play a crucial role in regulating Earth's climate by trapping heat in the atmosphere. While carbon dioxide is the most abundant anthropogenic GHG, N_2O and CH_4 contribute disproportionately to global warming due to their much higher global warming potential, approximately 298 and 25 times greater than CO_2, respectively. N_2O and CH_4 are particularly concerned due to their persistence in the atmosphere. Natural processes and human activities both contribute to the production of N_2O and CH_4. Agricultural activities are the predominant source, responsible for over two-thirds of global anthropogenic N_2O emissions and one-third of total CH_4 emissions. In these agricultural systems, microbial processes are fundamental to the production and mitigation of both N_2O and CH_4. To elucidate microbial mechanisms regulating GHG fluxes in agricultural systems, this dissertation presents two complementary studies: one focusing on mitigating N_2O emissions during forage conservation, and the other examining the role of biological nitrification inhibition (BNI) in controlling CH_4 oxidation. Building on the recognition that anaerobic forage conservation may serve as an unrecognized source of N_2O, I conducted an extensive investigation using three major silage crops in the U.S.—maize, alfalfa, and sorghum. The total N_2O emission from these silage processes was quantified and emission potential was calculated with USDA National Agriculture Statistics Services annual silage production report, revealing that silage ranks as the third largest source of anthropogenic N_2O emissions in the U.S. Through chemical and molecular analyses, denitrifying bacteria were identified as the primary contributors to these emissions. Subsequently, a chemical combination was developed using chlorate—a specific inhibitor of nitrate reductase— mitigating N_2O emissions from silage up to 99%, offering a practical solution to significantly reduce GHG emissions in agriculture.

The second part of this dissertation examines a novel phenomenon with significant environmental implications. Plant–microbe interactions in the rhizosphere strongly influence nitrogen cycling and GHG emissions. BNI through which plants release natural compounds that suppress nitrification, offers a sustainable alternative to synthetic inhibitors. However, the broader impacts of BNI on other microbial processes remain unclear. In particular, CH_4 oxidation by methanotrophs—the only biological sink for atmospheric CH_4—may be affected because the

key enzymes involved in nitrification and methanotrophy share similar catalytic mechanisms. This effect could be significant in paddy environments like wetlands and rice fields, which are major contributors to global GHG emissions. To investigate this interaction, a multi-scale experimental approach was undertaken. Soil column experiments with BNI-producing plants demonstrated that BNI compounds reduced CH_4 oxidation activity and altered methanotrophic community structures. Pure culture experiments confirmed the direct inhibitory effects of specific BNI compounds on methanotrophs. These findings provide the first multi-lines of evidence that BNI can adversely affect methanotrophy, suggesting that while BNI reduces nitrification and associated N_2O emissions, it may unintentionally suppress CH_4 oxidation, potentially increasing CH_4 emissions. This novel discovery underscores the need for a balanced assessment of BNI's environmental impacts. Understanding BNI's dual effects is essential for developing sustainable agricultural practices that mitigate GHG emissions without unintended consequences. Collectively, these two studies advance our understanding of how nitrogen and carbon management practices influence GHG emissions in agricultural systems, providing valuable insights for developing more sustainable and climate-resilient agricultural strategies.

Microbial and Biochemical Mechanisms Underlying Greenhouse Gas Mitigation in Agriculture

by

Seongmin Yang

B.S., Jeonbuk National University, 2017
M.S., Korea Advanced Institute of Science and Technology (KAIST), 2019

A DISSERTATION

submitted in partial fulfillment of the requirements for the degree

DOCTOR OF PHILOSOPHY

Department of Civil Engineering
Carl R. Ice College of Engineering

KANSAS STATE UNIVERSITY
Manhattan, Kansas

2026

Approved by:

Major professor
Dr.Jeongdae Im

Copyright

Abstract

Greenhouse gases (GHGs) such as carbon dioxide (CO_2), nitrous oxide (N_2O), and methane (CH_4) play a crucial role in regulating Earth's climate by trapping heat in the atmosphere. While carbon dioxide is the most abundant anthropogenic GHG, N_2O and CH_4 contribute disproportionately to global warming due to their much higher global warming potential, approximately 298 and 25 times greater than CO_2, respectively. N_2O and CH_4 are particularly concerned due to their persistence in the atmosphere. Natural processes and human activities both contribute to the production of N_2O and CH_4. Agricultural activities are the predominant source, responsible for over two-thirds of global anthropogenic N_2O emissions and one-third of total CH_4 emissions. In these agricultural systems, microbial processes are fundamental to the production and mitigation of both N_2O and CH_4. To elucidate microbial mechanisms regulating GHG fluxes in agricultural systems, this dissertation presents two complementary studies: one focusing on mitigating N_2O emissions during forage conservation, and the other examining the role of biological nitrification inhibition (BNI) in controlling CH_4 oxidation. Building on the recognition that anaerobic forage conservation may serve as an unrecognized source of N_2O, I conducted an extensive investigation using three major silage crops in the U.S.—maize, alfalfa, and sorghum. The total N_2O emission from these silage processes was quantified and emission potential was calculated with USDA National Agriculture Statistics Services annual silage production report, revealing that silage ranks as the third largest source of anthropogenic N_2O emissions in the U.S. Through chemical and molecular analyses, denitrifying bacteria were identified as the primary contributors to these emissions. Subsequently, a chemical combination was developed using chlorate—a specific inhibitor of nitrate reductase— mitigating N_2O emissions from silage up to 99%, offering a practical solution to significantly reduce GHG emissions in agriculture.

The second part of this dissertation examines a novel phenomenon with significant environmental implications. Plant–microbe interactions in the rhizosphere strongly influence nitrogen cycling and GHG emissions. BNI through which plants release natural compounds that suppress nitrification, offers a sustainable alternative to synthetic inhibitors. However, the broader impacts of BNI on other microbial processes remain unclear. In particular, CH_4 oxidation by methanotrophs—the only biological sink for atmospheric CH_4—may be affected because the

key enzymes involved in nitrification and methanotrophy share similar catalytic mechanisms. This effect could be significant in paddy environments like wetlands and rice fields, which are major contributors to global GHG emissions. To investigate this interaction, a multi-scale experimental approach was undertaken. Soil column experiments with BNI-producing plants demonstrated that BNI compounds reduced CH_4 oxidation activity and altered methanotrophic community structures. Pure culture experiments confirmed the direct inhibitory effects of specific BNI compounds on methanotrophs. These findings provide the first multi-lines of evidence that BNI can adversely affect methanotrophy, suggesting that while BNI reduces nitrification and associated N_2O emissions, it may unintentionally suppress CH_4 oxidation, potentially increasing CH_4 emissions. This novel discovery underscores the need for a balanced assessment of BNI's environmental impacts. Understanding BNI's dual effects is essential for developing sustainable agricultural practices that mitigate GHG emissions without unintended consequences. Collectively, these two studies advance our understanding of how nitrogen and carbon management practices influence GHG emissions in agricultural systems, providing valuable insights for developing more sustainable and climate-resilient agricultural strategies.

Table of Contents

List of Figures

List of Tables

Chapter 1 - Background and literature review

1.1. Introduction

Although global climate change is widely recognized as a long-term threat to humanity and the environment, atmospheric concentrations of GHGs continue to rise, primarily due to ongoing human activities (IPCC Core Writing Team, 2014; Montzka et al., 2011; D. Reay et al., 2007). GHGs regulate the Earth's energy balance by absorbing and re-emitting heat from the surface, effectively forming an insulating layer that elevates surface temperatures GHGs regulate the Earth's energy balance by absorbing and re-emitting heat from the surface, effectively forming an insulating layer that elevates surface temperatures (IPCC Core Writing Team, 2014; D. Reay et al., 2007; U.S. EPA, 2018). While CO_2 is the dominant driver of anthropogenic warming, other gases—particularly N_2O and CH_4—also contribute substantially due to their respective warming potentials, 298 and 25 times that of CO_2, respectively. Among various sectors, agriculture is a major source of these gases, accounting for over two-thirds of global N_2O and about 40% of CH_4 emissions (Davidson & Kanter, 2014a; D. S. Reay et al., 2012a; USEPA, 2019). Most agricultural N_2O emissions originate from nitrogen fertilizer use, which stimulates microbial processes such as nitrification and denitrification—key components of the respective cycle that convert ammonia to nitrate and nitrate to nitrogen gas, respectively, with N_2O produced as an intermediate (Hu et al., 2015a; Klimasmith & Kent, 2022a).

In addition to soil-based emissions, recent studies have identified forage conservation—particularly ensiling and storage—as an emerging but overlooked source of N_2O. These emissions result from microbial transformations of nitrogen compounds under anaerobic and partially aerobic conditions typical of silage fermentation. However, N_2O released during forage conservation is not currently included in the U.S. Environmental Protection Agency's GHG

inventory, suggesting a potential underestimation of agricultural emissions. Quantifying these emissions and elucidating their microbial drivers are critical steps toward developing mitigation strategies and improving national GHG inventories. Beyond mitigation during storage, reducing N_2O production at its microbial source—through strategies such as biological nitrification inhibition (BNI) – offers a complementary approach to minimizing nitrogen losses and enhancing agricultural sustainability.

Similarly, CH_4 emissions in agriculture are primarily due to enteric fermentation in ruminant livestock and the anaerobic decomposition of organic matter in rice paddies, wetland and manure storage facilities. In these oxygen-poor environments, methanogenic archaea produce CH_4 as a metabolic product. Conversely, CH_4 oxidation by methanotrophs—bacteria that consume CH_4 in aerobic conditions—can mitigate CH_4 emissions by converting it to CO_2, thereby playing a vital role in the carbon cycle (Colin Murrell & Jetten, 2009; Conrad et al., n.d.; Wahlen M, 1993). Additionally, the implementation of BNIs presents a promising strategy for mitigating N_2O emissions by suppressing the activity of nitrifying microbes in the soil(O'Sullivan et al., 2016b; Subbarao et al., 2007a, 2009a). However, there is emerging evidence that BNIs may also affect methanotrophic communities (Holmes et al., 2006; Lieberman & Rosenzweig, 2004; Sayavedra-Soto et al., 2011). Since methanotrophs are essential for oxidizing CH_4 and reducing its emission into the atmosphere, understanding the potential impacts of BNIs on these organisms is crucial. A comprehensive understanding of the microbial processes driving N_2O and CH_4 emissions in agricultural systems is essential for developing effective mitigation strategies. By exploring how forage conservation affects N_2O emissions and investigating the potential influence of BNIs on methanotrophs, we can identify agricultural

practices that reduce GHG emissions while maintaining or enhancing productivity. Such insights are vital for achieving global climate objectives and promoting sustainable agriculture.

1.2. Forage conservation

Forages, which are plants or parts of plants consumed by herbivorous animals, are essential for livestock nutrition and farming efficiency. Forage conservation is critical for feeding livestock during periods of limited pasture growth or inadequate pasture conditions, ensuring a consistent food supply throughout the year (Finch et al., 2014a; Owens, 2003a). Historically, throughout the world, forage conservation is a crucial element for productive and efficient livestock farming. Forages consist of highly digestible cell content—proteins, fats, and soluble carbohydrates—and less digestible cell walls composed of cellulose, hemicellulose, and lignin (Barnes et al., 2003). The primary methods of forage conservation are haymaking and silage production. Hay is produced by drying forage to a moisture content below 20% (typically 12–20% w/w) to inhibit microbial growth, and it is stored under aerobic conditions (Barnes et al., 2003). Silage, on the other hand, is prepared with higher moisture content (50~70%, w/w) and stored under strict anaerobic conditions to promote fermentation. In silage, indigenous or exogenous lactic acid bacteria (LAB) convert soluble carbohydrates to organic acids, mainly lactic acid, which act as a natural preservative to inhibit undesirable microorganisms (Müller et al., 2008a; Soundharrajan et al., 2017a). Therefore, commercial inoculants containing LAB and other anaerobic bacteria (such as *Lactobacillus buchneri*) are added in practice (Muck et al., 2018a). Silage production is a significant segment of the global livestock industry. In 2022, the United States alone harvested approximately 162.3 million metric tons of crops for silage (USDA, 2023). The global market for silage inoculants was valued at $503 million in 2021 and is projected to grow to $630 million by 2028, reflecting an annual growth rate of 3.8%. Despite its high production volume and

widespread use, the forage conservation process has been relatively understudied as a potential source of GHGs (Grossi et al., 2019). However, several researchers have reported the detection of N_2O emissions from silages. For instance, N_2O production was observed from corn silages stored in open bunker silos, where ambient N_2O concentrations were orders of magnitude higher than rural background levels (Maw et al., 2002). A few other studies reported N_2O production from silage (Bueno et al., 2020a; Krommweh et al., 2020a), but a comprehensive quantitative assessment has not been performed.

1.3. Nitrogen cycle and N_2O emissions

N_2O is the third-largest contributor of GHG emissions to the atmosphere after CO_2 and CH_4 (USEPA, 2023). N_2O is also the dominant ozone-depleting substance in the stratosphere (Ravishankara et al., 2009a). N_2O is produced by both natural and anthropogenic sources, but the emissions from human activities have increased 20% since the pre-industrial era, and its concentration has increased 15% since 1750 (USEPA, 2023). Approximately 40% of N_2O emissions come from human activities, and of those, the majority are from agricultural practices. In the US, about 75% of all anthropogenic N_2O emissions are attributed to agriculture (USEPA, 2023). The mechanism of N_2O production is not completely understood, but microbial production of N_2O is generally considered to be the main driver of N_2O emissions (Hu et al., 2015; Klimasmith & Kent, 2022b; Kuypers et al., 2018a; a. J. Thomson et al., 2012; Tian, Xu, Canadell, Thompson, Yao, et al., 2020b). Although nearly all microorganisms involved in biogeochemical nitrogen cycling can potentially produce N_2O, there are several key microbial pathways contributing the most to N_2O production including heterotrophic denitrification, ammonia oxidation, and nitrifier denitrification (Butterbach-Bahl et al., 2013; Kuypers et al., 2018a). Heterotrophic denitrification is a multistep respiratory process that reduces oxidized

mineral forms of nitrogen, i.e., NO_3^- and nitrite (NO_2^-) to the gaseous nitric oxide (NO), N_2O, and dinitrogen (N_2). The reaction typically occurs under anaerobic conditions, although a novel group of aerobic denitrifying bacteria has recently been discovered (J. Yang et al., 2020a). On the other hand, ammonia oxidation and nitrifier denitrification occur under aerobic conditions. Nitrification is a two-step process where ammonia (NH_3) is oxidized to NO_2^- by ammonia oxidizing bacteria (AOB) and archaea (AOA), and subsequently to NO_3^- by NO_2^- oxidizing bacteria. N_2O is known to be produced indirectly via chemical decomposition of ammonia oxidation intermediates or end-product (hydroxylamine, nitroxyl hydride, or NO_2^-) (S. Liu et al., 2017a). In addition, some AOB can directly produce N_2O via nitrifier denitrification where NH_3 is oxidized to NO_2^- followed by the reduction of NO_2^- to NO and N_2O (Kozlowski et al., 2016a; Wrage, Velthof, van Beusichem, et al., 2001; Wrage-Mönnig et al., 2018a).

1.4. BNI and its inhibition mechanisms

Globally, about 50-70% of the nitrogen fertilizer applied to cropping systems is lost to the environment mainly due to microbial nitrification (Cassman et al., 2002; Ladha et al., 2005). Nitrification, a key microbial process in the global nitrogen-cycle, transforming immobile ammonium (NH_4^+) to highly mobile NO_3^-, is known to enhance losses of fertilizer nitrogen by leaching and denitrification (Coskun et al., 2017). Nitrification has been known to be a two-step process where NH_4^+ is first oxidized to NO_2^- by AOB and/or AOA, and subsequently to NO_3^- by NO_2^--oxidizing bacteria, although recent studies demonstrated that *Nitrospira* spp. can carry out both reactions (Daims et al., 2015; van Kessel et al., 2015). Further, nitrification is the primary process of N_2O emissions in soils (R. Liu et al., 2016), which is the third most important GHG next to CO_2 and CH_4.

For these reasons, there have been attempts to mitigate nitrification in agriculture. Since the mid-1950s, studies on nitrification inhibitors have been conducted, and hundreds of synthetic nitrification inhibitors (SNIs) have been identified. However, these artificially synthesized nitrification inhibitors are not widely applied in practice, because (1) their biological stability is limited leading to shorter effective time of nitrification inhibition, (2) some of these artificially synthesized nitrification inhibitors have toxicity and adversely affect beneficial soil microorganisms, resulting in their limited usability, and (3) artificially synthesized nitrification inhibitors are in general expensive (Coskun et al., 2017; Subbarao, Ito, et al., 2006). On the other hand, despite many early studies, it has recently become apparent that certain plant species are capable of suppressing microbial nitrification by releasing inhibitory phytochemicals from roots, which is termed BNI (Subbarao et al., 2009a; Sun et al., 2016; Tesfamariam et al., 2014). This phenomenon has emerged as a promising new area of research not only because of its potential to improve NUE in cropping systems (Coskun et al., 2017; Subbarao et al., 2013), but also its implications for agricultural soil management, i.e., reduced N_2O emissions (Byrnes et al., 2017; Peters et al., 2013; Subbarao et al., 2017). For example, N_2O emission was also suppressed by 90% in the field of high-BNI *Brachiaria* pasture compared with soybean (*Glycine max*), which lacks BNI capacity (Subbarao et al., 2009a). Since the first report of BNI in *Brachiaria humidicola (B.humidicola)*, BNIs have been discovered in several crops, including sorghum *(Sorghum biocolor L.)* and wheat *(Triticum aestivum L.)* (O'Sullivan et al., 2016a; Zakir et al., 2008a). More recently, one of the major cereal crop rices *(Oryza sativa L.)* exudate was reported as crops which can produce detectable BNI activity (Pariasca Tanaka et al., 2010).

The first step of nitrification, the oxidation NH_3 to NO_2^- via hydroxylamine (NH_2OH), is catalyzed by two enzymes: ammonia monooxygenase (AMO) and hydroxylamine

oxidoreductase (HAO). Many studies measure BNI activity using nitrification inhibition assay (Subbarao, Ishikawa, et al., 2006) which measures NO_2^- concentration to identify the activity of several BNI exuded from roots with Nitrosomonas spp. in pure culture. The mode of inhibitory action of the BNIs varies for each species. For example, recent research has demonstrated that methyl 3-(4-hydroxyphenyl) propionate (MHPP) in sorghum and 1,9 decanediol (1,9-D) in rice specifically block the AMO step in bacterial ammonia oxidation (Coskun et al., 2017; Pariasca Tanaka et al., 2010; Zakir et al., 2008a). Also, Brachialactone, which is the exudate of *B. humidicola*, inhibited both AMO and HAO but had a greater inhibitory effect on AMO than the HAO (Subbarao et al., 2007b).

1.4. Methanotrophs and possibility of potential inhibition from BNI

Methanotrophs are specialized microbes capable of deriving all their carbon and energy from CH_4, the second most abundant GHG after CO_2 (Core Writing Team, 2014; Denman et al.,). The most widely studied methanotrophs belong to the classes Gammaproteobacteria and Alphaproteobacteria, and they have historically been divided into type I and type II methanotrophs based on physiological characteristics (Dedysh & Dunfield, 2011; Knief, 2015a). All aerobic methanotrophs initiate CH_4 oxidation using methane monooxygenase (MMO), which converts CH_4 to methanol. This reaction is followed by further oxidation of methanol to formaldehyde by methanol dehydrogenases (Keltjens et al., 2014). The MMO is catalyzed by two forms, cytoplasmic or soluble form of methane monooxygenase (sMMO) and membrane-bound or particulate methane monooxygenase (pMMO; Semrau et al., 2013, 2020). All pMMO-containing methanotrophs use copper as the catalytic metal in the first step of CH_4 oxidation to methanol, and? copper suppresses the expression of the sMMO (Knapp et al., 2007; Trotsenko & Murrell, 2008) which require iron as they belong to a diverse enzymatic family of di-iron

carboxylate enzymes (Crombie & Murrell, 2014; Nichol et al., 2019). Most extant methanotrophs, including those that have the ability to synthesize sMMO, also express pMMO and such expression and activity increases with increasing copper availability (Choi et al., 2003; Lontoh & Semrau, 1998). These two distinct MMOs have different kinetics for CH_4 oxidation, with sMMO having a much higher turnover, but lower affinity for CH_4 than pMMO (Lee et al., 2006). As a result, the type of MMO expressed can have a significant impact on the overall CH_4 consumption rate (Semrau et al., 2013). Interestingly, pMMO, which catalyzes the initial oxidation of CH_4 to methanol, is evolutionarily related to AMO found in AOB. Both pMMO and AMO are membrane-associated enzymes and share striking similarities in their genetic encoding (*pmoCAB* and *amoCAB*, respectively), structural configuration ($\alpha_3\beta_3\gamma_3$), metal requirements (copper in pMMO and possibly iron in AMO), substrate ranges, and inhibition patterns (Arp et al., 2007; Hakemian & Rosenzweig, 2007). These similarities suggest that certain BNIs, known to inhibit AMO, may also inhibit MMO, particularly pMMO (Holmes et al., 1995). Such inhibition could reduce the efficiency of CH_4 oxidation in methanotrophs, potentially increasing CH_4 release into the atmosphere. The evolutionary relationship between AMO and pMMO underscores the complex interactions between CH_4 and N_2 cycling and highlights the potential impacts of BNI compounds on atmospheric CH_4 dynamics.

Chapter 2 - Hypotheses and research objectives

The goal of the proposed research is to provide a comprehensive understanding of the impact of nitrogen and carbon management practices on GHG emissions in agricultural systems, thereby offering valuable insights for developing strategies that promote more sustainable and climate-resilient agriculture.

2.1. The role of microbial diversity in controlling greenhouse gas emissions from conserved forages

2.1.1 Hypotheses

2.1.1.1 Evaluation and optimization of lysis methods for microbial DNA extraction from epiphytic phyllosphere samples

This study hypothesizes that DNA extraction methods employing enzymatic lysis will yield higher total DNA concentrations in silage-derived phyllosphere samples compared to methods based primarily on mechanical disruption, due to more extensive lysis of both microbial and plant-derived cells. However, mechanical lysis approaches, such as bead-beating, are expected to provide greater specificity toward microbial cells, resulting in higher bacterial 16S rRNA gene copy numbers and reduced co-extraction of plant DNA and inhibitory compounds.

It is further hypothesized that optimizing the balance between enzymatic and mechanical disruption will improve DNA quality, as reflected by DNA integrity and downstream sequencing performance. Additionally, differences in extraction methodology are expected to influence the observed microbial community composition and diversity, with mechanically biased methods yielding more reproducible and biologically representative profiles of epiphytic microbial communities in silage samples.

2.1.1.2 Evaluation of N_2O emissions from conserved forages and validation of the role of denitrification in N_2O production

This study hypothesized that conserved forages, including maize, alfalfa, and sorghum, will exhibit distinct N_2O emission patterns driven by differences in their carbon-to-nitrogen ratios and associated microbial communities. Denitrification and nitrification are expected to serve as the dominant pathway for N_2O production during forage conservation, as evidenced by the upregulation of denitrification-associated genes such as *narG, nirK/nirS*, and *nosZ*, along with measurable increases in N_2O accumulation during the ensiling process. Additionally, N_2O production is hypothesized to correlate positively with nitrate availability and negatively with carbon availability and pH, linking emission magnitude to the nutritional and physicochemical parameters of conserved forages.

2.1.1.3 Optimization of N_2O emission mitigation methods for conserved forages

This study hypothesized that the controlled supplementation of chlorate will selectively inhibit nitrate reductase activity, thereby reducing N_2O accumulation without negatively impacting silage fermentation quality. The co-application of readily available carbon sources, such as acetate or glucose, is anticipated to stimulate complete denitrification to N_2, enhancing the inhibitory efficiency of chlorate and resulting in a synergistic mitigation of N_2O emissions. Consequently, an optimized combination of chlorate concentration and carbon amendment is expected to achieve a sustained reduction in N_2O flux while preserving the nutritional quality of the silage, presenting a practical and cost-effective GHG mitigation strategy.

2.1.2 Objectives

2.1.2.1 Evaluation and optimization of lysis methods for microbial DNA extraction from epiphytic phyllosphere samples

1. Compare the efficiency of two commercially available DNA extraction kits that employ different lysis methodologies.
2. Assess the impact of various cell lysis techniques under different extraction conditions on DNA yield, purity, DIN, and the bacterial 16S rRNA gene copy number per ng of template genomic DNA (gDNA).
3. Investigate the effects of distinct DNA extraction methods on microbial community composition, diversity, and reproducibility, utilizing 16S rRNA gene amplicon sequencing.
4. Optimize the DNA extraction procedure for conserved forage based on the obtained results.

2.1.2.2 Evaluation of N_2O emissions from conserved forages and validation of the role of denitrification in N_2O production

1. Monitor simulated silages from three major crops in the United States (maize, alfalfa, and sorghum) over a 4-week period.
2. Assess the influence of various treatments on N_2O production in conserved forages, including dynamics of gene and transcript abundance.
3. Evaluate N_2O production and its correlation with physicochemical parameters.
4. Examine the environmental implications of N_2O emissions originating from conserved forages

2.1.2.3 Optimization of N_2O emission mitigation methods for conserved forages

1. Optimize chlorate concentrations to minimize N_2O emissions from forage conservation while inhibiting the denitrification process.

2. Investigate the addition of supplemental carbon sources to enhance the denitrification process in conserved forages, thereby mitigating N_2O emissions.

2.2 Impact of BNI on methanotrophs

2.2.1 Hypothesis

2.2.1.1 Examination of the influence of BNI compounds on pMMO-expressing *Methylosinus trichosporium* OB3b

This study posits that BNI compounds—namely MHPP, 1,9-D, and linoleic acid (LA)—will significantly inhibit the activity of pMMO in *M. trichosporium* OB3b. The inhibitory effects are expected to manifest as measurable alterations in kinetic parameters, including maximum methane oxidation rate (V_{max}) and apparent substrate affinity (K_m).

2.2.1.2 Impact of BNI compounds on different conditions of *M. trichosporium* OB3b and various types of methanotrophs

It is anticipated that the inhibition patterns induced by BNI compounds will differ between the soluble methane monooxygenase (sMMO)-expressing and pMMO-expressing forms of *M. trichosporium* OB3b, given the structural and cofactor variations between these enzyme systems. Additionally, the inhibitory responses are hypothesized to vary among methanotroph types, with Type I methanotrophs (e.g., *Methylomicrobium album* BG8) showing different susceptibility patterns than Type II (*M. trichosporium* OB3b).

2.2.1.3 Molecular gene abundance and RNA sequencing analysis

I hypothesized that BNI compounds will trigger distinct transcriptomic responses in methanotrophic cultures, reflecting both enzyme-specific inhibition and broader stress responses. Also, RNA-seq analysis will reveal compound-specific transcriptional signatures, providing mechanistic insights into how BNIs modulate methanotroph metabolism at the molecular level.

2.2.2 Objective

2.2.2.1 Examination of the influence of BNI compounds on *M.trichosporium* OB3b

1. Evaluate the inhibitory effects of BNI compounds MHPP, 1,9-D, and LA on the kinetic parameters of *M. trichosporium* OB3b.

2.2.2.2 Impact of BNI compounds on different conditions of *M. trichosporium* OB3b and various types of methanotrophs

1. Assess the inhibition rates of BNI compounds on the kinetic values for sMMO-expressing *M. trichosporium* OB3b.
2. Evaluate the inhibition rates of BNI compounds on the kinetic values for Type I methanotrophs (*M. album* BG8)

2.2.2.3 Plants exudates affect the methanotrophs-enriched soil

1. Assess the inhibition of CH_4 oxidation in the presence of growing plants which exudate BNI compounds.

2.2.2.4 Molecular gene abundance and RNA sequencing

1. Elucidate the transcriptomic responses of pure cultures of methanotrophs upon exposure to BNI compounds.

Chapter 3 - The role of microbial diversity in controlling GHGs emissions from conserved forages

N_2O is the third most important GHG, following CO_2 and CH_4. Per mole, N_2O has a warming potential 298 times greater than CO_2 and remains in the atmosphere for an extended period, estimated at 100–150 years (USEPA, 2023). Recent studies have also emphasized N_2O as the primary ozone-depleting substance in the stratosphere (Fang et al., 2019a; Ravishankara et al., 2009a). While natural processes and human activities contribute to N_2O production, agricultural activities are the predominant source, responsible for over two-thirds of global anthropogenic N_2O emissions (Davidson & Kanter, 2014b; D. S. Reay et al., 2012b). Despite extensive research on agricultural N_2O sources such as soils and manure management, forage conservation remains a relatively overlooked contributor. Forage conservation plays a vital role in livestock farming, ensuring a reliable feed source during times when fresh pasture is limited due to seasonal changes or inadequate growing conditions (Finch et al., 2014; Owens, 2003). Silage, a common forage conservation method, involves the anaerobic fermentation of plant material, which preserves nutrients through the activity of lactic acid bacteria (LAB) that convert soluble carbohydrates to lactic acid. This process creates an acidic environment that inhibits spoilage organisms and enhances forage stability (Müller et al., 2008a; Soundharrajan et al., 2017a). However, the same anaerobic and microbially active conditions that stabilize silage can also facilitate nitrogen-transforming processes that generate N_2O. In particular, microbial denitrification is considered a primary pathway contributing to N_2O emissions under these conditions, as part of the broader biogeochemical nitrogen cycle (Butterbach-Bahl et al., 2013a; Kuypers et al., 2018a). These processes suggest that conserved forages may represent a

previously underappreciated source of N_2O emissions within agricultural systems. To elucidate the mechanisms driving N_2O production in these systems, it is essential to characterize the structure and function of the associated microbial communities. Within conserved forages, particularly in the phyllosphere—the aerial region of plants—microbial communities are highly diverse and metabolically dynamic. This environment hosts both epiphytic (surface-associated) and endophytic (internal) microorganisms that actively participate in nitrogen cycling and influence plant–microbe interactions (Vorholt et al., 2012). However, accurate characterization of these microbial communities remains a critical challenge. DNA extraction from plant-associated samples is often hindered by co-extraction of host plant DNA, low microbial biomass, and the presence of inhibitory compounds such as polyphenols and polysaccharides. These constraints can introduce substantial bias in downstream molecular analyses, leading to misrepresentation of microbial community composition and function. As a result, methodological limitations in DNA extraction represent a key bottleneck in linking microbial ecology to observed N_2O emissions.

Addressing this limitation requires systematic evaluation and optimization of DNA extraction strategies tailored to phyllosphere samples. Therefore, this chapter first examines the environmental significance of N_2O emissions from forage conservation systems and the microbial processes underlying their production. It then focuses on the methodological challenges associated with DNA extraction from plant-associated matrices, including a comparative evaluation of lysis techniques and their impact on microbial community profiling. In addition, this study investigates mitigation strategies aimed at reducing N_2O emissions during forage fermentation, including the application of chlorate to inhibit denitrification pathways and the supplementation of external carbon sources to manipulate microbial activity. Together, these

approaches aim to both improve mechanistic understanding and identify practical solutions for reducing greenhouse gas emissions from forage-based agricultural systems.

Understanding these microbial communities, especially their role in N_2O emissions, requires high-quality DNA extraction for accurate molecular analyses. This chapter will provide a comprehensive background on the environmental impact of forage conservation, with a focus on microbial processes contributing to N_2O emissions. Additionally, it will explore the challenges of DNA extraction from plant-associated samples, reviewing various lysis techniques and evaluating their effectiveness in capturing accurate microbial profiles for molecular analyses. Also, we will optimize reducing GHG emission from forage fermentation using chlorate and extra carbon sources. This understanding is crucial for advancing sustainable forage management practices and mitigating GHG emissions in agriculture.

3.1. Evaluation and optimization of lysis method for microbial DNA extraction from epiphytic phyllosphere samples

3.1.1 Introduction

The phyllosphere is the aerial region of the plant, which supports diverse groups of microorganisms that can live on the surface (epiphytic) and interior (endophytic) of plant tissues (Vorholt, 2012). The epiphytic phyllosphere is an important microbial habitat and plays a crucial role in the global carbon and nitrogen cycles (Bringel and Cou´ee, 2015; Delmotte et al., 2009) as well as in plant health and growth (Wang et al., 2015). Epiphytic microorganisms are also vital in many industrial applications, such as *Pseudozyma* in bioplastic production (Sato et al., 2017; Watanabe et al., 2014) and lactic acid bacteria in the anaerobic forage conservation process (e.g., silage) (Holzer et al., 2003). Understanding the abundance, diversity, and functions of the epiphytic microbiome often depends on culture-independent molecular techniques

(Lucaciu et al., 2019). Molecular analysis of the epiphytic microbiome necessitates applying additional pretreatment steps such as washing (Kadivar and Stapleton, 2003; Saito et al., 2007; Wang et al., 2019) and sonication (Cui et al., 2021; Yang and Crowley, 2000) to isolate and purify microbial cells. However, a cell pellet sometimes unavoidably contains residual plant debris, and DNA and PCR inhibitors released from the plant cells often interfere with downstream molecular analysis of the microbial communities (Dent et al., 2004; Ikeda et al., 2009; Saito et al., 2007). Particularly, chloroplast 16S rRNA genes may ultimately hinder the detection of the bacterial 16S rRNA gene in PCR amplification (Dent et al., 2004). It is critical to develop a simple and reproducible DNA extraction method optimized for each sample type to explore the microbial community in environmental samples using a molecular approach. Typical DNA extraction protocols from an epiphytic phyllosphere sample comprise three major steps: pretreatment, cell lysis, and subsequent DNA purification. This study focuses on the second step, cell lysis, to minimize contamination from plant-derived biomolecules. Notably, cell lysis relies on mechanical or enzymatic disruption in most commercial DNA isolation kits. Mechanical disruption is typically based on bead beating to break the cell membrane. The advantage of mechanical disruption is efficacy and concurrent sample homogenization; however, applications relying on intact chromosomes could be limited owing to DNA shearing (Bag et al., 2016; Corcoll et al., 2017; Pakpour et al., 2013; Salonen et al., 2010). Enzymatic disruption is more suitable for obtaining genomic DNA (gDNA) but may suffer from extraction bias owing to the limited spatial access to all target organisms and different sensitivity for different cell types (Robe et al., 2003; Saito et al., 2007). Using the Google Scholar database (accessed on 9/13/2022), we selected the first 100 recent articles published after 2020, searched using the keywords “phyllosphere” and “sequencing” and classified them based on the lysis method. A

total of 70 studies employed commercial kits with mechanical disruption, whereas 30 used commercial kits with enzymatic disruption (data available upon request), indicating that both methods are widely used in different research areas. However, to the best of our knowledge, there is no study examining the effect of cell lysis methods and extraction conditions on DNA quantity and quality and subsequent molecular analysis of the phyllosphere microbiome. Factors affecting DNA extraction efficiency by each lysis method include bead-beating time, speed, and temperature for mechanical disruption (Li et al., 2007) and temperature and contact time for enzymatic disruption (Qamar et al., 2017). For this study, we selected two commercially available DNA extraction kits employing different lysis methods and evaluated the effect of cell lysis methods under different extraction conditions on DNA extraction yield, purity, DNA integrity number (DIN), and bacterial 16S rRNA gene copy number per ng template gDNA as a measure of preferential lysis of bacterial cells over plant cells. Furthermore, the effect of DNA extraction methods on microbial community composition, diversity, and reproducibility was examined using 16S rRNA gene amplicon sequencing.

3.1.2 Materials and methods

3.1.2.1 Sample and pretreatment

An epiphytic phyllosphere sample was collected from a 30-day-old alfalfa silage. Silage is a form of forage conservation in an anaerobic environment (Collins et al., 2017). Silage is typically based on fermentation and, thus, is a microorganism-rich phyllosphere niche. As a conventional pretreatment method for epiphytic phyllosphere samples to isolate and purify microbial cells minimizing plant material, each sample (5 g) was suspended in 45 mL of sterile 0.85% NaCl solution for 2 h at 20 °C, filtered through two cheesecloth layers, and centrifuged at 12,000 ×g at 4 °C for 15 min (Li et al., 2020; Saito et al., 2007; Wang et al., 2019). The

supernatant was discarded, the pellet was stored at −80 °C until subsequent DNA extraction, and the solid residue was also collected and stored at −80 °C.

3.1.2.2 DNA extraction

Mechanical and enzymatic disruptions are two cell lysis methods commonly used for DNA extraction from phyllosphere samples. This study selected the DNeasy PowerSoil Pro kit and DNeasy Blood and Tissue kits from the same manufacturer (Qiagen, Hilden, Germany) to represent each lysis method. DNA extraction using the PowerSoil kit was conducted according to the manufacturer's instructions with the following modifications: (1) three different bead-beating times, i.e., 5, 10, and 15 min at (2) two temperatures, i.e., 20 °C and 30 °C. The protocol recommended by the manufacturer was bead-beating for 10 min at 20 °C. Mechanical cell disruption was performed using a Bead Mill 24 homogenizer (Fisher Scientific, Waltham, MA, USA) in a temperature-controlled room. DNA extraction using the Blood and Tissue kit was performed with the following modifications: (1) four incubation times with proteinase K (5, 10, 20, and 60 min) at (2) three temperatures (20 °C, 40 °C, and 56 °C). The manufacturer's protocol for prokaryotes was incubation for 10 min at 56 °C, and 30 min was recommended for gram-positive bacteria. A longer incubation time (60 min) was employed to evaluate the effect of lower incubation temperatures. The enzyme-sample mixture was incubated in a water bath set at different temperatures. The total DNA yield was obtained by repeated elutions until the DNA concentration was lower than 5 ng μL−1 (**Table 1**). All extractions were performed in triplicate. One gram of the solid residue on the cheesecloth was also subjected to DNA extraction using the DNeasy PowerSoil Pro kit to ensure the efficacy of the pretreatment process.

3.1.2.3 Determination of DNA yield, purity, and integrity

DNA yield and purity were determined using the Epoch 2 Microplate Spectrophotometer and TAKE3™ microvolume plate (Agilent Technologies, Santa Clara, CA, USA). An absorption ratio at 260/280 nm ($OD_{260/280}$) was used as an indicator of protein contamination, and the ratio of 260/230 nm ($OD_{260/230}$) was used for a secondary purity check. DIN was measured using the Agilent 2200 TapeStation system (Agilent Technologies, Santa Clara, CA, USA). Notably, DIN determines the level of DNA degradation by assessing the distribution of electrophoretic signals across the size range using a proprietary algorithm. The higher
the DIN value, the better the integrity of the gDNA sample.

3.1.2.4 Relative abundance of microbial DNA in the DNA extract

Quantification of PCR (qPCR) targeting bacterial 16S rRNA gene was performed using the CFX Opus 96 Real-Time PCR System (Bio-Rad, Hercules, CA, USA) in 20-µL reaction mixtures containing 10 µL of SsoAdvanced™ Universal SYBR Green Supermix (Bio-Rad, Hercules, CA, USA), 300 nM of each primer, and 2 µL of template DNA. A primer pair of 1055F and 1392R was used for amplification (Park et al., 2017). Standard curves for quantification were prepared in triplicate using double-stranded synthetic DNA fragments (gBlocks®, Integrated DNA Technologies, Coralville, IA, USA) as control templates. The primer sequences are presented in **Table 2**. The qPCR program was initiated at 95 °C for 10 min and continued at 40 cycles of 95 °C for 15 s and 59 °C for 1 min.

Table 1. DNA yield (μg) of each elution for the samples prepared by the enzymatic disruption under different conditions. The numbers in the parentheses indicate the standard errors of the estimates.

Elution	Incubation time	20°C			Avg	40°C			Avg	56°C			Avg
	min	1	2	3		1	2	3		1	2	3	
1st	5	12.5	11.7	13.7	12.6 (0.8)	7.8	6.6	7.2	7.2 (0.5)	10.9	11.0	12.0	11.3 (0.5)
	10	13.6	15.5	11.5	13.5 (1.6)	6.0	6.6	5.8	6.1 (0.3)	10.3	14.3	12.0	12.2 (1.6)
	20	14.2	6.9	7.6	9.6 (3.3)	5.0	6.3	6.1	5.8 (0.6)	12.7	16.2	12.8	13.9 (1.6)
	60	5.5	5.7	6.9	6.0 (0.6)	4.8	3.9	4.5	4.4 (0.4)	9.6	10.3	9.5	9.8 (0.3)
2nd	5	22.5	17.2	20.8	20.1 (2.2)	14.7	14.5	11.9	13.7 (1.3)	13.5	14.6	18.0	15.4 (1.9)
	10	12.1	19.9	19.9	17.3 (3.7)	13.7	14.1	8.9	12.2 (2.4)	14.4	18.5	14.3	15.7 (2.0)
	20	22.8	14.1	13.4	16.8 (4.3)	8.3	5.7	14.6	9.5 (3.8)	16.0	15.9	22.4	18.1 (3.0)
	60	14.1	12.5	13.1	13.2 (0.7)	7.9	8.9	7.7	8.2 (0.6)	16.4	18.4	17.8	17.6 (0.8)
3rd	5	13.4	21.6	16.9	17.3 (3.4)	9.6	8.9	9.5	9.4 (0.3)	12.1	12.4	10.6	11.7 (0.8)
	10	18.7	13.3	16.6	16.2 (2.2)	6.3	8.6	11.5	8.8 (2.1)	9.2	16.1	11.5	12.3 (2.9)
	20	12.1	9.9	12.3	11.4 (1.1)	14.2	12.6	11.0	12.6 (1.3)	15.4	15.3	10.5	13.7 (2.3)
	60	12.6	12.9	7.5	11.0 (2.5)	15.4	8.5	8.5	10.8 (3.3)	8.8	10.1	10.8	9.9 (0.8)
4th	5	7.9	11.7	11.1	10.2 (1.6)	11.0	9.8	10.4	10.4 (0.5)	8.4	7.9	8.0	8.1 (0.2)
	10	12.0	8.6	10.9	10.5 (1.4)	10.1	6.4	13.7	10.1 (3.0)	9.4	7.6	7.2	8.0 (1.0)
	20	9.6	6.5	8.6	8.2 (1.3)	7.1	9.7	7.4	8.1 (1.2)	5.4	6.6	6.7	6.3 (0.6)
	60	8.8	8.7	11.4	9.7 (1.3)	6.5	7.4	6.2	6.7 (0.5)	5.3	6.0	5.3	5.5 (0.3)
5th	5	6.9	8.4	7.2	7.5 (0.6)	12.7	12.8	17.8	14.4 (2.4)	5.1	5.7	5.2	5.4 (0.3)
	10	6.4	7.2	10.0	7.9 (1.5)	13.9	15.9	13.5	14.4 (1.0)	4.6	6.9	6.5	6.0 (1.0)
	20	14.3	18.7	12.4	15.1 (2.7)	16.0	18.5	14.1	16.2 (1.8)	6.7	6.3	7.2	6.7 (0.4)
	60	12.4	13.2	14.1	13.3 (0.7)	13.0	11.0	11.2	11.7 (0.9)	5.1	5.9	5.7	5.6 (0.3)
6th	5	4.1	5.6	5.9	5.2 (0.8)	2.9	3.0	3.9	3.3 (0.5)	3.5	3.4	3.8	3.6 (0.2)
	10	4.8	5.7	8.3	6.3 (1.5)	3.8	3.9	3.5	3.7 (0.2)	4.8	4.4	4.1	4.5 (0.3)
	20	2.3	3.8	1.8	2.6 (0.8)	3.2	2.8	2.9	2.9 (0.2)	3.1	3.7	4.0	3.6 (0.4)
	60	1.8	2.8	2.2	2.3 (0.4)	2.6	2.9	2.3	2.6 (0.2)	3.7	3.0	3.8	3.5 (0.4)
7th	5	4.1	5.6	5.9	5.2 (0.8)	2.9	3.0	3.9	3.3 (0.5)	3.9	5.4	4.7	4.7 (0.6)
	10	4.8	5.7	8.3	6.3 (1.5)	3.8	3.9	3.5	3.7 (0.2)	4.6	4.9	6.2	5.2 (0.7)
	20	2.3	3.8	1.8	2.6 (0.8)	3.2	2.8	2.9	2.9 (0.2)	4.5	4.7	5.0	4.7 (0.2)
	60	1.8	2.8	2.2	2.3 (0.4)	2.6	2.9	2.3	2.6 (0.2)	3.7	4.9	4.3	4.3 (0.5)
8th	5	5.7	6.2	4.8	5.5 (0.6)	3.3	3.7	4.0	3.7 (0.3)	4.0	4.6	4.5	4.4 (0.3)
	10	4.3	4.5	9.1	6.0 (2.2)	2.4	2.6	3.7	2.9 (0.6)	3.8	4.4	3.3	3.9 (0.5)

	20	3.2	3.4	2.6	3.1 (0.4)	3.4	3.6	2.9	3.3 (0.3)	3.8	4.4	4.1	4.1 (0.2)
	60	2.1	2.6	1.6	2.1 (0.4)	2.9	1.8	1.9	2.2 (0.5)	4.2	3.5	3.2	3.6 (0.4)
9th	5	2.9	2.9	3.3	3.0 (0.2)	2.9	3.4	3.2	3.2 (0.2)	2.5	2.8	2.8	2.7 (0.1)
	10	3.1	2.8	2.5	2.8 (0.2)	2.1	2.1	2.4	2.2 (0.1)	1.9	3.5	2.1	2.5 (0.7)
	20	2.2	2.1	1.9	2.1 (0.1)	1.9	2.4	2.2	2.2 (0.2)	2.2	2.5	2.5	2.4 (0.2)
	60	1.6	1.7	2.1	1.8 (0.2)	3.1	1.4	1.5	2.0 (0.8)	1.6	1.9	1.7	1.7 (0.1)
10th	5	2.6	2.3	2.2	2.4 (0.2)	2.8	2.9	2.2	2.6 (0.3)	1.7	1.7	2.2	1.9 (0.3)
	10	2.6	2.0	1.4	2.0 (0.5)	1.9	2.3	1.6	1.9 (0.3)	1.6	2.9	1.6	2.0 (0.6)
	20	1.7	2.1	1.7	1.8 (0.2)	2.2	1.4	1.4	1.7 (0.4)	1.6	1.8	2.2	1.9 (0.2)
	60	1.5	1.6	0.9	1.4 (0.3)	1.4	1.3	2.1	1.6 (0.3)	1.3	1.7	1.6	1.5 (0.2)
11th	5	2.7	2.1	2.1	2.3 (0.3)	2.0	3.0	1.6	2.2 (0.6)	1.5	1.8	1.7	1.6 (0.1)
	10	2.8	2.0	0.8	1.9 (0.9)	2.2	1.8	1.1	1.7 (0.4)	1.2	2.1	0.8	1.4 (0.6)
	20	1.7	1.8	1.5	1.6 (0.1)	1.7	1.2	1.4	1.4 (0.2)	1.3	1.6	1.7	1.5 (0.2)
	60	1.1	1.2	0.9	1.1 (0.1)	1.5	0.9	1.1	1.2 (0.2)	1.1	1.7	0.9	1.2 (0.3)
12th	5	1.5	1.6	1.6	1.6 (0.0)	2.0	2.6	1.6	2.1 (0.4)	1.2	1.3	1.4	1.3 (0.1)
	10	1.8	2.0	2.1	2.0 (0.1)	1.8	2.0	1.0	1.6 (0.4)	1.4	2.3	0.7	1.5 (0.7)
	20	1.2	1.6	2.9	1.9 (0.7)	1.2	1.2	1.4	1.3 (0.1)	1.1	1.3	1.5	1.3 (0.2)
	60	2.0	1.3	1.2	1.5 (0.4)	1.7	0.9	1.0	1.2 (0.4)	0.8	0.9	1.0	0.9 (0.1)
13th	5	1.2	1.3	1.3	1.3 (0.0)	1.0	2.4	1.4	1.6 (0.6)	1.0	1.1	1.9	1.3 (0.4)
	10	1.9	1.2	1.1	1.4 (0.4)	1.1	1.5	0.8	1.1 (0.3)	0.9	2.2	0.4	1.2 (0.7)
	20	0.8	2.9	0.8	1.5 (1.0)	1.4	1.4	0.8	1.2 (0.3)	0.9	1.1	1.2	1.1 (0.1)
	60	1.0	1.0	1.4	1.1 (0.2)	0.8	0.9	1.1	0.9 (0.1)	0.7	0.8	0.8	0.7 (0.1)
14th	5	1.1	1.2	1.3	1.2 (0.1)	0.2	1.7	1.6	1.2 (0.7)	0.9	0.9	1.1	1.0 (0.1)
	10	1.4	1.0	0.8	1.1 (0.2)	1.6	1.0	1.6	1.4 (0.3)	0.7	1.5	0.4	0.9 (0.5)
	20	1.0	2.2	0.8	1.3 (0.6)	1.2	0.7	0.9	0.9 (0.2)	0.7	0.8	0.9	0.8 (0.1)
	60	0.9	0.7	0.5	0.7 (0.1)	1.3	0.7	0.5	0.8 (0.4)	0.6	0.7	0.5	0.6 (0.1)
15th	5	0.7	0.8	1.0	0.8 (0.1)	1.0	2.0	1.5	1.5 (0.4)	0.0	0.0	0.0	0.0 (0.0)
	10	1.9	0.9	0.9	1.2 (0.5)	1.8	0.9	1.0	1.2 (0.4)	0.0	0.0	0.0	0.0 (0.0)
	20	0.5	1.0	1.8	1.1 (0.5)	0.0	0.0	0.0	0.0 (0.0)	0.0	0.0	0.0	0.0 (0.0)
	60	0.5	0.5	0.4	0.5 (0.0)	0.0	0.0	0.0	0.0 (0.0)	0.0	0.0	0.0	0.0 (0.0)
16th	5	0.9	0.7	0.9	0.8 (0.1)	1.6	1.2	1.0	1.3 (0.2)	0.0	0.0	0.0	0.0 (0.0)
	10	0.4	0.7	0.1	0.4 (0.2)	1.1	1.0	0.5	0.9 (0.3)	0.0	0.0	0.0	0.0 (0.0)
	20	0.0	0.0	0.0	0.0 (0.0)	0.0	0.0	0.0	0.0 (0.0)	0.0	0.0	0.0	0.0 (0.0)
	60	0.0	0.0	0.0	0.0 (0.0)	0.0	0.0	0.0	0.0 (0.0)	0.0	0.0	0.0	0.0 (0.0)

Table 2. Summary of primers information

Target gene	Primer	Nucleotide sequence (5'-3')	Reference
Universal 16S rRNA	1055F	ATGGCTGTCAGCT	(Ferris et al., 1996)
	1392R	ACGGGCGGTGTGTAC	
V3 and V4 region	Forward	CCTACGGRRBGCASCAGKVRVGAAT	(Teng et al., 2018)
	Reverse	GGACTACNVGGGTWTCTAATCC	
V4 and V5 region	Forward	GTGYCAGCMGCCGCGGTAA	(Teng et al., 2018)
	Reverse	CTTGTGCGGKCCCCCGYCAATTC	

where, N=G,A,T,orC;Y=C or T;M=A or C;K=G or T;S=G or C;R=G or A;B=C,T or G;W=A or T;V=A, C or G

3.1.2.5 Amplificon sequencing and bioinformatic analysis

Bacterial 16S rRNA amplicon sequencing was conducted at GENEWIZ, Inc. (South Plainfield, NJ, USA). DNA samples were quantified using a Qubit 2.0 Fluorometer (Invitrogen, Carlsbad, CA, USA), and 30–50 ng DNA was used to generate amplicons using a MetaVx™ Library Preparation kit (GENEWIZ, Inc., South Plainfield, NJ, USA). The V3/V4/V5 hypervariable regions were analyzed using two amplicons—one each for the V3/V4 and V4/V5 regions. **Table 2** presents the primer sequences targeting each region. The amplicons were sequenced on the same run using the Illumina MiSeq™ with a 2 × 250 bp paired-end configuration. The Quantitative Insights Into Microbial Ecology (QIIME) 1.1.9, an open-source bioinformatics pipeline, was used for data analysis. Quality filtering on sequence reads was performed to remove low-quality or ambiguous reads. Beta diversity was calculated using weighted and unweighted Unifrac, and principal coordinate analysis (PCoA) was performed with R v.4.1.1 software. The sequencing data have been deposited at NCBI under accession numbers SRR22404852, SRR22404853, SRR22404854, SRR22404855, and SRR22404856.

3.1.2.6 Statistical analysis

One-way ANOVA analysis was employed with the Tukey Honestly Significant Difference test to assess differences between the extraction methods for DNA yield, purity, DIN, and normalized microbial 16S rRNA gene copy number. P-values were adjusted for multiple testing using the false discovery rate method. All statistical analyses were performed using the R v.4.1.1 software.

3.1.3 Results and discussion

3.1.3.1 DNA yield, purity, and integrity

The effect of the cell lysis methods on microbial DNA extraction from the phyllosphere sample was examined using two commercially available kits with modifications. The Blood and Tissue kit was used for enzymatic disruption, and the PowerSoil kit was used for mechanical disruption. As shown in **Table 3**, enzymatic disruption exhibited one to two orders of magnitude higher DNA yields (66.5–97.1 μg) than mechanical disruption (0.54–5.24 μg) regardless of the extraction conditions. However, such a high yield by enzymatic disruption was possible only after repeated elutions up to 16 times (**Table 1**). In contrast, mechanical disruption required a single elution (data not presented). In multiple elutions, similar amounts of DNA (6–20 μg) were retrieved for the first three to four elutions, and then the DNA concentrations gradually decreased. At the first elution, the DNA yield was 10.39 ± 2.83 μg on average, only two times higher than the sample prepared via mechanical disruption at 20 °C (4.73 ± 0.41 μg). The $OD_{260/280}$ of the samples prepared by the enzymatic disruption ranged from 1.46 to 1.52 (**Table 1**), which is considered "appreciably lower" (<1.6) (Corcoll et al., 2017). Severe contamination by plant cell materials was observed with enzymatic disruption even in the mildest lysis conditions (i.e., incubation with proteinase for 5 min at 20 °C). Given that the recommended protocol by the manufacturer of the Blood and Tissue kit for the prokaryote is much more intense (i.e., incubation for 10 min at 56 °C for bacteria in general and 30 min at 56 °C for gram-positive

bacteria), extra care should be taken when enzymatic disruption is used for microbial DNA extraction from an environmental sample containing plant materials. We performed an additional DNA purification step to improve the $OD_{260/280}$ using a commercial kit, but the purity was not noticeably improved (data not shown). The $OD_{260/280}$ for mechanical disruption was higher than 1.8, not exceeding 2.0 (**Table 3**), which is generally accepted as "pure" for DNA (Carrigg et al., 2007; Jorgez et al., 2006). For enzymatic disruption, as the lysis intensity increased, i.e., the incubation temperature or incubation time increased at fixed temperatures, the DNA yield decreased, but there were no significant differences in the $OD_{260/280}$. The highest DNA yield was observed in the mildest lysis condition (incubation for 5 min at 20 °C), indicating that further optimization of this method may result in a higher yield. The temperature significantly affected the DNA yield ($P < 0.001$) for mechanical disruption. DNA yields at 20 °C (4.73 ± 0.54 μg) were 10 times higher than those at 30 °C (0.57 ± 0.03 μg) regardless of the bead-beating time. At the same temperature, variations in the bead-beating time had no impact on the DNA yield and the $OD_{260/280}$. There were no significant differences in the $OD_{260/280}$ regardless of the extraction conditions. The $OD_{260/230}$ values were low (0.7 – 0.86) irrespective of the extraction methods, typically indicating the presence of polysaccharides from plant materials (Varma et al., 2007). Higher DINs indicate larger DNA fragments, and low DINs indicate fragmented DNA. Sequencing prefers higher DINs. Unexpectedly, lower DINs (< 2), i.e., more severe DNA shearing, were observed for enzymatic disruption regardless of the extraction conditions, whereas mechanical disruption samples showed significantly higher DINs (> 5, $P < 0.001$). In general, mechanical disruption is the most popular and commercially available method with high throughput and high efficiency (Husseini et al., 2022), but it can result in extensive shearing of DNA. Enzymatic disruption is typically considered the most common alternative to mechanical

disruption to extract longer DNA fragments. However, in this study, the DINs were consistently lower in the samples prepared with enzymatic disruption than those with mechanical disruption. Further optimization with enzymatic disruption, such as shorter incubation time and lower temperature, may improve DNA integrity. For mechanical disruption, as the bead-beating time increased, DIN decreased significantly at 20 °C ($P < 0.01$) and only numerically at 30 °C. This suggests that temperature is the controlling factor in minimizing DNA shearing for the mechanical lysis method.

3.1.3.2 Quantification of bacterial 16S rRNA gene

The total copy numbers of the bacterial 16S rRNA gene in the solid residue samples were two orders of magnitude smaller than the pellets, suggesting that the pretreatment method used in this study was suitable for collecting bacterial biomass. The bacterial 16S rRNA gene copy numbers normalized by the template DNA concentration were used to assess the microbial DNA extraction efficiency from the epiphytic phyllosphere sample, where a lower value indicates high plant DNA content. Mechanical disruption exhibited 2–12 times higher bacterial 16S rRNA gene copies per ng template gDNA ($2.7 \pm 0.1 \times 10^7 – 6.5 \pm 0.1 \times 10^7$) than enzymatic disruption ($5.2 \pm 0.0 \times 10^6 – 1.8 \pm 0.0 \times 10^7$) (**Fig. 1**). The copy numbers were consistent for mechanical disruption when extraction was performed at the same temperature irrespective of the bead-beating time, suggesting that the extraction temperature is a controlling factor for the preferential lysis of bacterial rather than plant cells (**Fig. 1b**). At 30 °C, two times higher copy numbers ($6.5 \pm 0.1 \times 10^7$) were detected than at 20 °C ($3.4 \pm 0.0 \times 10^7$). For enzymatic disruption, there were significant variations in the gene copy numbers depending on extraction conditions (**Fig. 1a**). At 56 °C, no significant differences were observed in the copy number as the incubation time varied. At 20 °C and 40 °C incubation temperatures, the 16S rRNA gene copy numbers increased

Table 3. Effects of cell lysis methods and extraction conditions on DNA yield (μg), purity (absorbance ratios of 260/280 nm ($OD_{260/280}$) and 260/230 nm ($OD_{260/230}$)), and DNA integrity (DIN). The numbers in the parentheses indicate the standard errors of

Blood & tissue kit												
Incubation	Temperature	20 °C				40 °C				56 °C			
	Time (min)	5	10	20	60	5	10	20	60	5	10	20	60
DNA total yield		97.1 (4.6)	96.6 (5.4)	80.9 (7.3)	67.9 (1.0)	80.9 (1.8)	74.1 (0.5)	70.0 (0.2)	57.0 (6.2)	74.3 (3.2)	77.3 (10.4)	80.1 (3.3)	66.5 (2.7)
DIN		1.33 (0.29)	1.40 (0.1)	1.20 (0.16)	1.00 (0.00)	1.2 (0.28)	1.13 (0.12)	1.00 (0.00)	1.05 (0.05)	1.00 (0.00)	1.27 (0.05)	1.53 (0.12)	1.13 (0.09)
$OD_{260/230}$		0.73	0.73	0.74	0.73	0.73	0.73	0.73	0.72	0.70	0.70	0.71	0.71
$OD_{260/280}$		1.49	1.46	1.52	1.51	1.49	1.50	1.52	1.50	1.50	1.47	1.49	1.50

Power Soil kit							
Incubation	Temperature	20 °C			30 °C		
	Time (min)	5	10	15	5	10	15
DNA total yield		4.2 (0.1)	4.8 (0.2)	5.2 (0.1)	0.5 (0.0)	0.6 (0.0)	0.6 (0.0)
DIN		6.23 (0.12)	5.83 (0.17)	5.37 (0.05)	6.33 (0.12)	6.20 (0.08)	6.07 (0.09)
$OD_{260/230}$		0.81	0.86	0.78	0.80	0.82	0.79
$OD_{260/280}$		1.85	1.84	1.85	1.80	1.98	1.85

as the incubation time increased. The results suggest that mechanical disruption is more suitable for the preferential lysis of bacterial cells than enzymatic disruption.

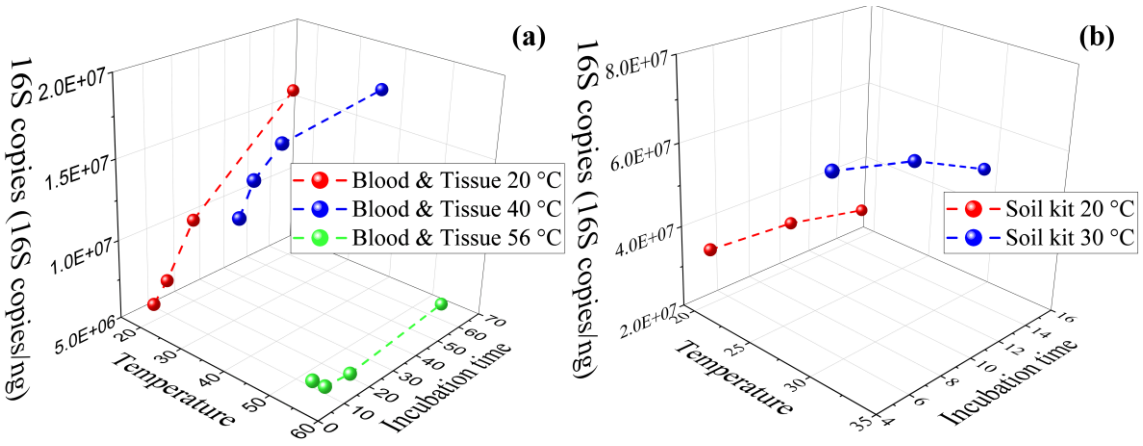

Figure 1. The copy numbers of bacterial 16S rRNA gene normalized by the template DNA amount in the samples prepared by (a) enzymatic and (b) mechanical lysis methods, respectively, under different extraction conditions.

3.1.3.3 Composition and diversity of the bacterial community

Bacterial 16S rRNA amplicon sequencing was performed on selected DNA extracts in duplicate to examine the effects of different DNA extraction methods on the patterns of soil bacterial community structure and diversity. The sequences per sample ranged from 15,094 to 445,904, clustered at a 97% sequence identity threshold. A total of 2767 OTUs were identified at both phylum and genus levels. Depending on the extraction conditions, distinctive variations were observed in the bacterial community compositions between the samples prepared via enzymatic disruption. In contrast, the samples prepared via mechanical disruption exhibited consistent community compositions irrespective of the extraction conditions (**Fig. 2**). At the phylum level, there was a high abundance of unclassified phyla (72%) in the samples prepared via enzymatic disruption for 5 min at 20 °C (BT 5m20c) but not in the samples prepared using the same lysis method for 60 min at 40 °C (BT 60m40c, <5%) (**Fig. 2a**). In the samples prepared via

mechanical disruption, the compositions were consistent. In all the samples, firmicutes was the predominant phylum, followed by proteobacteria, actinobacteria, and cyanobacteria. At the genus level, BT 5m20c exhibited the highest abundance of unclassified genera (up to 88%), whereas BT 60m40c displayed the lowest abundance of unclassified genera (20%). A positive correlation between small-sized (sheared) DNA and an abundance of unclassified sequences was previously reported (De Lipthay et al., 2004; Desneux and Pourcher, 2014; Teng et al., 2018). However, in this study, DIN did not correspond to the abundance of unclassified sequences (**Table 3**). It can be speculated that the proportion of plant DNA may have been significant in the extracts prepared via enzymatic disruption, and the DINs did not represent the DIN of microbial DNA. Simultaneously, microbial DNA may have been released earlier than plant DNA and may have been exposed to the proteinase longer, resulting in more small-sized DNA in BT 60m40c than in BT 5m20c. The samples prepared using mechanical disruption also showed consistent community compositions at the genus level regardless of the extraction conditions. In all samples, *Pediococcus* was a dominant genus, followed by *Weissella, Lactobacillus, and Lactococcus* (**Fig. 2b**). Previous studies have shown that differences in the bacterial cell wall and membrane structures cause DNA extraction to be more or less effective from some organisms. Such a discrepancy can introduce bias in the estimates of relative abundances of microbes in samples; thus, mechanical lysis methods are considered less biased than enzymatic lysis methods (Carrigg et al., 2007; Krsek and Wellington, 1999). Indeed, in this study, the samples prepared using the mechanical lysis method exhibited consistent microbial community compositions irrespective of the extraction conditions. PCoA analysis also confirmed that mechanical disruption allowed consistent analysis of microbial community structure (**Fig. 3**). The first axis of the PCoA explains 59.98% of the variance, whereas the second axis explains 14.02% of the

variance from the samples prepared using the Blood and Tissue and PowerSoil kits under different conditions. All duplicate samples were clustered close to each other, suggesting that both lysis methods are reproducible. Irrespective of the extraction conditions, the samples prepared via mechanical disruption were clustered together, whereas those prepared via enzymatic disruption were located separately in response to the different extraction conditions. This indicates that the mechanical lysis method is less biased than the enzymatic approach.

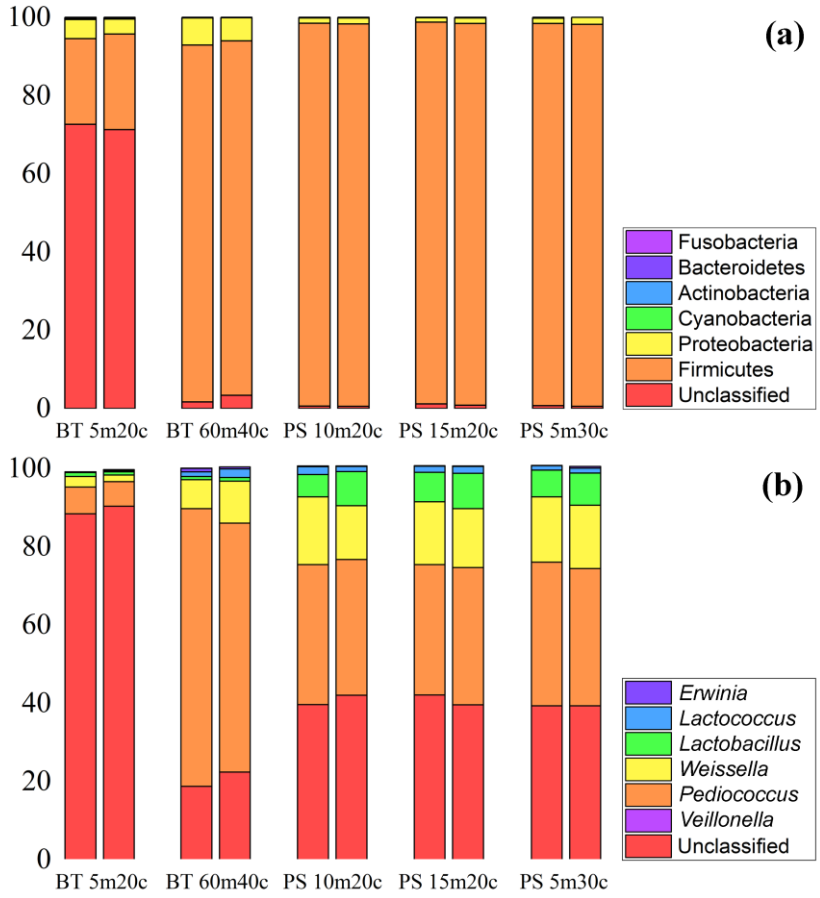

Figure 2. Comparison of relative abundance of 16S rRNA OTUs in the samples prepared by two different lysis methods under different extraction conditions at the phylum (a), the genus (b) level. Each bar represents one replicate sample.

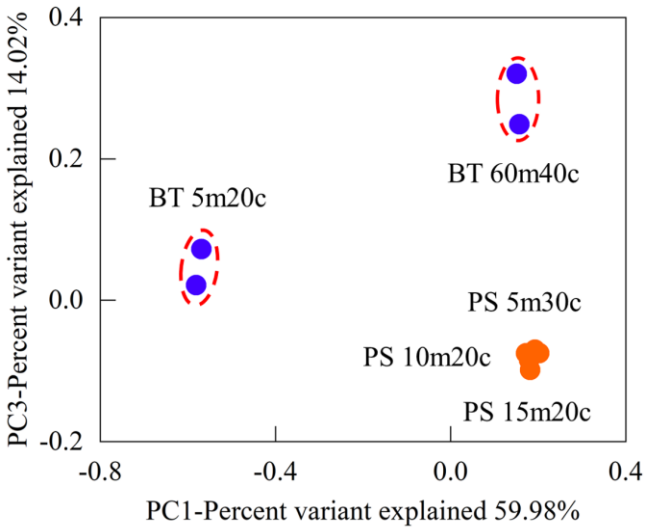

Figure 3. PCoA plot of 16S rRNA OTU abundance in all samples. Each symbol represents different samples prepared by the following extraction conditions: 5 min incubation at 20°C using Blood and Tissue kit (BT 5m20c), 60 min incubation at 40°C using Blood and Tissue kit (BT 60m40c), 10 min bead-beating time at 20°C using PowerSoil kit (PS 10m20c), 15 min bead-beating time at 20°C using PowerSoil kit (PS 15m20c), and 5 min bead-beating time at 30°C using PowerSoil kit (PS 5m30c).

3.1.4 Conclusion

We hypothesized that an optimized cell lysis protocol would allow preferential bacterial cell lysis over plant cells. With enzymatic disruption, the DNA quality was suboptimal for downstream applications, and more importantly, the bias in the microbial community profiles was prominent, albeit with high DNA yield. In the meantime, the samples prepared via mechanical disruption exhibited high DNA quality and consistent microbial compositions irrespective of extraction conditions. Therefore, this study demonstrates that the mechanical disruption method is more suitable for epiphytic phyllosphere samples than the enzymatic disruption method, and disruption at 20 °C for 5 min was found to be optimal for the fermented forage samples used in this study.

3.2 Forage conservation is a neglected N_2O source

3.2.1 Introduction

N_2O is the third most important GHG, following CO_2 and CH_4. On a molar basis, N_2O has a warming potential 300 times greater than CO_2 and remains in the atmosphere for an extended period, estimated at 100–150 years (USEPA, 2019). Recent studies have also emphasized N_2O as the primary ozone-depleting substance in the stratosphere (Fang et al., 2019b; Ravishankara et al., 2009b). Atmospheric N_2O concentrations have increased by over 20% compared to preindustrial levels, with the fastest increase occurring in the last five decades (Hall et al., 2007; Tian, Xu, Canadell, Thompson, Yao, et al., 2020b). While natural processes and human activities contribute to N_2O production, agricultural activities are one of the dominant sources, responsible for over two-thirds of global anthropogenic N_2O emissions (Davidson & Kanter, 2014a; D. S. Reay et al., 2012a; Tian, Xu, Canadell, Thompson, Yao, et al., 2020b). Numerous countries compile GHG emission inventories following the technical guidelines provided by the Intergovernmental Panel on Climate Change. For example, the USEPA annually publishes a report titled "Inventory of U.S. Greenhouse Gas Emissions and Sinks," which accounts for N_2O emissions from agricultural activities through three sources: agricultural land management, manure management, and the burning of agricultural residues. Forages, the plant materials consumed by herbivores, are conserved to sustain livestock during periods of limited pasture growth or inadequate grazing conditions (Finch et al., 2014b; Owens, 2003b).

Globally significant for productive and efficient livestock production, forage conservation methods mainly involve hay and silage. For long-term storage, hay is dried to below 20% moisture (12–20%, w/w) to curtail microbial growth and stored under aerobic conditions(Owens, 2003b). Conversely, silage is produced at higher moisture levels (40–70%,

w/w) and stored strictly under anaerobic conditions to facilitate fermentation. Indigenous or exogenous lactic acid bacteria (LAB) convert soluble carbohydrates into organic acids, predominantly lactic acid, which acts as a natural preservative that inhibits unwanted microorganisms (Müller et al., 2008b; Soundharrajan et al., 2017b). Commercial silage inoculants containing LAB, such as *Lentilactobacillus buchneri* and other facultative anaerobic bacteria, are used as additives to enhance silage fermentation (Muck et al., 2018b). The fermentation process typically takes 2 to 4 weeks to complete, and most silages can be stored for 6 to 12 months, although the length of storage time depends on the crop and weather conditions (Owens, 2003b). The market for global silage inoculants reached USD 503 million in 2021 and is projected to grow to USD 630 million by 2028 at a compound annual growth rate of 3.8%. Silage is a significant segment of the global livestock industry, with 162.3 million metric tons (MMT) harvested in the United States in 2022 (Grossi et al., 2019b; USDA, 2023b). Despite its high production volume and extensive use, forage conservation has been limitedly studied as a potential source of GHG emissions (Grossi et al., 2019b).

While gas production during forage conservation has been investigated, previous studies have primarily focused on odorous chemicals, such as volatile organic compounds and ammonia (NH_3) (Hafner et al., 2013; Morgan & Pereira, 1962; Pusede & Cohen, 2012). At best, the detection of N_2O has been reported in previous studies (Bueno et al., 2020b; Chuan Wang & Burris, n.d.; Krommweh et al., 2020b; Schmithausen et al., 2022), but a quantitative assessment is still lacking. That is, our study, to our knowledge, is the first to provide comprehensive quantitative estimates on a per-crop basis, which can be scaled to national and sector-level estimates for N_2O emission from forage conservation. The precise mechanism underlying N_2O production remains partially understood, but microbial processes are widely considered the main

contributors to N_2O emissions (Hu et al., 2015c; Klimasmith & Kent, 2022c; Kuypers et al., 2018b; A. J. Thomson et al., 2012; Tian, Xu, Canadell, Thompson, Winiwarter, et al., 2020). While nearly all microorganisms involved in the biogeochemical nitrogen cycle can potentially produce N_2O, specific microbial pathways including heterotrophic denitrification, NH_3 oxidation, and nitrifier denitrification, are pivotal to N_2O production (Butterbach-Bahl et al., 2013b; Kuypers et al., 2018b). Heterotrophic denitrification is a multistep respiration process that involves the reduction of oxidized mineral forms of nitrogen (i.e. NO_3^- and NO_2^-) to gaseous nitric oxide (NO), N_2O, and dinitrogen (N_2). This process typically occurs under anaerobic conditions, although recent discoveries have identified a new group of aerobic denitrifying bacteria (J. Yang et al., 2020b). Conversely, NH_3 oxidation and nitrifier denitrification occur under aerobic conditions. Nitrification involves a two-step process: the oxidation of NH_3 to NO_2^- by AOB and AOA, followed by further oxidation to NO_3^- by NO_2^--oxidizing bacteria. N_2O is indirectly produced through the chemical decomposition of intermediate or end products of NH_3 oxidation (hydroxylamine, nitroxyl hydride, or NO_2^-) (S. Liu et al., 2017b). Additionally, certain AOB can directly produce N_2O through nitrifier denitrification by oxidizing NH_3 to NO_2^- and subsequently reducing it to NO and N_2O (Kozlowski et al., 2016b; Wrage, Velthof, Van Beusichem, et al., 2001; Wrage-Mönnig et al., 2018b). In this study, we conducted a comprehensive quantitative assessment of N_2O emissions during forage conservation, especially in silage form. Simulated silages derived from three major silage crops in the United States–maize, alfalfa, and sorghum—were monitored for N_2O emissions over a 4-week period. Our findings showed significant N_2O release from silages, making forage conservation the third-largest source of N_2O emissions within the agricultural

sector. Further experiments confirmed the significant role of denitrification in N_2O production in conserved forages, as validated by molecular analyses.

3.2.2 Materials and methods

3.2.2.1 Forage sample preparation

Maize (Dyna Gro D53VC55RIB) and sorghum (Dyna Gro Super Sile 20) were harvested from a private farm near Manhattan, KS (39°38′ N, 96°88′ W) at their optimal maturity stages (i.e. 2/3 milk line and soft dough stages, respectively). The plants were chopped to a theoretical length of 2 cm using a standard forage harvester without inoculation. Two distinct alfalfa varieties, HVX MegaTron (WinField United L.L.C., Arden Hills, MN, USA) and HybriForce 3400 (Dairyland Seed Co.), were grown in experimental plots at the Kansas State University Agronomy Research Farm in Manhattan, Kansas (39°20′ N, 96°59′ W). Each variety was harvested at two different stages of maturity (mid-bud and early flowering) using a sickle bar mower. The harvested alfalfa was subsequently chopped to a length of 2 cm using a stationary forage chopper.

3.2.2.2 Experimental design

We used a simulated silage model known as mini silos. These mini-silos comprised a 1-L glass jar (Contreras-Govea et al., 2011) connected to a 3-L Tedlar bag (**Fig. 4**). Each crop was ensiled with four treatments: (i) no inoculant (control, I^-), (ii) crop-specific commercial silage inoculant (brand names omitted for confidentiality) following the manufacturer's instructions (I^+), (iii) inoculant + chlorate (0.1%, w/w, potassium salt) (I^+ Ch^+), and (iv) inoculant + acetate (0.1%, w/w, sodium salt) (I^+ Ac^+). Chlorate was added to inhibit denitrifiers (Kučera, 2006; Oremland & Capone, 1988), and acetate was added as a readily available external carbon source to increase the initial C/N ratio (Itokawa et al., 2001; Kampschreur et al., 2009). And for the optimization of the chlorate concentration and finding the economical method, each crop was ensiled with seven

different chlorate concentrations (0, 0.002, 0.005, 0.01, 0.05, 0.1, and 0.5%) to optimize the chlorate concentrations. Also, each crop was ensiled with 0.002% of chlorate and three different extra carbons (acetate, glucose, molasses) to find the best combination.

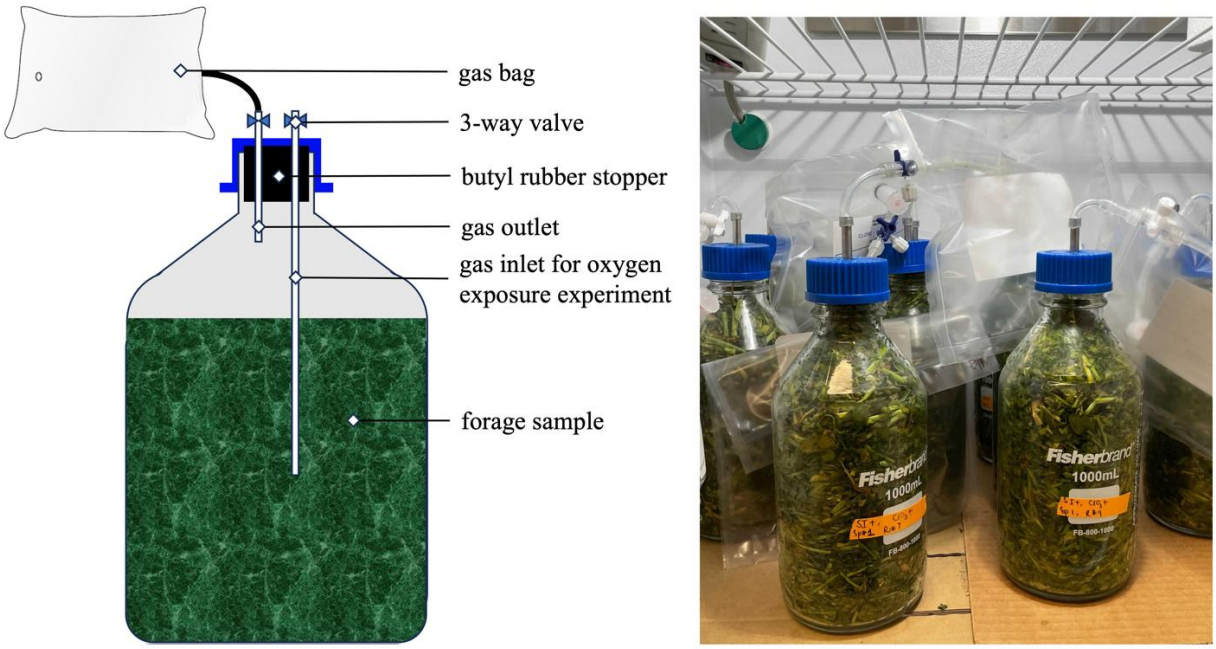

Figure 4. A schematic (left) and photo (right) of mini-silos used in this study. Gas inlet was only used for the oxygen exposure experiment.

Separate inoculant, chlorate, and acetate solutions were prepared and sprayed onto the plants. The initial moisture content was measured using the conventional microwave oven method (Lacerda et al., 2009) and adjusted to 70% (w/w, wet weight basis) by adding deionized water to the treatment solutions. All crops were packed in mini-silos with a bulk density of 650 kg/m^3 (41 lb/ft^3) (Darby & Jofriet, 1993), and each silo contained 650 g of the crops (wet weight), which was equivalent to 195 g_{DM}. The mini-silos were incubated at 30 °C in the dark, and N_2O production was monitored regularly for up to 4 weeks. Gas bags were removed on days 1, 2, 3, 5, and 20 to characterize temporal variations in the volume and composition of gas production and

replaced with new bags at each sampling. Fresh feed samples were collected and stored at −80˚C for chemical analysis. Additionally, for molecular analysis, four mini-silos were prepared for each treatment and sacrificed on days 1, 3, 5, and 20. A subset of the samples (5 g) was preserved in 5 mL RNA preservation solution (RNAprotect, QIAGEN, Hilden, Germany) and stored at −80 °C. Each treatment comprised three replicates of the mini-silos.

3.2.2.3 Contribution of nitrification to N_2O emissions

To investigate the relative contribution of nitrification to N_2O production, mini-silos were prepared with alfalfa (HVX Megatron) harvested at the early flowering stage, and acetylene (10 Pa) (Jia & Conrad, 2009) was added at the beginning of incubation. In addition, the mini-silos were intermittently exposed to oxygen on days 3, 5, and 10, achieved by supplying 20 mL of air (4 mL of oxygen) through a stainless-steel tube that reached the center of the mini-silos (**Fig. 5**). Oxygen was added to separate bottles on each injection date.

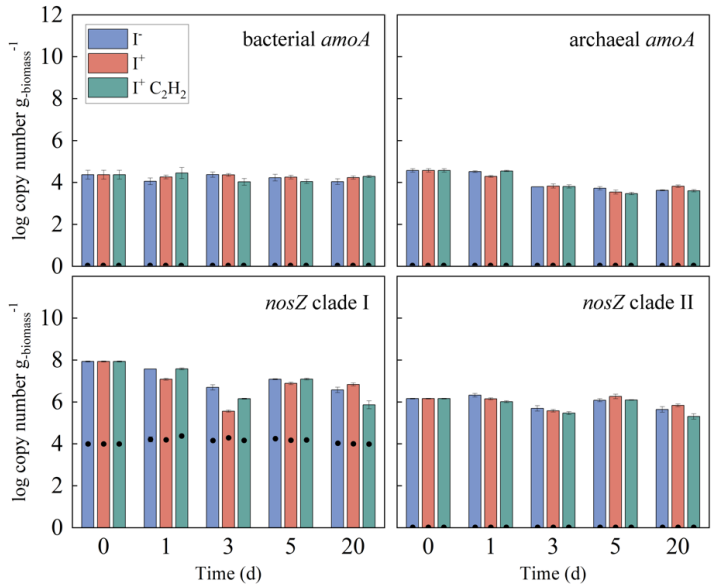

Figure 5. Effect of acetylene (C_2H_2) on the abundance of bacterial/archaeal *amoA* genes and clade I/II *nosZ* genes (bar) and their transcripts (black circle). The error bars represent the standard deviations of the triplicate incubations. Error bars may not be visible if their magnitude is smaller than the symbols.

3.2.2.4 Analytical methods

The total gas production volume was measured using the water displacement method. N_2O was quantified using an Agilent 7890 gas chromatograph with an electron capture detector and an HP-PLOT/Q column (30 m × 0.53 mm × 40 m). Fresh forage samples were sent to Rock River Laboratory, Inc., Watertown, WI, USA for nutritional analysis. The following parameters were examined: crude protein (CP), total amino acid, NH_3-N content, ADF, amylase-treated neutral detergent fiber (aNDF), lignin, starch, and ethanol-soluble carbohydrate (ESC). NO_3^--N content (% of DM) was measured at the Kansas State University Soil Testing Laboratory.

3.2.2.5 Nucleic acid extraction and quantitative PCR

Microbial nucleic acid extraction from plant material, particularly from the epiphytic phyllosphere, poses challenges due to plant derived biomolecules such as proteins and nucleic acids (Dent et al., 2004; Ikeda et al., 2009). In this study, we used a microbial DNA extraction method optimized for silage samples, as detailed in our previous study(S. Yang et al., 2023). Briefly, for DNA extraction, five grams of the sample was suspended in 45 mL of sterile 0.85% NaCl solution, shaken on a rotary shaker at 120 rpm for 2 h at room temperature, filtered through two layers of gauze cloth to remove large plant debris, and centrifuged at 12,000 g for 15 min at 4°C. The supernatant was discarded, and the pellet was stored at −80°C until subsequent DNA extraction. The RNA preservation solution containing the sample was shaken on a rotary shaker at 120 rpm for 2 h at room temperature. Four milliliters of the supernatant were collected, pelleted by centrifugation at 12,000 g for 15 min at 4°C, and immediately subjected to RNA extraction. DNA and RNA extractions from the pellets were performed using the DNeasy and RNeasy PowerSoil kits (Qiagen, Hilden, Germany), following the manufacturer's instructions, with slight modifications. Cells were lysed by bead beating at 20°C for 5 min. RNA samples

were subjected to DNase treatment (ezDNaseTM, Invitrogen, CA, USA) and reverse transcribed into complementary DNA (cDNA) using SuperScriptIV Reverse Transcriptase (Thermo Fisher Scientific, Waltham, MA, USA). PCR was conducted with universal 16S rRNA gene primers on DNase-treated RNA samples to confirm the absence of DNA contamination. Target genes and transcripts were quantified by qPCR using a CFX Opus 96 Real-Time PCR System (Bio-Rad, Hercules, CA, USA) in 20 μL reaction mixtures containing 10 μL of SsoAdvancedTM Universal SYBR Green Supermix (Bio-Rad, Hercules, CA, USA), 300 nM of each primer, and 2 μL of template DNA. Quantification was performed using standard curves prepared from serial 10-fold dilutions of cloned plasmids or double-stranded synthetic DNA fragments (gBlocks®, Integrated DNA Technologies, Coralville, IA, USA) in triplicate. Detailed information on primer sequences, standard sequences, and detection limits can be found in **Table 4**.

3.2.2.6 Statistical analysis

Statistical analyses were conducted using the MIXED procedures of SAS/STAT software, Version 9.4 (SAS Institute Inc., Cary, NC, USA). A two-way ANOVA was applied to the N_2O emission data, crop, treatment, and their interaction term as fixed effects. A Bonferroni multiplier adjustment was performed when comparing N_2O emissions between crops in each treatment group or treatments in each crop group (conditional pairwise comparison). Probability values of $P < 0.05$ (two-tailed) were considered statistically significant for all comparisons. The correlation coefficients between N_2O production and nutrient variables were calculated as Pearson correlation coefficients. A Pearson correlation coefficient > 0.8 or < -0.8 with $P < 0.05$ (two-tailed) was deemed indicative of a strong correlation between the two variables.

Table 4. Quantitative PCR primers, standards, and detection limits of each assay.

Target gene	Primer set	Primer sequences (5'-3')	Quantification range
16S rRNA (Amann et al., 1990)	1055F 1392R	ATGGCTGTOGTCAGCT ACGGGCGGTGTGTAC	10^2-10^9
napA(Henry et al., 2008)	V67m V17m	AAYATGGCVGARATGCACCC GRTTRAARCCCATSGTCCA	10^2-10^9
narG (Bru et al., 2007)	narG-F narG-R	TCGCCSATYCCGGCSATGTC GAGTTGTACCAGTCRGCSGAYTCSG	10^2-10^9
nirK (Wei et al., 2015)	nirKC1-F nirKC1-R	ATGGCGCCATCATGGTNYTNCC TCGAAGGCCTCGATNARRTTRTG	10^4-10^9
nirS (Braker et al., 1998)	nirS-1F nirS-6R	CCTAYTGGCCGCCRCART CGTTGAACTTRCCGGT	10^3-10^9
qnorB **(Braker & Tiedje, 2003)**	qnorB-2F qnorB-5R	GGNCAYCARGGNTAYGA ACCCANAGRTGNACNACCCACCA	10^2-10^9
Clade I *nosZ* (Henry et al., 2006)	nosZ-1F nosZ-1R	WCSYTGTTCMTCGACAGCCAG ATGTCGATCARCTGVKCRTTYTC	10^2-10^9
Clade II *nosZ* (Chee-Sanford et al., 2020)	nosZ 1374F nosZ 1577R	CCBYTBCAYACSCARTTYG TGSGASAGCTTGTTSAGSS	10^2-10^9
Bacterial - *amoA* (Rotthauwe et al., 1997)	amoA-1F amoA-2R	GGGGTTTCTACTGGTGGT CCCCTCKGSAAAGCCTTCTTC	10^2-10^9
Archaeal - *amoA* (Francis et al., 2005)	arch-amoAF arch-amoAR	STAATGGTCTGGCTTAGACG GCGGCCATCCATCTGTATGT	10^2-10^9

Abbreviations for degenerate nucleotide positions are as follows: R =A or G; K = G or T; M =A or C; S =C or G;W=A or T; Y =C or T; B =C, G, or T; D = A, G, or T; V =A, C, or G; H =A, C, or T. References for the primers and probes are included in the first column.

3.2.3 Results

3.2.3.1 Chemical properties of silage materials

The freshly chopped, non-inoculated plant materials showed characteristic nutritional properties for each crop (**Fig. 6**). Among them, alfalfa, a leguminous crop, showed notably higher concentrations of proteins and amino acids than maize and sorghum. Conversely, cereal crops like maize and sorghum exhibited a higher starch content than alfalfa. The total protein and amino acid contents in alfalfa decreased as it matured, accompanied by an increase in fiber (acid detergent fiber [ADF] and neutral detergent fiber [aNDF]) and lignin contents. Notably, the

alfalfa variety HybriForce 3400 consistently showed higher protein and amino acid contents than HVX MegaTron, regardless of maturity stage.

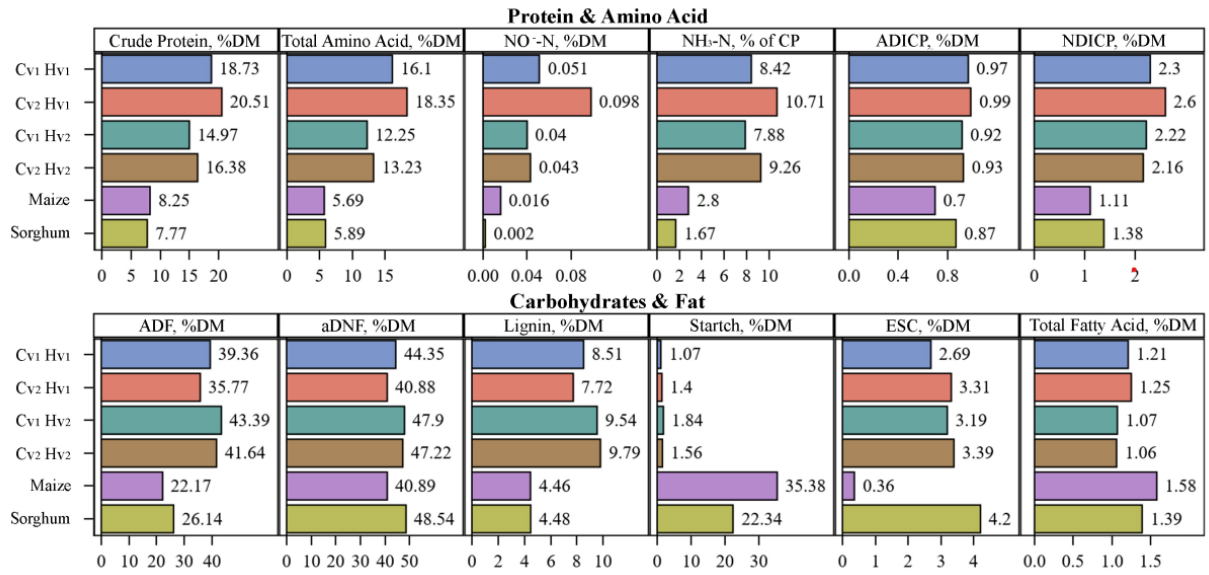

Figure 6. Nutritional parameters of fresh maize, alfalfa (two distinct varieties harvested at two different stages of maturity), and sorghum samples. The labels Cv_1 and Cv_2 denote two alfalfa varieties, HVX MegaTron and HybriForce 3400, respectively. The labels Hv_1 and Hv_2 denote alfalfa samples harvested at the mid-bud and early flowering stages, respectively. DM: dry matter; CP: crude protein; ADICP: acid detergent-insoluble CP; NDICP: neutral detergent-insoluble CP; ADF: acid detergent-treated fiber; aNDF: amylase-treated neutral detergent fiber; ESC: ethanol-soluble carbohydrates. The numerical annotations next to the individual bars are their respective measured values.

3.2.3.2 N_2O emissions from simulated silage

The total amount of N_2O produced in the maize, alfalfa (HybriForce 3400, harvested at mid-bud stage, Cv_2 Hv_1), and sorghum silage over 28 d of incubation was 6.7 (±0.7), 62.3 (±4.0), and 1.8 (±0.1) mL, which corresponded to 18.2 (±1.9), 169.7 (±10.9), and 4.8 (±0.2) g CO_2 equivalent (eq.) per kgDM, respectively (**Fig. 7a**). N_2O emissions began immediately after incubation commenced, with the majority (>90%) being produced within 24 h for maize and sorghum and 5 days for alfalfa. For alfalfa harvested at the same growth stages, no significant difference in N_2O production was observed between the varieties ($P > 0.05$) (**Fig. 7b**). However, incubations with

alfalfa harvested at the later maturity stages (i.e. early flowering stage, Hv2) produced significantly lower N_2O emissions ($P < 0.05$) regardless of the varieties (**Fig. 7b**). The statistical analysis is summarized in **Fig. 8**.

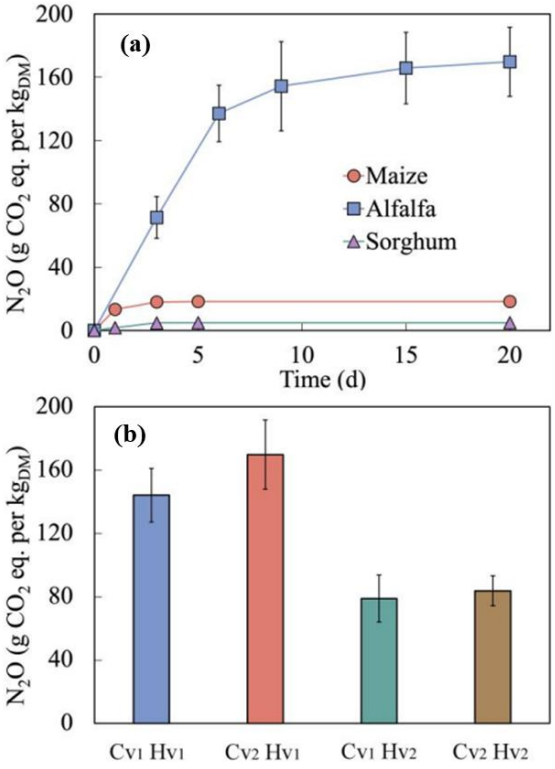

Figure 7. Cumulative N_2O production of (a) maize, alfalfa, and sorghum and (b) two distinct alfalfa varieties harvested at two different stages of maturity. The labels Cv_1 and Cv_2 denote the two alfalfa varieties, HVX MegaTron and HybriForce 3400, respectively. Similarly, the Hv_1 and Hv_2 denote alfalfa samples harvested at the mid-bud and early flowering stages. The error bars represent the standard deviations derived from the triple incubations. Error bars may not be visible if their magnitude is smaller than the symbols.

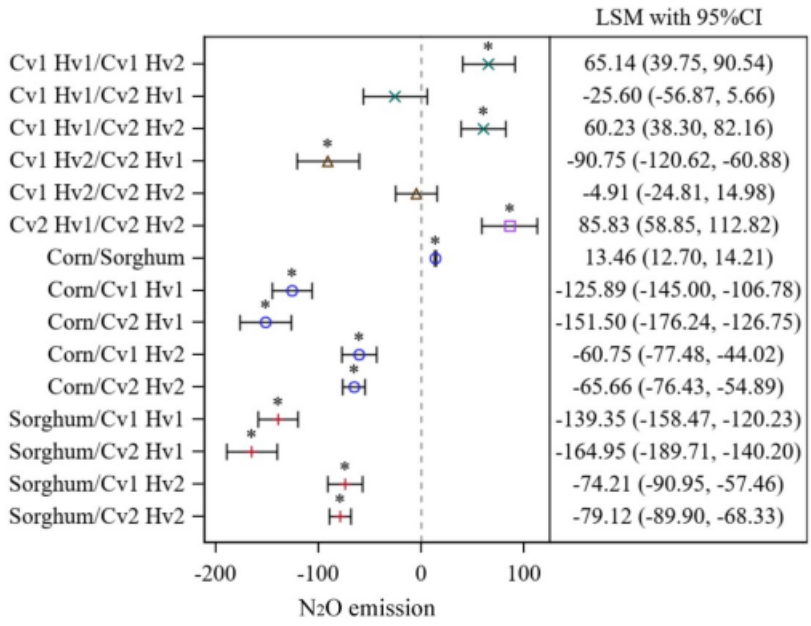

Figure 8. Pairwise comparisons N_2O emissions for crops under the controls (I^-) group. Results are reported as lease square means for N_2O emissions with 95% confidence intervals. '*' indicates a significant difference observed between the two crop groups.

3.2.3.3 Effects of different treatments on N_2O production

The effects of various treatments on N_2O production were examined within the same sample group, revealing consistent trends regardless of the crops or alfalfa varieties harvested at different growth stages (**Fig. 9a**). Compared to the controls (I^-), the addition of inoculants (I^+) had no significant effect on N_2O production ($P > 0.05$), except for sorghum, where a significant difference was observed ($P < 0.05$). Notably, applying chlorate treatment and the inoculant (I^+ Ch^+) significantly reduced N_2O production by up to 99%. The addition of acetate as an external carbon source alongside the inoculant (I^+ Ac^+) resulted in a statistically insignificant but numerically lower N_2O production than I^+ ($P > 0.05$). However, the effect of acetate on N_2O reduction was significant in alfalfa Cv_2 Hv_1 and sorghum ($P < 0.05$). Conversely, neither acetylene (C_2H_2) addition nor intermittent O_2 exposure at different periods (days 3, 5, and 10) impacted N_2O production (**Fig. 9b**). Lower chlorate concentrations, as low as 0.01% (w/w), still

achieved 92% N_2O reduction (**Fig. 9c**). Residual chlorate could not be quantified due to technical limitations in ion chromatography. The statistical analysis is summarized in **Table 5**.

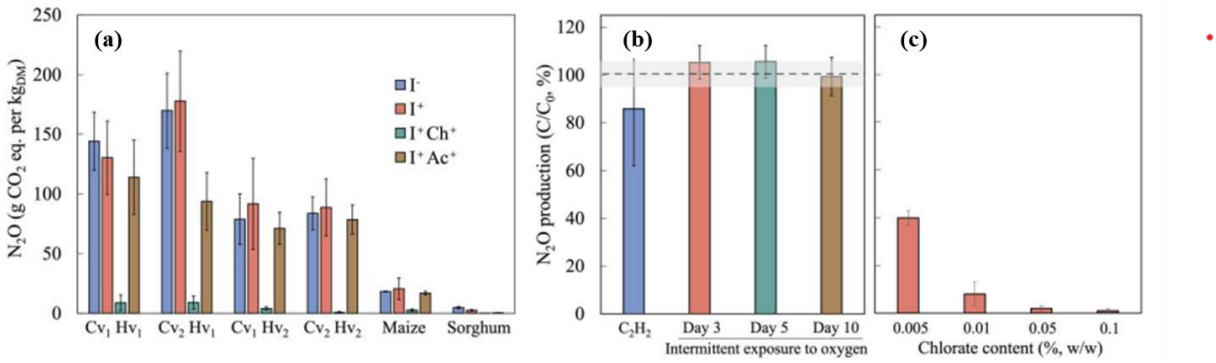

Figure 9. Cumulative N_2O production of (a) maize, alfalfa, and sorghum and (b) two distinct alfalfa varieties harvested at two different stages of maturity. The labels Cv_1 and Cv_2 denote the two alfalfa varieties, HVX MegaTron and HybriForce 3400, respectively. Similarly, the Hv_1 and Hv_2 denote alfalfa samples harvested at the mid-bud and early flowering stages. The error bars represent the standard deviations derived from the triple incubations. Error bars may not be visible if their magnitude is smaller than the symbols.

Table 5. Least square means for N_2O emissions (g-CO_2 eq. per kgDM-forage) with standard error (SE) of the two-way analysis of variance (ANOVA) model under variance heterogeneity.[1,2,3]

	Treatments			
Crops	I^-	I^+	I^+Ch^+	I^+Ac^+
$Cv_1\ Hv_1$	144.14 ± 10.90^a	130.33 ± 10.90^a	8.90 ± 10.90^b	114.07 ± 10.90^a
$Cv_2\ Hv_1$	169.74 ± 10.90^a	177.72 ± 10.90^a	9.01 ± 10.90^c	93.84 ± 10.90^b
$Cv_1\ Hv_2$	78.99 ± 7.77^a	91.82 ± 7.77^a	4.15 ± 7.77^b	71.23 ± 7.77^a
$Cv_2\ Hv_2$	83.91 ± 7.77^a	88.79 ± 7.77^a	0.83 ± 7.77^b	78.71 ± 7.77^a
Maize	18.24 ± 1.87^a	20.57 ± 1.87^a	2.70 ± 1.87^b	16.96 ± 1.87^a
Sorghum	4.79 ± 0.22^a	2.46 ± 0.22^b	0.07 ± 0.22^c	0.52 ± 0.22^c

[a, b, c]Means in the same row with different superscript letters differ significantly ($P < 0.05$).
[1]Treatments are no inoculant (I^-), crop-specific commercial silage inoculant (I^+), inoculant and chlorate (I^+Ch^+), and inoculant and acetate (I^+Ac^+). The notations Cv_1 and Cv_2 indicate two alfalfa cultivars, HVX MegaTron and HybriForce 3400, respectively. The notations Hv_1 and Hv_2 indicate samples harvested at two different maturity stages, i.e., mid-bud and early-flowering, respectively.
[2]Results are reported as lease square means ± standard error (SE) for each combination group of crop and treatment.
[3]P values of two-way analysis of variance (ANOVA) under variance heterogeneity for crop, treatment, and crop by treatment interaction are < 0.01, <0.01, and <0.01, respectively.

3.2.3.4 Analysis of the correlation between N_2O production and fresh matter nutrient parameters

The relationship between various nutrient parameters and N_2O production in the controls (I^-) was measured using a Pearson correlation coefficient (**Fig. 3**). Parameters related to protein and amino acids, including crude protein ($r = 0.98$, $P = 0.031$), total amino acids ($r = 0.99$, $P = 0.001$), $NO_3^- - N$ ($r = 0.94$, $P = 0.017$), $NH_3 - N$ ($r = 0.96$, $P = 0.010$), and NDICP ($r = 0.92$, $P = 0.029$), exhibited strong correlations with N_2O production ($r > 0.8$ and $P < 0.05$). Conversely, parameters related to carbohydrates and fats, including ADF, aNDF, lignin, starch, ethanol-soluble carbohydrates, and total fatty acids, exhibited no significant correlation with N_2O production ($r < 0.4$ or $P > 0.05$).

3.2.3.5 Gene and transcript abundance dynamics

The abundance of the genes and transcripts in incubations with alfalfa harvested at the early flowering stage (Hv_2) under various treatments is summarized in **Fig. 11**. Notably, the abundance of *narG*, the gene encoding membrane-bound NO_3^- reductase, exhibited a marked two-order-of-magnitude decrease with the addition of chlorate (I^+ Ch^+), in which N_2O production was reduced by up to 99%, compared to I^+. The abundance of other denitrification genes showed no trend across the various treatments over time. Notably, the abundances of bacterial and archaeal *amoA* gene encoding AMO were lower than those of denitrification genes, and no trend was observed over time across the various treatments. Transcript analysis revealed the expression of *narG* was completely suppressed by the addition of chlorate (I^+ Ch^+), similar to the gene abundance. Transcripts of archaeal and bacterial *amoA,* both *nir* genes encoding NO_2^- reductase, and *nosZ* gene encoding N_2O reductase clade II were not detected. The expression level of *napA* gene

encoding periplasmic NO_3^- reductase, *norB* gene encoding nitric oxide reductase, and *nosZ* gene encoding N_2O reductase clade I were not affected by the treatments used.

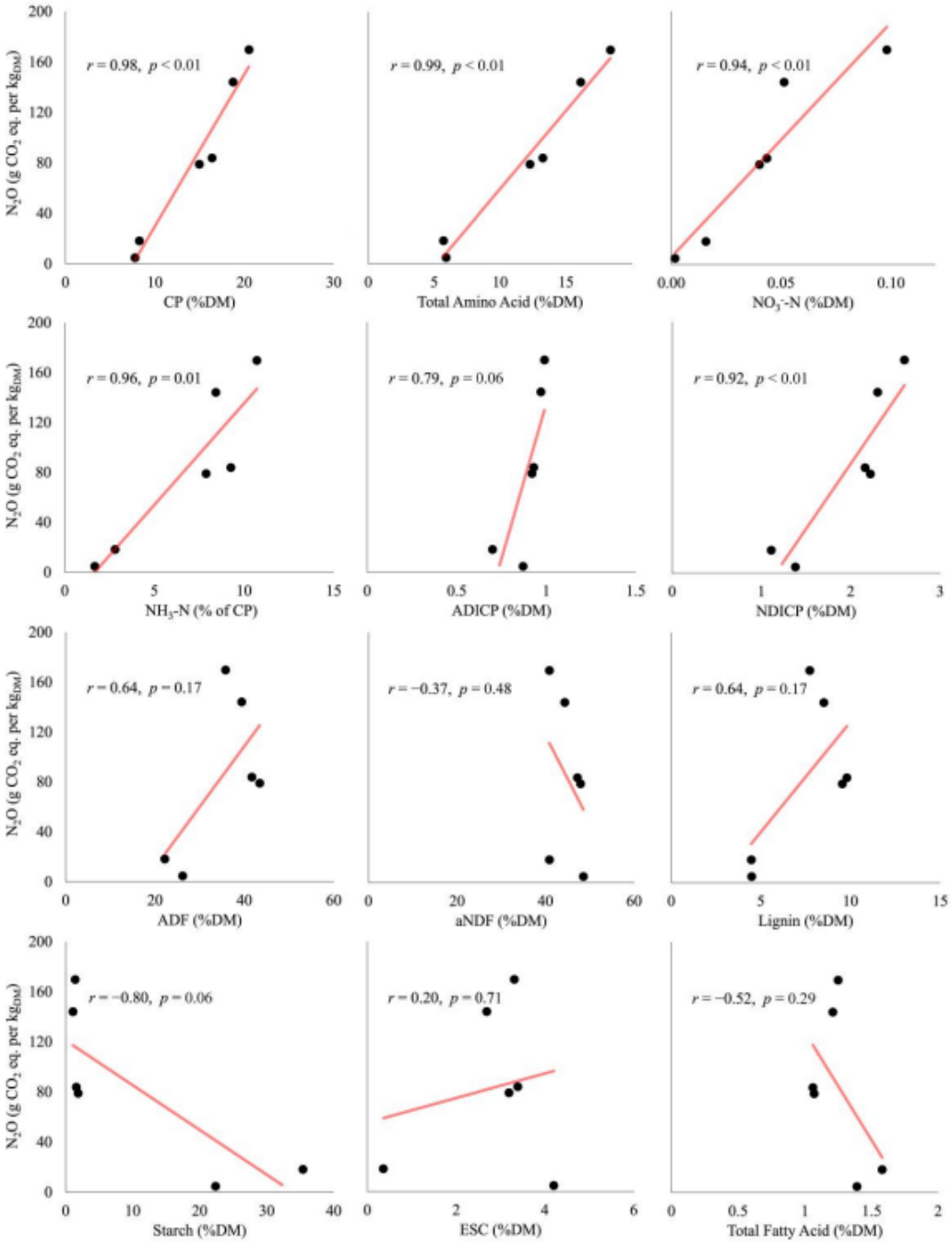

Figure 10. Correlation analysis of N_2O production and fresh matter nutrient parameters. DM, dry matter; CP, crude protein; ADICP, acid detergent insoluble CP; NDICP, neutral detergent insoluble CP; ADF, acid detergent treated fiber; aNDF, amylase-treated neutral detergent fiber; ESC, ethanol-soluble carbohydrates

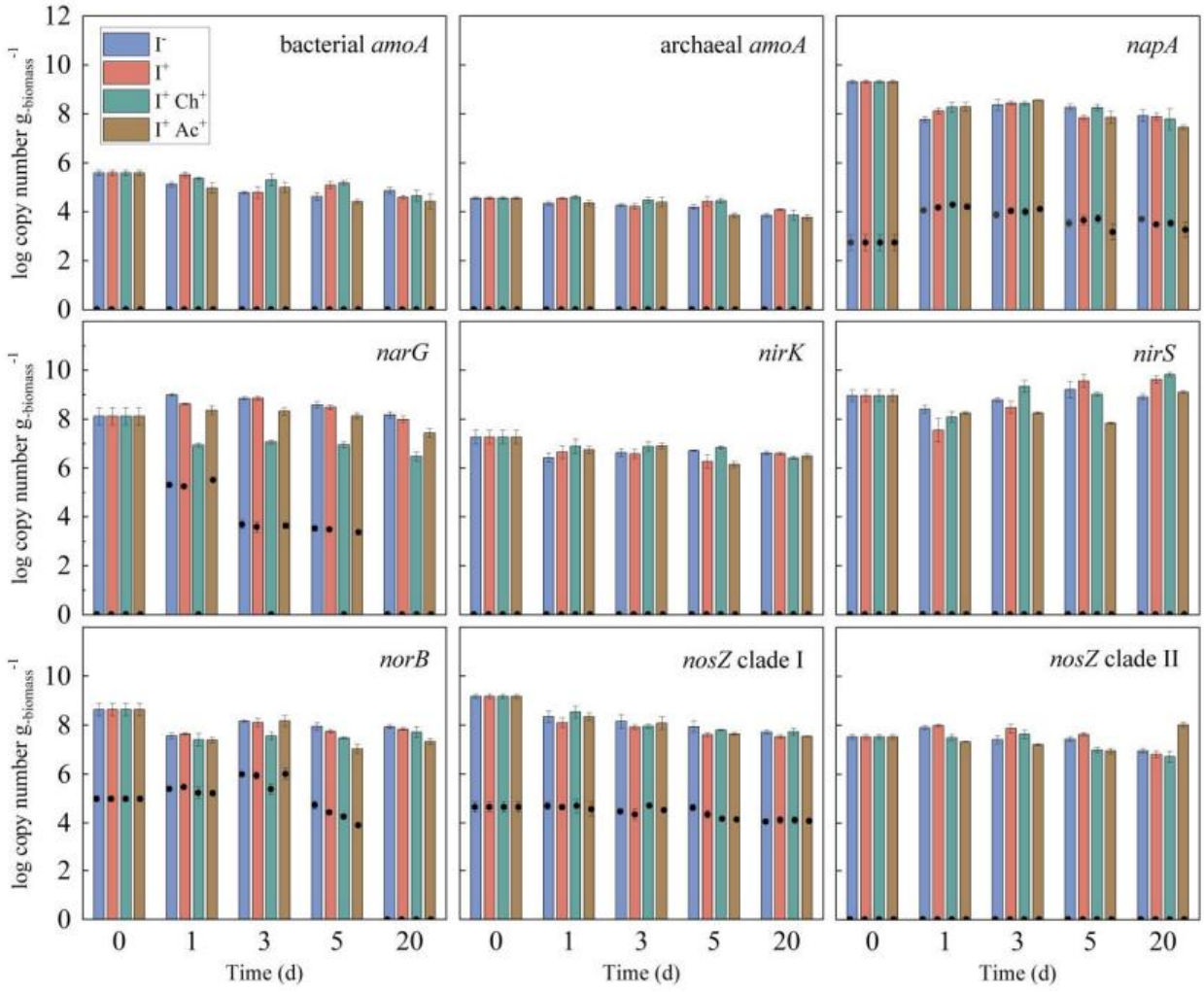

Figure 11. Abundance of functional genes (bar) and their transcripts (black circle) in incubation with alfalfa harvested at the early flowering stage (Hv_2) under various treatments. The error bars represent the standard deviations of the triplicate incubation. Error bars may not be visible if their magnitude is smaller than the symbols.

3.2.3.6 Optimization of chlorate and additional carbon sources combination

The cumulative N_2O produced from alfalfa silage controls was 16.6 ± 2.3 mL, equivalent to 45.2 g CO_2-eq kg^{-1} dry matter (DM). Chlorate sharply suppressed N_2O in a dose-dependent manner: 0.01% (w/w) achieved a 92% reduction, while 0.005% reduced N_2O by 60% (**Fig. 12**). To evaluate potential co-benefits with added carbon and to retain an interpretable dynamic range, 0.005% chlorate was selected as the working dose for combination tests. At this dose,

supplemental glucose or acetate increased the inhibition from 62.9% (chlorate alone) to 79.8% and 85.0%, respectively, on Day 1 and maintained ~80% inhibition through Day 20. In contrast, molasses did not improve inhibition relative to chlorate alone.

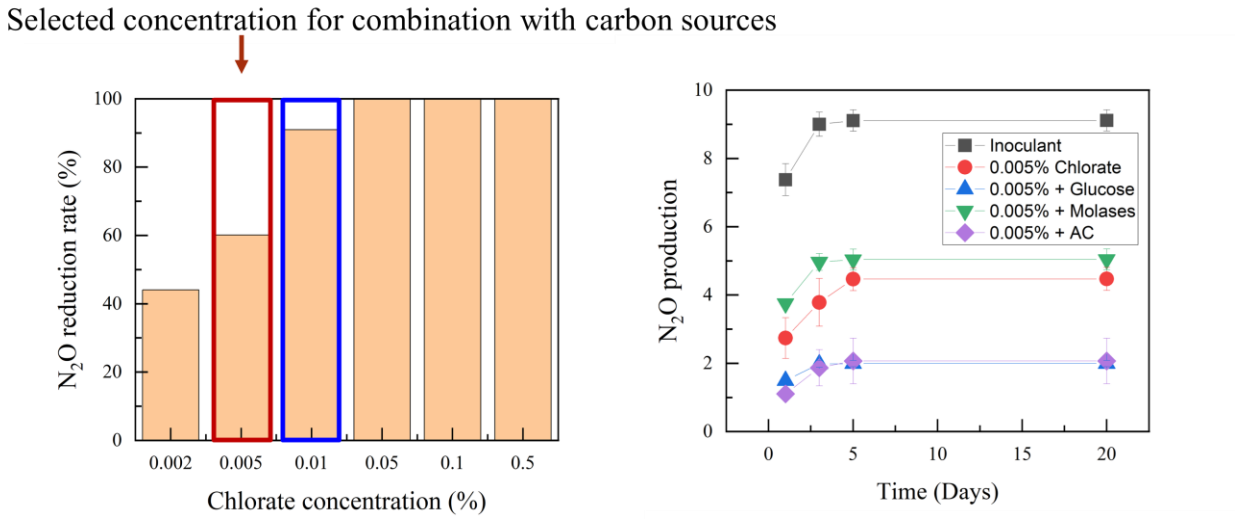

Figure 12. N_2O reduction rate for different chlorate concentrations

3.2.4 Discussion

3.2.4.1 N_2O production mechanism

The majority of N_2O production in this study occurred within the first week of incubation (**Fig. 7a**), which is consistent with previous studies (Krommweh et al., 2020b; Schmithausen et al., 2022). During this initial phase, transient aerobic or microaerobic conditions can be expected due to residual oxygen, followed by anaerobic conditions (Ávila & Carvalho, 2020). Under these conditions, both ammonia oxidizers and denitrifiers are potential contributors to N_2O production (Barnard et al., 2005; Schinner et al., 1996). Ammonia oxidizers are recognized for producing N_2O through direct (i.e. nitrifier denitrification) and indirect (i.e. abiotic processes) mechanisms. Furthermore, ammonia oxidizers can contribute to N_2O production by converting NH_3 to NO_3^-, subsequently fueling denitrification. If nitrification contributes to N_2O production, we

hypothesize that additional O_2 could stimulate N_2O production since nitrification activity is dependent on residual O_2 levels. However, N_2O production did not increase when O_2 was added at different time points ($P > 0.05$, **Fig. 9b**), indicating that the contribution of nitrification to N_2O production may not be significant. This finding is further supported by the observation that C_2H_2 (10 Pa), a potent inhibitor of bacterial and archaeal NH_3 oxidation (Berg et al., 1982; Jia & Conrad, 2009), did not affect N_2O production ($P > 0.05$**, Fig. 9b**). The absence of bacterial and archaeal *amoA* transcripts also confirmed the noninvolvement of ammonia oxidizers in N_2O production (**Fig. 11**). At high concentrations (1 – 20 kPa), C_2H_2 has been shown to inhibit N_2O reductase activity of denitrifying micro-organisms (Knowles, 1996; Yoshinari et al., 1977). However, such inhibition (i.e. increased N_2O production) was not observed in this study (**Fig. 9b**). The expression of Clade I *nosZ* remained unaffected in the samples supplemented with C_2H_2 (**Fig. 5**), suggesting that C_2H_2 did not inhibit denitrifying bacteria at the concentration used in this study (i.e. 10 Pa). Furthermore, although recent studies have demonstrated that active nitrification can occur at pH levels as low as 3.0 (Norton & Stark, 2011), nitrification is typically limited in acidic conditions due to the unavailability of substrate (NH_3) for AMO, the enzyme catalyzing NH_3 oxidation. In silage, low pH caused by organic acids generated during fermentation may also inhibit nitrification. Due to the chemical similarities between NO_3^- and chlorate, chlorate has been used as an inhibitor for dissimilatory NO_3^- reduction, the first step in denitrification (Kučera, 2006; Oremland & Capone, 1988). The significant decrease in N_2O production, by up to 99% upon the addition of chlorate (**Fig. 9a**), indicates that denitrifiers are the main contributors to N_2O production. This finding was further confirmed by the diminished abundance of the *narG* genes and transcripts in the chlorate-amended samples (**Fig. 11**). In another study, the same concentration of chlorate (0.1% w/w) was used as a ruminant

supplement to reduce *E. coli* O157:H7 population (Callaway et al., 2002), suggesting that chlorate has the potential to be used as a silage additive to reduce N_2O emissions. Further studies are warranted to assess the potential hazards, such as the ultimate fate of the added chlorate and its impact on animal health if it remains in the silage. Denitrification is a microbial process wherein NO_3^- is reduced to N_2 via intermediates including N_2O. Factors such as a low C/N ratio have been reported to lead to N_2O accumulation during denitrification (Itokawa et al., 2001; Kampschreur et al., 2009). When the C/N ratio is low, the amount of available organic carbon is insufficient to fully reduce NO_3^- to N_2 (J. Wang et al., 2023; W. Zhou et al., 2020). Moreover, low C/N ratios affect microbial community dynamics, i.e., a low C/N ratio can favor populations less efficient at the N_2O reduction step, further contributing to higher N_2O levels (Xu et al., 2024). Additionally, conditions with a low C/N ratio often lead to residual oxygen or higher NO_2^- concentrations, both of which inhibit N_2O reductase, exacerbating N_2O accumulation (W. Zhou et al., 2020). In our study, adding acetate as an external carbon source, effectively increasing the C/N ratio, resulted in a slight reduction in N_2O production (**Fig. 9a** and **Table 5**). This suggests that N_2O production in conserved forage may be influenced, at least in part, by a low C/N ratio. Overall, these findings suggest that denitrification inhibitors, such as chlorate, can be combined with an external carbon source, such as acetate, as an effective additive to mitigate N_2O emissions from the forage conservation process.

3.2.4.2 Chlorate combination with extra carbon sources

Chlorate is a structural analog of NO_3^- and selectively inhibits the membrane-bound NO_3^- reductase, blocking the first step of respiratory denitrification and preventing downstream N_2O formation. Parallel observation of suppressed *narG* expression aligns with this primary target. At a low operational dose (0.005%), residual N_2O persists—useful for detecting whether added

carbon shifts electron flow toward the nitrous oxide reductase and completion to N_2. Both extra carbon sources (glucose and acetate) are readily bioavailable, low-complexity substrates that (i) elevate C: N, (ii) provide fast electron supply at low redox potential, and (iii) minimize metabolic overhead for denitrifiers. These traits favor complete denitrification and support *nosZ* activity, explaining the jump from ~63% to ~80–85% inhibition and its persistence through Day 20.

3.2.4.3 N_2O production and its relationship with nutritional parameters

N_2O production was closely correlated with most parameters related to protein and amino acids, including NO_3^-−N (**Fig. 10**), presumably the main source of N_2O production. The NO_3^-−N content in forages varies with the stage of plant maturity (Murphy & Smith, 1967), and both alfalfa varieties harvested at later growth stages, which produced significantly less N_2O ($P < 0.05$) (**Fig. 7b**), contained lower NO_3^-−N levels (**Fig. 6**). Reports have also demonstrated that nitrogen fertilization directly impact NO_3^-−N content (Murphy & Smith, 1967), implying that nitrogen fertilization, especially preceding harvest, may contribute to higher N_2O production at ensiling. Further studies are needed to investigate the effects of nitrogen fertilization schedule on N_2O production. Simple changes in agricultural practice may reduce N_2O emissions. A source of organic carbon is an important component of denitrification, serving as an electron donor. Many studies have shown that external carbon sources, such as methanol, ethanol, and acetate, stimulate denitrification and usually reduce N_2O production (Fu et al., 2022). Consistent with these findings, our study showed that the addition of acetate reduced N_2O production (**Fig. 9a**). However, carbohydrate-related parameters, such as ADF, aNDF, lignin, starch, and ethanol-soluble carbohydrates, did not correlate with N_2O production (**Fig. 10**), which could be due to the recalcitrance of these carbon sources. Similarly, denitrification was promoted by plant-based

carbon substrates, such as rice straw, but there was a significant lag before denitrification became active (B. Zhou et al., 2019).

3.2.4.4 Environmental implications

What gets measured gets managed. The first step in reducing GHG emissions is to measure them. The US EPA publishes an annual report titled "Inventory of US Greenhouse Gas Emissions and Sinks," which estimates total GHG emissions by source across all sectors of the economy at the national level (1). Notably, agriculture is the largest contributor to N_2O emissions in the United States, accounting for 80% in 2021. The EPA monitors major sources in the agricultural sector, including agricultural land management, manure management, and the field burning of agricultural residues (**Table 1**) (USEPA, 2023;). In our study, 18.2 (± 1.9), 169.7 (± 10.9), and 4.8 (± 0.2) g CO_2 eq. per kg_{DM}-forage of N_2O were produced from maize, alfalfa, and sorghum, respectively (**Fig. 7a**). These values correspond to 2.3, 9.1, and 0.7 mg-N_2O-N/g-N based on the assumption that the total nitrogen content in silage is 16% of the protein content (Collins & Owens, 2003). According to the Crop Production 2022 Summary of the United States Department of Agriculture National Agricultural Statistics Service, the total production volumes of maize, alfalfa, and sorghum for silage in 2022 were 128.6, 17.4, and 5.6 MMT, respectively, comprising 93% of the total silage production combined (USDA, 2023b). Assuming a similar amount of N_2O can be produced from each crop, the total N_2O emission potential amounts to 5.3 MMT CO_2 eq.. This makes forage conservation the third largest N_2O emitter in the agricultural sector, surpassing the field burning of agricultural residues by a factor of 30 (**Table 1**). Notably, N_2O emissions from silage of uncategorized crops (total production volume: 10.7 MMT in 2022, comprising 7% of the total silage production) were not considered in this study (USDA, 2023b). Again, the first step to reducing GHG emissions is to measure them, as policymakers and

decision-makers use GHG inventories to develop strategies and track progress in GHG emission reduction efforts (Gidden et al., 2023; Iyer et al., 2017).

3.2.4.5 Limitations and perspectives

While our assessment provides valuable insights, it is important to acknowledge its limitations, particularly when attempting to extrapolate the data to a national scale. The microbial N_2O production, like any other microbial process, is sensitive to various environmental factors such as temperature and nutritional parameters, which could result in underestimation or overestimation of the outcomes. There are additional uncertainties associated with the heterogeneity of farmers' practices, such as storage types (e.g. silo, bunker, bag), harvest time, inoculant use, moisture content (i.e. wilting), and oxygen exposure. Therefore, N_2O emission measurements from actual silage fermentation systems spanning a range of environmental and management variations worldwide are warranted to achieve more accurate estimation results. Additionally, we demonstrated that a simple treatment could significantly reduce N_2O emissions from silage. With that, we aim to underscore the critical importance of the silage process as a significant source of N_2O emissions, advocating for targeted research and intervention strategies to mitigate this environmental impact. The nitrogen cycle within our study system is complex, where multiple processes such as nitrification, nitrifier-denitrification, and denitrification may occur simultaneously. This complexity introduces potential sources of error in distinguishing the contributions of these concurrent N_2O-producing reactions. Further efforts are warranted to develop more refined methodologies that can accurately assess and differentiate the contributions of each individual process. Our study highlights the need for such advancements to enhance our understanding of N_2O emissions in silage systems. In this study, chlorate was proposed as a simple and effective remedy to significantly reduce N_2O emissions (**Fig. 9a**). Additional

experiments demonstrated that even at low concentrations, such as 0.01% (w/w), chlorate achieved a 92% reduction in N_2O emissions (**Fig. 9c**). The chlorate (as sodium salt) price at the end of 2023 in the United States was 795 USD per ton. The estimated cost to add 0.01% (w/w) chlorate as an additional silage additive is 0.08 USD per ton forage (dry weight), which is only approximately 5–8% compared to the silage inoculant cost (i.e. 1–1.5 USD per ton). Assessing the social cost of GHG emissions has become a common yardstick for estimating the benefits of formulating and implementing abatement policies (Aldy et al., 2021). The social cost estimates of N_2O shown in recent studies range from 16 to 174 USD per kg − N_2O − N (Kanter et al., 2021; Rennert et al., 2022; J. Wang et al., 2023). Assuming that chlorate (0.01%, w/w) is added to achieve 90% N_2O reduction (**Fig. 9c**), the social cost saving could be 81–882 million USD with the expected total cost of 12 million USD for applying chlorate as an additive.

Chapter 4 - Impact of BNI on methanotrophs

4.1 Background

Nitrogen use efficiency (NUE) of agricultural plants, defined as the yield of grain achieved per unit of nitrogen available to the crop from soil and applied fertilizer, is notoriously low. Globally, about 50-70% of the nitrogen fertilizer applied to cropping systems is lost to the environment mainly due to microbial nitrification (Cassman et al., 2002; Ladha et al., 2005). Nitrification, a key microbial process in the global nitrogen-cycle, transforming immobile NH_4^+ to highly mobile NO_3^-, is known to enhance losses of fertilizer nitrogen by leaching and denitrification (Coskun et al., 2017). Nitrification has been known to be a two-step process where NH_4^+ is first oxidized to NO_2^- by AOB and/or AOA, and subsequently to NO_3^- by NO_2^--oxidizing bacteria, although recent studies demonstrated that *Nitrospira* spp. can carry out both reactions (Daims et al., 2015; van Kessel et al., 2015). Further, nitrification is one of the primary processes inducing N_2O emissions in soils (R. Liu et al., 2016), which is the third most important GHG, next to CO_2 and CH_4.

For these reasons, there have been attempts to repress nitrification in agriculture. Since the mid-1950s, studies on nitrification inhibitors have been conducted, and hundreds of SNIs have been identified. However, these artificially synthesized nitrification inhibitors are not widely applied in practice, because (1) their biological stability is limited leading to shorter effective time of nitrification inhibition, (2) some of these artificially synthesized nitrification inhibitors have toxicity and adversely affect beneficial soil microorganisms, resulting in their limited usability, and (3) artificially synthesized nitrification inhibitors are in general expensive (Coskun et al., 2017; Subbarao, Ito, et al., 2006). On the other hand, despite many early studies, it has recently become apparent that certain plant species are capable of suppressing microbial

nitrification by releasing inhibitory phytochemicals from roots, which is termed BNI (Subbarao et al., 2009a; Sun et al., 2016; Tesfamariam et al., 2014). This phenomenon has emerged as a promising new area of research not only because of its potential to improve NUE in cropping systems (Coskun et al., 2017; Subbarao et al., 2013), but also its implications for agricultural soil management, i.e., reduced N_2O emissions (Byrnes et al., 2017; Peters et al., 2013; Subbarao et al., 2017). For example, N_2O emission was also suppressed by 90% in the field of high-BNI *Brachiaria* pasture compared with soybean (*Glycine max*), which lacks BNI capacity (Subbarao et al., 2009a). Since the first report of BNI in *B.humidicola*, BNIs have been discovered in several crops, including sorghum *(Sorghum biocolor L.)* and wheat *(Triticum aestivum L.)* (O'Sullivan et al., 2016a; Zakir et al., 2008a). More recently, one of the major cereal crop rice *(Oryza sativa L.)* exudate was reported as crops which can produce detectable BNI activity (Pariasca Tanaka et al., 2010).

The first step of nitrification, the oxidation NH_3 to NO_2^- via hydroxylamine (NH_2OH), is catalyzed by two enzymes: AMO and HAO. Many studies measure BNI activity using nitrification inhibition assay(Subbarao, Ishikawa, et al., 2006) which measures NO_2^- concentration to identify the activity of several BNI exuded from roots with *Nitrosomonas* spp. in pure culture. The mode of inhibitory action of the BNIs varies for each species. For example, recent research has demonstrated that MHPP in sorghum and 1,9-D in rice specifically block the AMO step in bacterial ammonia oxidation (Coskun et al., 2017; Pariasca Tanaka et al., 2010; Zakir et al., 2008a). Also, Brachialactone, which is the exudate of *B. humidicola*, inhibited both AMO and HAO but had a greater inhibitory effect on AMO than the HAO (Subbarao et al., 2007b).

Meanwhile, CH_4 can be oxidized by MOB, a.k.a., methanotrophs, the only group of bacteria that utilize CH_4 as their sole carbon and energy source (Hanson & Hanson, 1996). pMMO, catalyzing the first step of CH_4 oxidation, is evolutionarily related to AMO. In these distinctive groups of Gram-negative bacteria, pMMO and AMO are both membrane associated enzymes and share many similarities in their encoding genes (*pmoCAB* and *amoCAB* respectively), structure ($\alpha_3\beta_3\gamma_3$ and subunit composition known for pMMO and possibly for AMO), metal content (Cu and possibly Fe), substrate ranges and inhibition patterns (Arp et al., 2007; Hakemian & Rosenzweig, 2007), suggesting that certain BNI compounds may inhibit MMO as well as AMO(Holmes et al., 1995), leading to increased CH_4 release to atmosphere.

4.2 Unexpected inhibition of methanotrophy by BNI: Mechanistic insights and ecological implications

4.2.1 Introduction

Plant–microbe interactions are fundamental drivers of terrestrial ecosystems, shaping nutrient cycles and influencing global climate dynamics. One critical and environmentally relevant interaction occurs in the plant rhizosphere, where plants and microbes compete intensely for nitrogen. Despite heavy nitrogen fertilizer use in modern agriculture, approximately 50–70% of applied nitrogen is not utilized by crops, instead lost primarily due to nitrification (Cassman et al., 2002; Coskun et al., 2017)—a microbial process converting immobile NH_4^+ to highly mobile NO_3^-, contributing to nitrogen loss through leaching and denitrification. This transformation ultimately increases emissions of N_2O, a potent GHG (USEPA, 2023) and primary ozone depleting substance (Ravishankara et al., 2009a).

To mitigate these losses, SNIs have been developed; however, they face limitations due to limited biological stability, potential toxicity to beneficial soil organisms, and high costs

(Coskun et al., 2017; Subbarao, Ito, et al., 2006). In contrast, recent research has identified a natural plant-based alternative: BNI, where plants release specific root exudates capable of suppressing nitrifying microbes (Coskun et al., 2017; Subbarao et al., 2009b, 2021; Subbarao & Searchinger, 2021). BNI represents a promising strategy to enhance NUE and reduce N_2O emissions (Byrnes et al., 2017; Peters et al., 2013; Subbarao et al., 2017). For instance, introducing a chromosomal segment from wild wheat into high-yielding cultivars significantly enhanced nitrogen uptake by 30% and reduced N_2O emissions by 25% without compromising grain yield and quality (Subbarao et al., 2021).

While BNI shows promise in improving agricultural sustainability (Coskun et al., 2017; Ghatak et al., 2023; Stein, 2023), its broader ecological level consequences remain insufficiently understood. Nitrification is a two-step process where NH_4^+ is first oxidized to NO_2^- by ammonia-oxidizing microorganisms and subsequently to NO_3^- by NO_2^--oxidizing bacteria. The entire nitrification process is usually limited by the initial step, i.e., NH_4^+ oxidation to NO_2^- via NH_2OH, which is sequentially catalyzed by AMO and HAO. Various BNI compounds from different chemical groups have been successfully isolated, and their mode of inhibition has been identified (Nardi et al., 2020; X. Wang et al., 2021). For example, 1,9-D from rice (*Oryza sativa*), MHPP from sorghum (*Sorghum bicolor*) specifically inhibit AMO (Sun et al., 2016b; Zakir et al., 2008b), similar to most SNIs (Coskun et al., 2017). In contrast, LA, derived from the pasture grass *B. humidicola*, inhibits both AMO and HAO (Subbarao et al., 2008).

Meanwhile, CH_4, another potent GHG, is oxidized by (MOB; hereafter referred to as methanotrophs), which serve as the sole biological CH_4 sink and play a critical role in mitigating CH_4 emissions (Hanson & Hanson, 1996). Given the chemical similarity between CH_4 and NH_4^+, pMMO —the enzyme catalyzing the first step of CH_4 oxidation—is evolutionarily related to

AMO and shares extensive genetic, structural, and catalytic homology (Holmes et al., 1995). Consequently, many SNIs—including nitrapyrin (Topp & Knowles, 1984), thiourea, allylthiourea (Hubley et al., 1975), and acetylene (Bédard & Knowles, 1989)—also inhibit MOB activity. These parallels raise the possibility that naturally produced BNIs, similar to some SNIs, may unintentionally suppress CH_4 oxidation. Understanding the impact of BNI on controlling GHG emissions is thus crucial, especially in wetland and rice paddy ecosystems(Calvo Buendia et al., 2019) where plants, MOB, and ammonia oxidizers coexist. These environments significantly contribute to global GHG budgets, underscoring the importance of comprehensively evaluating BNI's coupled impacts on nitrogen and carbon cycling.

To address this critical knowledge gap, we undertook a multi-scale investigation into the effects of BNI on CH_4 oxidation. We first employed controlled plant growth chamber experiments to examine how BNI-producing plants influence methanotrophic activity and community structure. Subsequently, pure culture assays were conducted to directly evaluate the inhibitory effects of specific BNI compounds on MOB. To elucidate the underlying inhibition mechanisms, we combined molecular docking, dynamic simulations, and chemical analog experiments to pinpoint the interactions between BNIs and the key CH_4-oxidizing enzyme, pMMO. Finally, RNA-seq analysis was conducted to gain molecular-level insights into the transcriptional responses of MOB exposed to BNIs. Our findings reveal, for the first time, that BNIs can significantly suppress CH_4 oxidation activity in addition to their established role in inhibiting nitrification. This dual action provides mechanistic insight into how specific BNI compounds interfere with CH_4-oxidizing enzymes and highlights the need to assess the previously unrecognized impacts of BNI activity on CH_4 oxidation and its broader implications for coupled carbon and nitrogen cycling in terrestrial ecosystems.

4.2.2 Material and Methods

4.2.2.1 Soil characterization.

The soil mixture was composed of 14% sand, 58% silt and 28% clay, and classified as silty clay loam according to the United State of Department of Agriculture (USDA) system for soil taxonomy. The soil physico-chemical characteristics were pH of 7.3; TC of 1.43%; TN of 0.13%; TP of 390 ppm; NO_3^--N of 8 ppm; NH_4^+-N of 7 ppm; Ca of 3,111 ppm; Cu of 1 ppm; Mg of 131 ppm; Mn of 9 ppm; Na of 13 ppm; K of 258 ppm; Zn of 0.3 ppm; and Fe of 29 ppm.

4.2.2.2 Soil Column Experiment: Plant-Mediated Effects on Methanotrophy

Acrylic soil columns (10 in i.d., 22 in length) (**Fig. 13**) were fabricated from transparent tubing with airtight lids. Each column base was filled with a 2-cm layer of 3-mm glass beads to ensure uniform gas distribution. Soil was packed to a depth of 25 cm, yielding a bulk density of 1.9 – 2.0 g·cm³. A gas mixture of CH_4 and CO_2 (50:50 v/v) was delivered from the base at 5 ± 0.5 mL·min^{-1}, while humidified ambient air was continuously flushed into the headspace at 20 mL·min^{-1} to simulate natural diffusion and wind. Soil moisture was monitored at 5 cm depth with an EC-5 probe (Decagon Devices, Pullman, WA, USA), and an automated irrigation system maintained 45–55% water-holding capacity. Ambient temperature and headspace relative humidity were monitored by a wireless thermo-hygrometer (Model H5074001, Govee, Hong Kong). Lighting was supplied by LED strips mounted under the reactor lids, providing 200 μmol·m^{-2}·s^{-1} photosynthetically active radiation under a 16 h light / 8 h dark cycle. Experimental treatments (n = 3 per condition) included: (1) control soil; (2) NH_4^+ amendment (25 mg NH_4^+-N·kg^{-1} soil); and (3) NH_4^+ amendment with ten *Brachiaria* seedlings (purchased from Hancock Seeds, Dade City, FL, USA). Seedlings were transferred at the 3–4 leaf stage. After two months, soils were collected from the rhizosphere (10-15 cm depth). CH_4 oxidation kinetics were assayed

within 24 h. Subsamples (30 g wet weight) were incubated in 160 mL serum bottles with 1% CH_4 (1.6 mL headspace). Bottles were incubated at 30 °C in the dark. Headspace samples (100 µL) were withdrawn every 40 min with gas-tight syringes and analyzed on an Agilent 7890 GC-FID. CH_4 oxidation rates were calculated from depletion curves, and Michaelis-Menten parameters (V_{max}, K_m) were fitted to the Michaelis-Menten model using OriginLab.

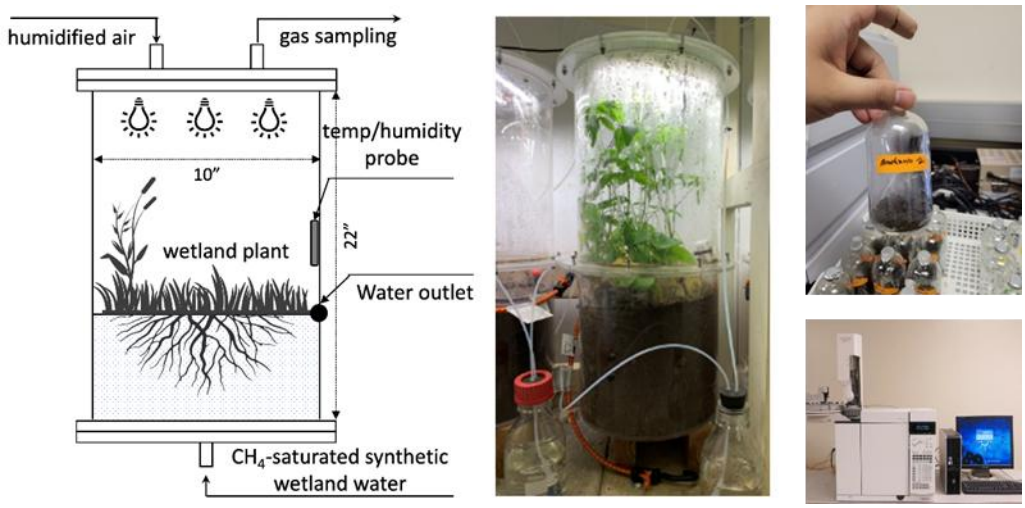

Figure 13 Acrylic soil columns to plant-mediated effects on methanotrophy and kinetic experiments set up.

4.2.2.3 Axenic culture experiment

BNI Compound Preparation.

Three BNIs were tested: 1,9-D (Activate Scientific, 95%), MHPP (Thermo Scientific, 98%), and LA (Thermo Scientific, 99%). Stocks were freshly prepared in DMSO (Thermo Scientific, 99%) and sterilized through 0.45-µm filters. Final solvent concentrations were 0.01% (methanotroph) or 0.1% (*N. europaea*). Additional experiments confirmed that these DMSO levels had no effect on growth, CH_4 oxidation, or NO_2^- formation. DMSO-containing controls served as appropriate baselines.

Direct Inhibition of Methanotrophy.

M. trichosporium OB3b and *M. album* BG8 were cultivated in NO_3^- mineral salts (NMS) medium supplemented with 10 µM $CuSO_4$ at 30 °C. For induction of sMMO, cultures were subcultured twice on copper-free NMS agar before transfer into liquid medium. Cultures were grown in 1 L NMS medium in 4 L Erlenmeyer flasks under a CH_4/air atmosphere with shaking at 120 rpm. CH_4 was replenished whenever depleted. Growth continued until OD_{600} ~ 0.3 (exponential phase). Cells were harvested by centrifugation (5,000 × g, 10 min, 20 °C), washed with fresh medium, and resuspended to OD_{600} = 0.3. For inhibition assays, 50 mL aliquots were transferred into 250 mL side-arm flasks for OD_{600} monitoring, sealed, and supplemented with 1% CH_4 (v/v). Inhibitor ranges were: 1,9-D (0.29 – 5.74 mM), MHPP (00.28 – 2.78 mM), and LA (5.8 – 58.2 µM). Positive controls contained 0.01% DMSO without BNIs. CH_4 depletion was monitored by GC-FID, and oxidation rates were fitted to Michaelis-Menten curves with OriginLab. V_{max} values were normalized to total protein concentration (Bradford assay).

Comparative Sensitivity of Nitrosomonas europaea.

N. europaea (ATCC 19718) was grown in ATCC medium 2265 at 30 °C in the dark with shaking (120 rpm). Cultures were harvested in exponential phase, centrifuged (5,000 × g, 10 min, 20 °C), washed twice, and resuspended in fresh medium to OD_{600} = 0.1. Assays were performed in 96-well plates with negative controls (medium only) and positive controls (0.1% DMSO without BNIs). Cultures were exposed to varying concentrations of BNIs. Parallel plates were used for baseline and 1 h incubations. Ammonia oxidation was stopped by adding 0.1 M allylthiourea (AT). NO_2^- accumulation was quantified by the Griess method, reading absorbance at 548 nm with an Epoch2 Microplate Reader (BioTek). Each treatment was performed in triplicate. Inhibition (%) was plotted against inhibitor concentration, and IC_{50} values were estimated using OriginLab.

Reversibility

To evaluate whether BNI-mediated inhibition of methane oxidation was reversible, *M. trichosporium* OB3b cultures were exposed to BNI compounds at their respective IC_{50} (MHPP and 1,9-D) or IC_{40} (LA) concentrations under the same conditions described above. Methane oxidation kinetics were first measured in triplicate cultures to quantify inhibited activity (V_{max}). Following this measurement, triplicate cultures were pooled prior to centrifugation (5,000 × g, 10 min) to minimize variability associated with cell harvesting. Cells were washed once with fresh NMS medium to remove residual inhibitors, centrifuged again, and resuspended in fresh medium. The resuspended culture was then redistributed into triplicate serum bottles, amended with methane, and methane oxidation kinetics were re-measured as described above.

Copper-dependent inhibition assays

To assess whether inhibition was associated with pMMO, additional assays were conducted under copper-replete (+Cu) and copper-limited (–Cu) conditions to modulate expression of pMMO and sMMO, respectively. OB3b cultures used for copper-limited (–Cu) assays were preconditioned on Cu-free NMS agar plates prior to liquid cultivation to minimize residual copper carryover and facilitate sMMO expression (Lee et al., 2006). Copper-replete conditions were established using NMS medium supplemented with 10 μM Cu, consistent with the conditions used in the kinetic assays, whereas copper-limited conditions were established using NMS medium without added Cu. Methane oxidation kinetics were then measured following exposure to BNI compounds at the same IC_{50} or IC_{40} concentrations as described above. V_{max} was measured for BNI-treated and control (BNI-free) cultures under both copper-replete (+Cu) and copper-limited (–Cu) conditions, and relative activity was calculated by

normalizing V_{max} values of BNI-treated samples to their corresponding control within each condition.

Molecular docking and dynamics simulations

The trimeric pMMO complex (PmoA–PmoB–PmoC) from *M. trichosporium* OB3b was modeled using both SWISS-MODEL(Waterhouse et al., 2018) and AlphaFold3(Abramson et al., 2024). Structural templates were selected based on sequence coverage and model quality metrics, including Global Model Quality Estimation (GMQE) and Quaternary Structure Quality Estimation (QSQE). The resulting models were evaluated by comparison with the available crystal structure (PDB ID: 3CHX),(Tucci et al., 2023) and the model with the lowest root-mean-square deviation (RMSD) was selected for subsequent analyses. Molecular docking was performed to identify potential binding sites of BNI compounds. Docking simulations were conducted using SwissDock (Bugnon et al., 2024; Grosdidier et al., 2011) with the AutoDock Vina algorithm in blind docking model, (Eberhardt et al., 2021) allowing exploration of the entire protein surface exposed to the periplasm. Ligand structures were provided as SMILES inputs. Binding poses were ranked based on predicted binding energy (kcal mol^{-1}), and clusters of low-energy conformations were used to identify candidate binding regions. Binding sites that were inaccessible from the protein exterior, including internal cavities and membrane-embedded regions, were excluded from further analysis. Docking results were visualized and analyzed using PyMOL. (Schrödinger LLC, 2015) In addition to native BNI compounds, structural analogues of 1,9-D, including dodecanoic acid and 1-decanol, were selected to probe structure–activity relationships and evaluated using the same methane oxidation inhibition assay described above, under identical experimental conditions. IC_{50} values were determined by testing a range of concentrations and fitting the resulting data to the Michaelis–Menten model.

Nucleic acids extraction, qPCR, and RT-qPCR

Soil DNA was extracted using the DNeasy PowerSoil kit (Qiagen, Hilden, Germany). DNA and RNA from axenic cultures were extracted using the MagMAX Microbiome Ultra Kit (Applied Biosystems, USA) on the Duo Prime automated platform (Thermo Fisher). RNA was DNase-treated (TURBO DNase, Thermo Fisher) and quantified by microvolume spectrophotometry (Epoch2, Agilent Technologies). RNA was reverse-transcribed with SuperScript IV Reverse Transcriptase (Thermo Fisher). qPCR and RT-qPCR were performed on a CFX Opus 96 (Bio-Rad) in 20 µL reactions containing 10 µL SsoAdvanced SYBR Green Supermix (Bio-Rad), 300 nM primers, and 2 µL template. Standard curves were generated using cloned plasmids or gBlocks (IDT). All reactions were run in triplicate. Primer sets and cycling conditions are listed in **Table.6**.

Table 6. qPCR/RT-qPCR primers

Target gene	Primer	Nucleotide sequence (5'-3')	Reference
Universal 16S rRNA	1055F	ATGGCTGTCAGCT	(Orschler et al., 2019)
	1392R	ACGGGCGGTGTGTAC	
pmoA	A189f	GGNGACTGGGACTTCTGG	(McDonald et al., 2008)
	Mb661r	CCGGMGCAACGTCYTTACC	
mmoX	mmoX 206f	ATCGCBAARGAATAYGCSCG	(Antony et al., 2010)
	mmoX 886r	ACCCANGGCTCGACYTTGAA	

where, N=G,A,T,orC;Y=C or T;M=A or C;K=G or T;S=G or C;R=G or A;B=C,T or G;W=A or T;V=A, C or G

Metagenomic analyses

Paired-end metagenomic reads were first subjected to quality control using Novogene's in-house pipeline. Low-quality bases and adaptor sequences were trimmed, and high-quality reads were merged with FLASH (Fast Length Adjustment of Short reads) under default parameters (minimum overlap length: 10 bp, maximum overlap length: 65 bp, mismatch ratio: 0.25).

MergeFASTQ files were converted to FASTA format using Seqtk (https://github.com/lh3/seqtk). The FunGene (Functional Gene Pipeline and Repository) database previously served as a curated reference for functional gene classification but is no longer maintained. To enable accurate classification of methanotrophic sequences, we constructed a custom pmoA reference library by compiling published *pmoA* sequences from all known methanotroph genera and species. Sequences were grouped into four phylogenetic types (Type I, Type II, and Type III) based on established frameworks. Environmental metagenomic reads were aligned to this custom reference using BLASTN (e-value $< 1 \times 10^{-6}$, minimum sequence identity > 80%). For each query sequence, only the top-scoring hit was retained, and type-level assignments were aggregated to estimate the relative abundances of methanotroph groups.

Transcriptomic analyses.

For transcriptomic profiling, *M. trichosporium* OB3b cultures were exposed to each BNI compound MHPP, 1,9-D, and LA—at their respective estimated IC_{50} concentrations determined in this study, alongside untreated controls. Cultures were harvested in mid-exponential phase. Total RNA was extracted, and RNA quality was verified by agarose gel electrophoresis and an Agilent 2100 Bioanalyzer (RIN > 7). Ribosomal RNA was removed using the Ribo-Zero rRNA Removal Kit (Illumina). Strand-specific cDNA libraries were prepared following Illumina's protocols and sequenced by Novogene (Beijing, China) on an Illumina NovaSeq 6000 platform, yielding 150 bp paired-end reads. Raw reads were processed by Novogene's pipeline, including adaptor trimming, removal of low-quality bases, and exclusion of reads with > 5% ambiguous nucleotides. Clean reads were aligned to the *M. trichosporium* OB3b reference genomeusing HISAT2 with default parameters. Read counts were generated using featureCounts, and differential expression analysis was performed with DESeq2 (v1.34.0) in R. Counts were

normalized with the median-of-ratios method, and dispersion was estimated with the default shrinkage approach. Genes with adjusted *p*-values (Benjamini-Hochberg correction) < 0.05 and $|\log_2$ fold-change$| > 1$ were considered significantly differentially expressed. Functional enrichment analysis was performed using Gene Ontology (GO) annotations. Overrepresented GO categories among up- and downregulated genes were identified using Fisher's exact test with Benjamini-Hochberg correction (padj < 0.05). For visualization, enrichment scores were calculated as (Up – Down) / (Up + Down) per GO category, and the top enriched categories for each compound were plotted as heatmaps.

Statistical Analysis

All statistical analyses were performed using OriginLab (OriginLab Software, Northhampton, MA, USA). Nonlinear regression was used to estimate kinetic parameters (V_{max}, K_m) and inhibitory concentrations (IC_{50}) from CH_4 oxidation and NO_2^- accumulation assays. For comparative analyses among treatments, one-way ANOVA followed by Tukey's post hoc test was applied unless otherwise noted. Data are presented as mean ± s.d. from at least three biological replicates. Statistical significance was accepted at $P < 0.05$ or $P < 0.01$, as indicated in the figure legends. Correlations between predicted binding affinities and inhibition intensities were tested using Pearson's correlation coefficients.

Analytical procedures

CH_4 concentrations in the headspace were measured by an Agilent 7890 GC equipped with a DB-624 capillary column (60 m × 0.32 mm × 1.8 μm) and an FID. For each measurement, 100 μL headspace gas was withdrawn and manually injected. Calibration curves ($R^2 > 0.99$) were generated before each experiment.

4.2.3 Results

4.2.3.1 BNI-producing plants suppress CH_4 oxidation in soil bioreactors

To determine whether BNI-producing plants influence CH_4 oxidation in complex soil-plant systems, we established soil bioreactors under three conditions: unamended control, NH_4^+ amendment (25 mg NH_4^+-N·$kg_{\text{-soil}}^{-1}$), and NH_4^+ amendment with *Brachiaria*. NH_4^+ addition significantly enhanced CH_4 oxidation ($P < 0.001$), with the maximum CH_4 consumption rate (V_{max}) increasing from 18.0 (± 4.4) to 105.7 (± 8.8) nmol·min^{-1}·$g_{\text{-soil}}^{-1}$. In contrast, *Brachiaria* incubation strongly suppressed CH_4 oxidation (13.5 nmol·hr^{-1}·g-$soil^{-1}$), reducing activity to levels below those observed in the unamended control, despite NH_4^+ amendment ($P < 0.001$) (**Fig.14a**), and thus were not considered further.

Metagenomic shotgun sequencing was performed to assess methanotrophic community shifts under the three treatments. Across the dataset, 21,283,174 sequences were obtained from the control, 14,678,467 from the NH_4^+-amended soil, and 12,969,658 from the NH_4^+ plus *Brachiaria* soil. Screening for methanotroph-specific *pmoA* genes recovered 21,976 sequences, which were classified into Type I (9,882 sequences), Type II (4,084), Type III (20), and Type IV (7,990) groups. The relative abundance of Type I MOB was significantly reduced in the *Brachiaria* treatment compared to both the control and NH_4^+-only treatments ($P < 0.01$). Type II MOB exhibited a modest decline, while Type III and IV groups were largely unaffected. (**Fig.14b**) These results demonstrate that BNIs from *Brachiaria* suppress CH_4 oxidation in soils, with metagenomic evidence pointing to a disproportionate effect on Type I MOB.

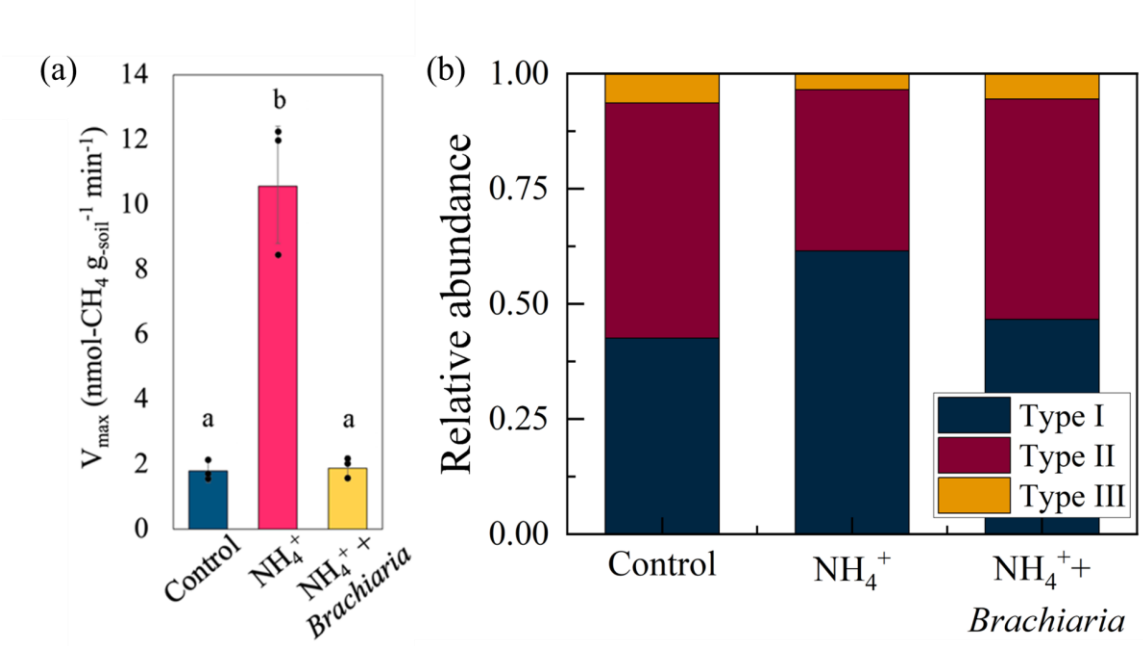

Figure 14. (a) Maximum methane oxidation rates (V_{max}) measured in soils recovered from the bioreactors. Bars indicate mean ± s.d. and dots represent individual biological replicates (n = 3). NH_4^+ amendment stimulated methane oxidation, whereas *Brachiaria* largely abolished this effect. Different letters indicate statistically significant differences ($P < 0.05$, one-way ANOVA with post hoc test). (b) Community profiles for the bioreactor with *B. humidicola* species. Sequences were used to screen related FunGene *pmo*A sequences with an e-value threshold of $1e^{-6}$ and minimum identity of 80%. Based on this screening, separate and non-overlapping databases for each *pmo*A type were constructed.

4.2.3.2 Axenic culture experiments: Methanotrophs inhibition assays

To evaluate the inhibitory effects of BNI compounds on methanotrophic activity, *M. trichosporium* strain OB3b was incubated with varying concentrations of 1,9-D (0.29–5.74 mM), MHPP (0.28–2.78 mM), and LA (5.7–57.1 µM), and Michaelis–Menten parameters were determined. For all three compounds, both the maximum CH_4 oxidation rate (V_{max}) and the substrate affinity constant (K_m) decreased with increasing inhibitor concentration, consistent with an uncompetitive mode of inhibition (**Fig. 15a and b**). In contrast, LA exhibited measurable inhibition at micromolar concentrations **(Fig. 15c).** indicating that LA interacts with OB3b at substantially lower concentrations than 1,9-decanediol or MHPP. At its aqueous solubility limit

(5.7 µM), LA reduced CH_4 oxidation by ~20%. As prior studies in *N. europaea* reported ~80% inhibition at 55 µM—above the aqueous solubility threshold tested here—(Subbarao et al., 2008) we additionally tested LA at 57.1 µM (nominal concentration exceeding aqueous solubility) for comparison. Under these conditions, inhibition increased to ~42%, but did not reach 50%, precluding reliable IC_{50} estimation. These data indicate that LA displays higher apparent potency but limited maximal inhibition under the experimental conditions tested. These results suggest that LA can inhibit CH_4 oxidation more strongly at artificially elevated concentrations, but under physiologically relevant conditions its overall inhibitory capacity remains limited compared with 1,9-D and MHPP.

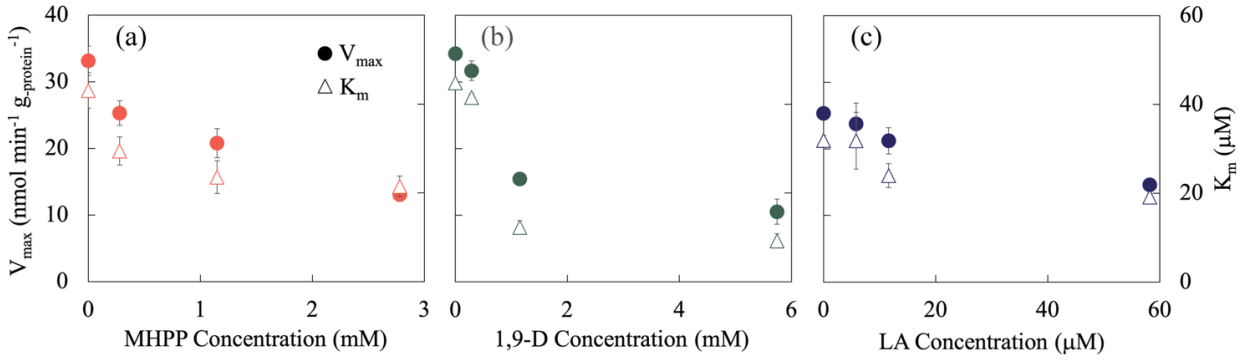

Figure 15. Effects of individual BNI compounds on methane oxidation kinetics. Increasing concentrations of each compound resulted in concurrent decreases in V_{max} and K_m, consistent with an uncompetitive-like inhibition pattern.

4.2.3.3 Type I methanotroph BG8 exhibits enhanced sensitivity to BNIs

Because metagenomic analysis of the soil bioreactors indicated that Type I methanotrophs were disproportionately reduced under *Brachiaria* incubation, inhibition assays were performed with *Methylomicrobium album* BG8, a representative Type I methanotroph, to determine whether this lineage-level pattern could be reproduced in pure culture. Across all compounds tested, BG8 was more sensitive to BNIs than *M. trichosporium* OB3b. The IC_{50} for MHPP was lower in BG8 (432 µM) than in OB3b (730 µM). Similarly, the IC_{50} for 1,9-D was lower in BG8 (391 µM) than in

OB3b (1076 µM). For LA, the IC_{40} was also lower in BG8 (14 µM) than in OB3b (53 µM). Although these results are based on representative strains, this pattern is consistent with the preferential reduction of Type I taxa observed in soil metagenomes under *Brachiaria* incubation. (**Fig. 16**).

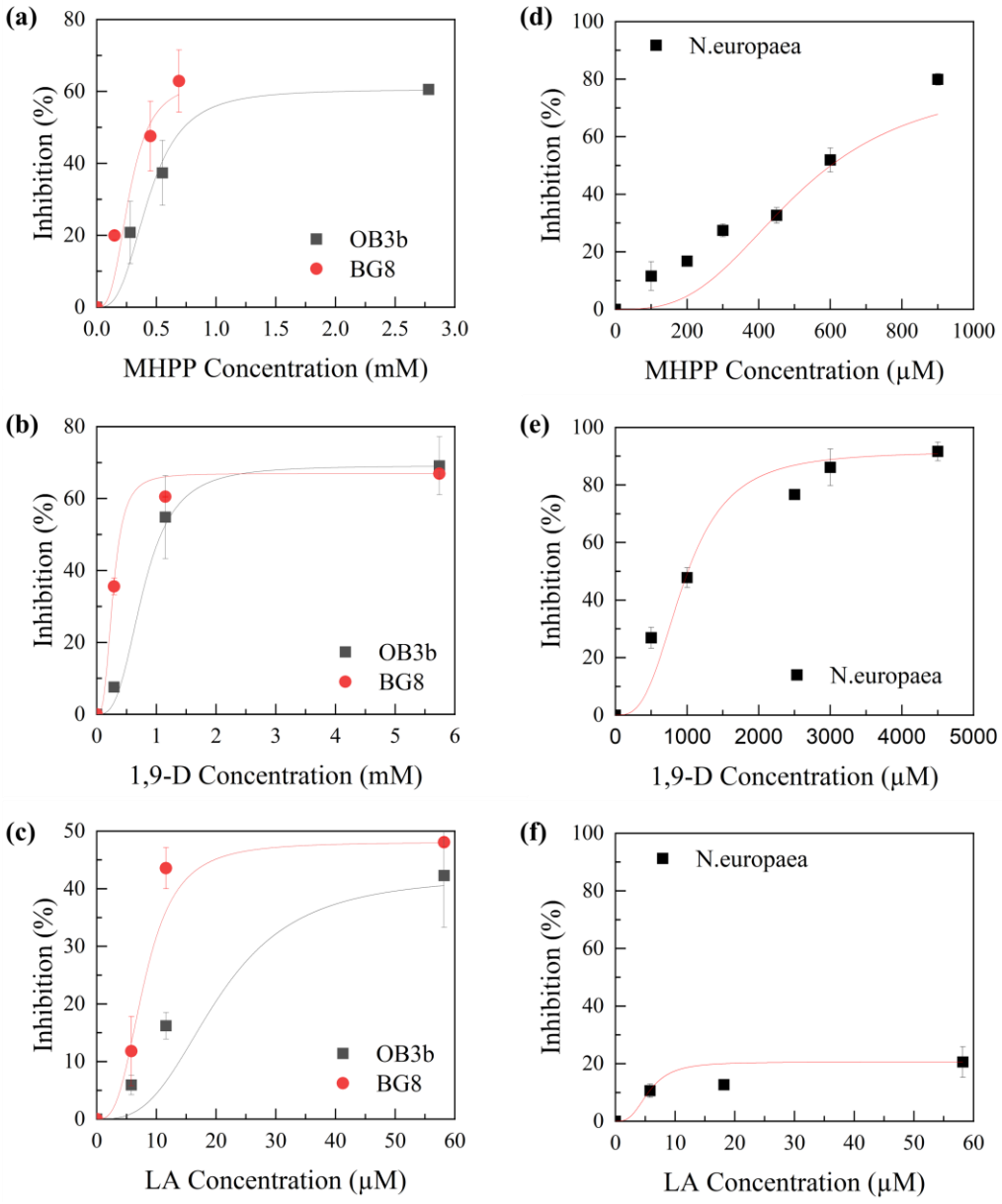

Figure 16. Kinetic analyses comparing the V_{max} inhibition in three different BNI compounds in *M. trichosporium* OB3b, *M. album* BG8, and *N. europaea.* (a) *M. trichosporium* OB3b and *M. album* BG8 of V_{max} inhibition for various concentrations of MHPP. (b) *M. trichosporium* OB3b and *M. album* BG8 of V_{max} inhibition for various concentrations of 1,9-D. (c) *M. trichosporium* OB3b and *M. album* BG8 of V_{max} inhibition for various concentrations of LA. (d) *N.europaea*

V_{max} inhibition for various concentrations of MHPP. (e) *N.europaea* V_{max} inhibition for various concentrations of 1,9-D. (f) *N.europaea* V_{max} inhibition for various concentrations of LA.

4.2.3.4 BNI is largely pMMO-specific with compound-dependent nonspecific effects

To determine enzyme specificity, strain OB3b was assayed under copper-limited conditions that repress pMMO and induce sMMO. While IC_{50} concentrations were estimated under copper replete conditions, inhibition was markedly alleviated under copper limitation, resulting in only 12-20% residual inhibition for MHPP and LA. In contrast, 1,9-D exhibited the highest residual values, reaching up to 38%, suggesting a partial inhibitory effect independent of pMMO (**Fig.17**).

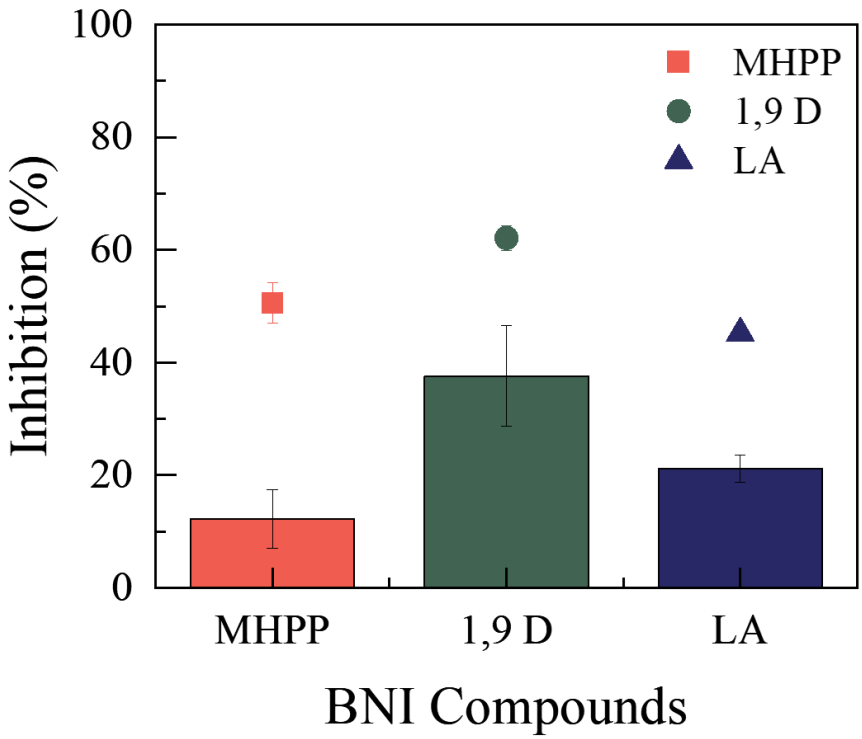

Figure 17. *M. trichosporium* OB3b inhibition analysis under copper-limited conditions with IC50 concentrations for BNIs compounds. Dotted line is inhibition ratio of same concentration of each BNI compounds for *M.trichosporium* OB3b with copper.

4.2.3.5 Reversibility of BNI-mediated inhibition

To determine whether BNI-mediated inhibition was reversible or indicative of irreversible enzyme inactivation, OB3b cultures were incubated with each compound at their respective IC_{50} concentrations and to LA at its IC_{40} concentration, followed by removal of the compounds through washing and resuspension in fresh inhibitor-free medium prior to kinetic analysis. Following washout, methane oxidation activity recovered to 85–95% of untreated controls across treatments. (**Fig. 18**). These results indicate that BNI-mediated inhibition is reversible under the conditions tested and does not reflect suicidal inactivation of methane monooxygenase.

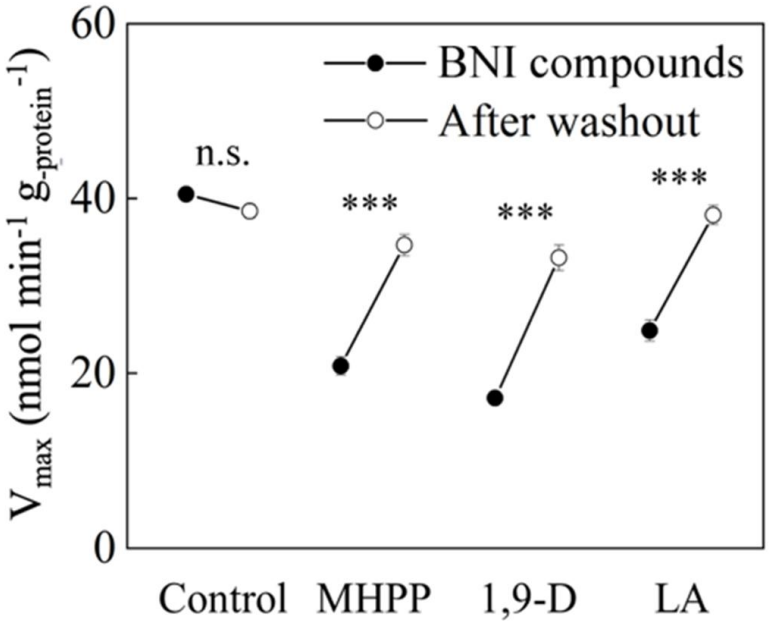

Figure 18. Reversibility of inhibition by BNI compounds following inhibitor removal. Methane oxidation activity recovered substantially after washout of each BNI compound, indicating that inhibition was reversible. Control samples showed no significant change following washout, whereas BNI-treated samples exhibited significant recovery of activity (paired two-tailed t-test, n = 3; *** $P < 0.001$; ns, not significant). Data are shown as V_{max} values. Error bars indicate s.d. and are shown where visible; in some cases they are smaller than the symbols.

4.2.3.6 Molecular docking and dynamics simulations

To investigate the structural basis of the pMMO-associated inhibition observed in the methanotroph assays, molecular docking was performed using a homology model of *M. trichosporium* OB3b pMMO (**Fig. 19a**) with three representative BNI compounds: MHPP, 1,9-

D, and LA. Across docking simulations, the highest-affinity poses were consistently located within the PmoB-PmoC interfacial pocket (**Fig. 19b and 19c**). Predicted binding energies for these compounds ranged from −4.6 to −6.1 kcal mol^{-1} (**Fig. 19d**).

To test whether this predicted binding site reflects a broader structural feature of hydrophobic inhibitors, two structural analogues of 1,9-D—dodecanoic acid and 1-decanol—were subsequently examined. Docking simulations predicted that both analogues bind within the same PmoB–PmoC interfacial pocket. Consistent with this prediction, both compounds inhibited CH_4 oxidation in *M. trichosporium* OB3b (IC_{50} values of 909 μM and 1290 μM for dodecanoic acid and 1-decanol, respectively). These results support the predicted interaction of hydrophobic inhibitors with the PmoB–PmoC interfacial pocket. Notably, all five chemically distinct compounds converged on the same PmoB–PmoC interfacial pocket in docking simulations.

When the two structural analogues were included, predicted binding energy across all five compounds was strongly associated with experimentally determined IC_{50} values (**Fig. 19e**), indicating that both the native BNIs and their structural analogues follow the same structure–activity relationship. Binding energy exhibited a perfect monotonic relationship with IC_{50} (Spearman's $\rho = 1.00$, two-tailed $p = 0.017$) and a strong linear correlation between binding energy and IC_{50} (Pearson's $r = 0.97$, $p = 0.006$). Although docking energies provide relative estimates rather than direct measures of binding affinity, the observed correlation supports the functional relevance of the PmoB–PmoC interfacial pocket as a plausible interaction site for BNI compounds.

The identified interfacial pocket lies adjacent to a channel-like cavity extending toward the Cu_C/Cu_D region of the PmoC subunit, proposed to harbor the catalytic copper center of pMMO,(Koo et al., 2022; Tucci et al., 2023) and is also located near the Cu_B site (**Fig. 19c**).

Ligand binding at this site may influence molecular flux through this channel, for example by affecting substrate access or product egress, without directly occupying the catalytic center. This spatial arrangement is consistent with the inhibition pattern observed in the kinetic assays.

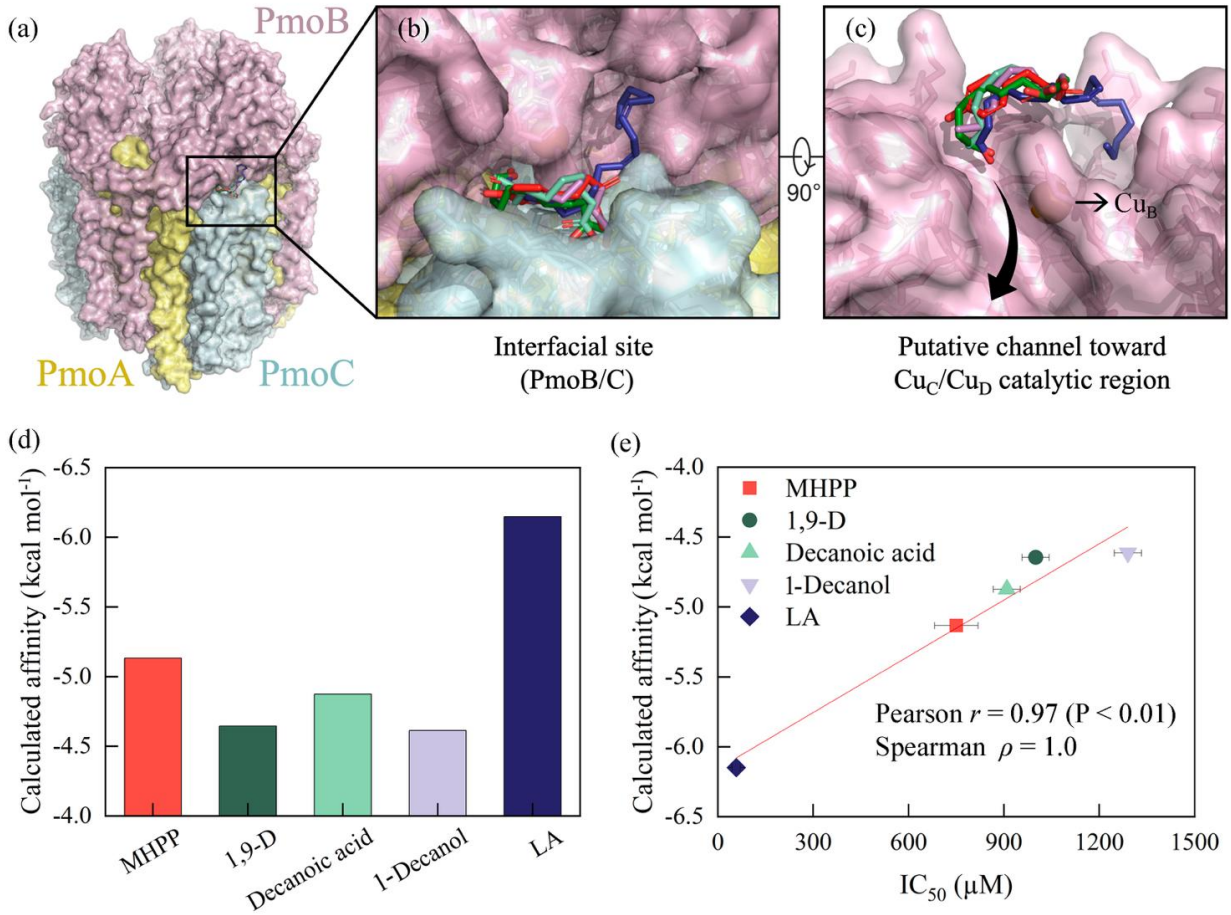

Figure 19. Molecular docking identifies a putative BNI-binding site in pMMO and links binding affinity to inhibitory potency. (a) Predicted homology model of pMMO showing the location of a putative binding site at the PmoB–PmoC interface.

(b) Close-up view of docked poses for MHPP (red), 1,9-D (dark green), decanoic acid (light green), 1-decanol (light purple), and LA (navy blue) within the interfacial pocket.

(c) Rotated view of the same pocket, showing its position near a putative channel toward the CuC/CuD catalytic region and in proximity to the CuB site.

(d) Calculated binding affinities of the docked compounds.

(e) Relationship between calculated binding affinity (kcal mol-1) and inhibitory potency (IC50, except LA where IC_{40} is shown). Stronger binding was associated with lower IC50 values.

Colors are consistent across panels.

4.2.3.7 Mechanistic insights from RNA-Seq analysis

To further examine how methanotroph cells respond to BNI exposure at the transcriptional level, RNA-seq analysis was performed. Principal component analysis revealed clear separation of MHPP-treated samples from controls, whereas 1,9-D induced broader dispersion consistent with widespread transcriptional perturbation. LA-treated samples showed a more moderate shift in global transcriptomic space (**Fig. 20a**). Differential expression analysis further highlighted these differences (**Fig. 20b-d**). 1,9-D triggered the broadest response, affecting a large number of genes with moderate fold changes across diverse functional categories, including stress responses, transporters, and membrane-associated processes. MHPP induced a more structured transcriptional shift, with coordinated changes in specific metabolic pathways. In contrast, LA elicited fewer differentially expressed genes but produced high-amplitude and high-significance expression changes in a subset of loci. These patterns were further resolved at the gene level (**Fig. 20e**), where LA induced pronounced upregulation of *nuoL* and *dksA* and strong downregulation of *pmoA* and *kdp* operon genes, consistent with a selective but high-impact transcriptional response. Cultures were exposed to MHPP and 1,9-D at their estimated IC_{50} concentrations and to LA at its IC_{40} concentration. Under these conditions, methane oxidation was inhibited by 48.5%, 58.6%, and 38.6% for MHPP, 1,9-D, and LA, respectively. Taken together, these results indicate that BNIs induce fundamentally distinct transcriptional programs in methanotrophs: 1,9-D acting as a broad stressor, MHPP producing a structured metabolic shift, and LA eliciting a selective but high-amplitude response.

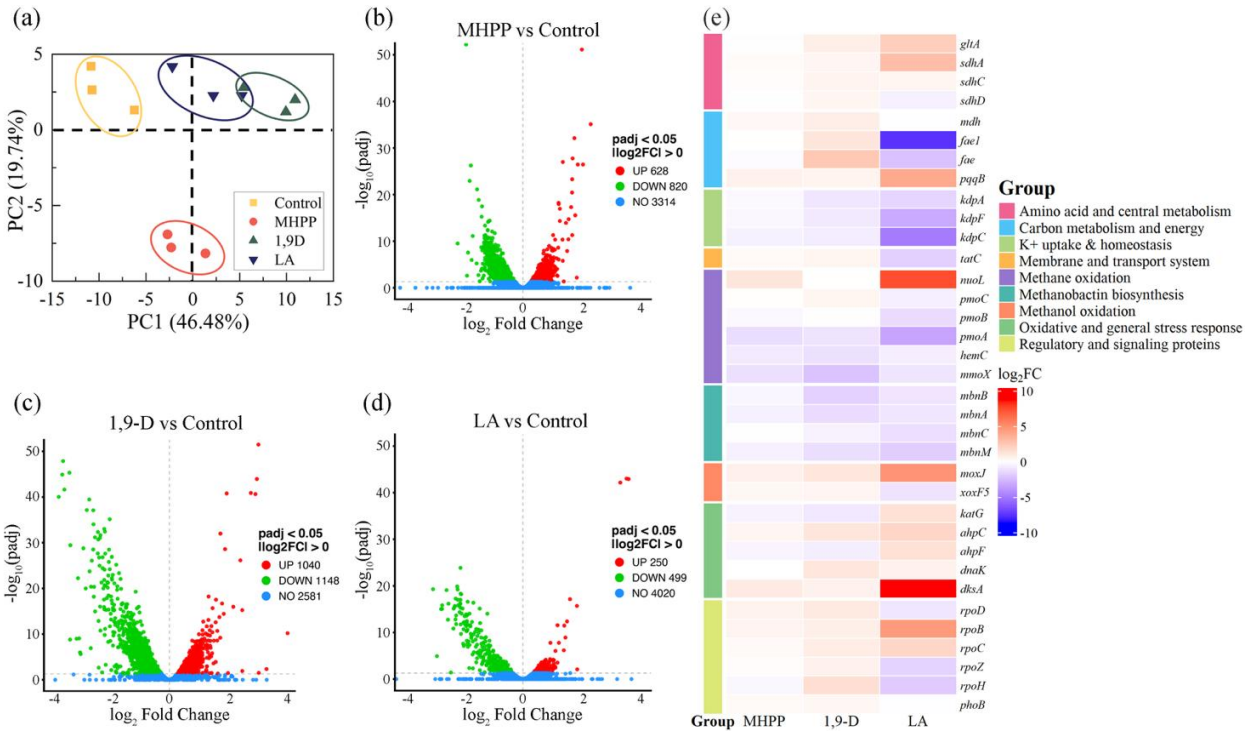

Figure 20. Compound-specific transcriptomic responses of Methylosinus trichosporium OB3b to BNI exposure.

(a) Principal component analysis (PCA) showing global transcriptomic differences among treatments.

(b–d) Volcano plots showing differential gene expression relative to control (adjusted $P < 0.05$).

(e) Heatmap of selected genes involved in methane oxidation, central metabolism, transport, and stress response. Notable responses include upregulation of nuoL and dksA and downregulation of pmoA and kdp operon genes under LA treatment. Cultures were exposed to MHPP and 1,9-D at their estimated IC50 concentrations and to LA at its IC40 concentration, corresponding to 47.5%, 58.6%, and 38.6% inhibition of methane oxidation, respectively.

4.2.3.6 Comparative sensitivity of ammonia-oxidizing and CH_4-oxidizing bacteria

To directly compare the inhibitory effects of BNIs on ammonia-oxidizing bacteria and methanotrophs, parallel inhibition assays were performed with *N. europaea*, a model ammonia-oxidizing bacteria, using the same three BNI compounds evaluated with methanotrophs: MHPP, 1,9-D, and LA. Because inhibitory responses depend on the ratio of inhibitor concentration to microbial biomass (Udekwu et al., 2009; X. Wang et al., 2023), inhibitory potency was normalized to cell abundance (16S rRNA copy number corrected) prior to comparison. In these

assays, *N. europaea* cultures were tested at $OD_{600} \approx 0.1$, whereas methanotrophs assays were performed at higher biomass ($OD_{600} \approx 0.3$). For MHPP and 1,9-D, inhibitory potency was expressed as the negative $\log_{10}$ of the cell-normalized IC_{50} values ($-\log_{10} IC_{50}$) to facilitate comparison across orders of magnitude. Under this normalization, both methanotrophic strains were markedly more sensitive than N. europaea, indicating that BNIs inhibit CH_4 oxidation at lower per-cell exposure levels than those required to suppress nitrification. For LA, inhibition did not reach 50% in either ammonia-oxidizing bacteria or methanotrophs assays, precluding IC_{50} estimation. In *N. europaea*, inhibition reached its maximum (~13%) at 57.1 μM, corresponding to a biomass-normalized exposure of 3.6×10^{-8} μM $cell^{-1}$. Achieving the same normalized exposure in methanotrophs assays as in the *N. europaea* experiment would require substantially higher LA concentrations, estimated at approximately 734 μM for OB3b and 985 μM for BG8. However, inhibition in both methanotrophic strains had already reached a plateau within the tested concentration range (approximately 42% for OB3b and 48% for BG8), with maximal suppression observed at ~57.1 μM. Thus, even at normalized exposures far below those required to match the ammonia-oxidizing bacteria assay, methanotrophs exhibited markedly stronger inhibition than *N. europaea*. Together, these results suggest that BNIs may suppress methanotrophic activity to a similar or greater extent than nitrification.

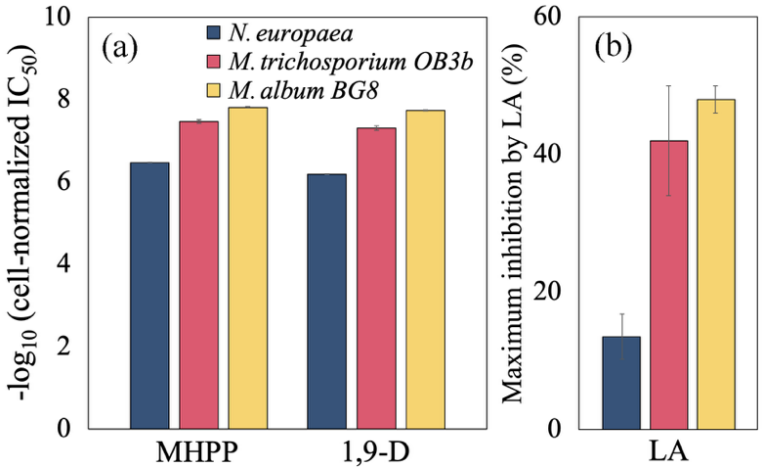

Figure 21. Comparative sensitivity of ammonia- and methane-oxidizing bacteria to BNI compounds.

(a) Cell-normalized inhibitory potency of MHPP and 1,9-D toward Nitrosomonas europaea, Methylosinus trichosporium OB3b, and Methylomicrobium album BG8. Inhibitory potency is expressed as −log10(IC50) of the cell-normalized values (M cell-1). Error bars represent propagated standard deviations following log transformation of IC50 values.

(b) Maximum inhibition by LA observed within the tested concentration range. Error bars represent standard deviations of triplicate measurements.

4.2.4 Discussion

This study reveals that BNIs, naturally released by plants, not only suppress ammonia oxidation but also curtail CH_4 oxidation by MOB. By integrating evidence from soil bioreactors, metagenomic profiling, pure-culture kinetics, and molecular docking, we show that BNIs can substantially reduce the microbial capacity for CH_4 oxidation in soil systems. These findings uncover a previously unrecognized ecological tradeoff (Florio et al., 2021; Peters et al., 2013; Subbarao, Rao, et al., 2013; Zhang et al., 2023),: while BNIs limit nitrification and thereby lower N_2O emissions, they may simultaneously diminish CH_4 consumption. Because nitrification and methanotrophy are central microbial processes linking the global nitrogen and carbon cycles, the dual action of BNIs has consequences that extend beyond local soil environments. Our comparative assays extend this tradeoff beyond nitrification. Although BNIs were originally characterized as inhibitors of AMO in AOB, we found that MOB were equally or more sensitive

on a per-cell basis (**Fig. 21**). In particular, LA, which was constrained by solubility and produced only weak inhibition in *N. europaea* (~15%), substantially suppressed CH_4 oxidation in MOB (40–50%). These findings highlight that BNIs can simultaneously constrain both nitrogen and carbon transformations, amplifying their potential to reshape coupled C–N cycling and GHG fluxes.

Building on these observations, we next examined the mechanistic basis of inhibition. Kinetic assays with *M. trichosporium* strain OB3b revealed an uncompetitive mode of inhibition with simultaneous decreases in V_{max} and K_m (Fig. 15). Molecular docking supported this pattern, identifying a hydrophobic region near the entrance of the pMMO active site where multiple BNIs localized, consistent with peripheral binding rather than direct competition with CH_4. This aligns with recent structural work revealing a hydrophobic cavity adjacent to the *PmoC* copper site in active pMMO (Koo et al., 2022) and with prior observations that hydrophobic cavities between *PmoC* and *PmoB* may guide substrate to the pMMO active site (Ross & Rosenzweig, 2017). Analog experiments confirmed that hydrophobic chain interactions were the primary determinant of binding, with terminal functional groups playing a minor role. Importantly, predicted binding affinities correlated strongly with experimentally determined IC_{50} values across all compounds tested (**Fig. 19**), providing evidence for a structure–activity relationship in which hydrophobicity and binding strength govern inhibitory potency. However, compound-specific differences were also apparent: MHPP acted in a primarily pMMO-specific manner, 1,9-D exhibited additional nonspecific inhibition (residual inhibition under sMMO conditions, reduced E. coli growth, and weaker predicted binding affinity), and LA showed limited maximal inhibition. It should be noted that 1,9-D was previously reported to affect AMO only (Sun et al., 2016b), underscoring that its broader inhibitory effects in MOB diverge from earlier findings. In addition, peripheral

binding near the pMMO active-site entrance is consistent with scenarios such as perturbation of access/egress channels or allosteric effects on catalytic cycling, both of which could explain the observed uncompetitive kinetics, as has been reported in other systems where product release is slowed. (Kokkonen et al., 2021).

Our choice of MHPP, 1,9-D, and LA was motivated by prior studies with *N. europaea*, where MHPP and 1,9-D were identified as AMO (Sun et al., 2016b; Zakir et al., 2008b), whereas LA inhibited both AMO and HAO (Subbarao et al., 2008). In those studies, LA was tested at concentrations far exceeding its aqueous solubility (1.6 mg L^{-1}, ~5.7 μM), with in vitro assays conducted up to 16 mg L^{-1} (~57.1 μM) and reported IC_{80} values at this level (Subbarao et al., 2008). By contrast, in our experiments with MOB (OB3b, BG8), inhibition by LA plateaued at its solubility limit, with no further suppression at higher tested concentrations. While LA reduced CH_4 oxidation only up to ~40% (**Fig. 16**), the calculated IC_{40} was the lowest among the three BNIs tested, indicating strong inhibitory potency at low concentrations despite limited maximal inhibition. This contrasts with MHPP and 1,9-D, which exhibited more classical dose–response curves consistent with pMMO-specific inhibition. (**Fig. 16**) Transcriptomic profiles further reinforced these distinctions, with 1,9-D eliciting broad stress-associated responses, MHPP producing a more targeted shift consistent with pMMO inhibition, and LA causing comparatively modest transcriptional changes, in line with its limited maximal inhibition. Taken together with prior findings in ammonia oxidizers, our results demonstrate that BNIs represent a chemically diverse class of inhibitors, each with distinct inhibition profiles and ecological implications.

Moving beyond individual compounds, we next evaluated the ecological consequences of BNI release. These were evident in our soil bioreactor experiments, where CH_4 oxidation was

suppressed in the presence of *Brachiaria* and metagenomic analysis revealed a disproportionate decline in Type I MOB. This lineage-level effect was further supported by pure culture assays: M. album BG8 (Type I) exhibited greater sensitivity to MHPP, 1,9-D and LA than the Type II strain OB3b (**Fig. 16**), Type I organisms being more vulnerable in some cases. Because Type I and Type II MOB occupy distinct ecological niches—Type I often dominating in nitrogen-rich soils and Type II in nitrogen-limited environments(Hanson & Hanson, 1996; Knief, 2015b)—such selective inhibition could shift methanotroph community structure in BNI-affected systems. One possible factor contributing to this pattern is the auxiliary CH_4 oxidation capacity of Type II MOB, many of which can express the sMMO under copper limitation (Liebner & Svenning, 2013; Semrau et al., 2010). Although convincing evidence for sMMO expression in terrestrial environments is still lacking, it has been suggested that its apparent rarity may reflect primer bias and methodological constraints in detecting *mmoX* (Semrau et al., 2010). Thus, while the ecological role of sMMO remains uncertain, the potential for its conditional expression raises the possibility that Type II MOB may, under some circumstances, be less sensitive to BNIs than Type I.

Having established the effects of BNIs at the cellular and community levels, it is important to consider their broader implications for the global CH_4 cycle, particularly given the widespread occurrence of BNI across the plant kingdom, ranging from agricultural crops (Coskun et al., 2017; Nardi et al., 2020) to forest trees(Andrianarisoa et al., 2010; Laffite et al., 2020). Wetlands, the largest natural source of atmospheric CH_4, and rice paddies, the largest anthropogenic source, both rely on methanotrophy in surface soils and rhizospheres as a key sink that attenuates gross CH_4 production (Conrad, 2009; Saunois et al., 2020). Our findings raise the possibility that BNIs released from plants may interfere with this sink function, thereby

modulating net CH_4 fluxes in these ecosystems. In wetlands, BNI exudation by native vegetation could influence not only nitrification and other processes in the nitrogen cycle but also methanotrophy, thereby modulating the balance of GHG fluxes. Accordingly, global and regional CH_4 models should represent BNI-driven constraints on methanotrophy in wetlands and flooded ecosystems to more accurately capture net fluxes. In rice paddies, the relevance is more direct, as rice itself produces BNI compounds such as 1,9-D (Sun et al., 2016b). Thus, BNI-based breeding programs aimed at enhancing NUE and reducing N_2O emissions should also evaluate their impacts on CH_4 uptake, ensuring that progress in nitrogen management does not come at the expense of CH_4 sink strength. Together, these considerations highlight the need to integrate BNI effects into our understanding of CH_4–climate feedbacks.

Several limitations of this study also point toward promising avenues for future research. The bioreactor and pure-culture experiments, although mechanistically informative, may not fully capture the complexity of plant–soil–microbe interactions in natural environments, where fluctuating oxygen availability, soil redox dynamics, microbial competition, and spatial heterogeneity in root exudation could all influence the magnitude of BNI effects. While our molecular docking analyses support the kinetic results, they rely on predicted structures and simplified binding assumptions, and experimental structural confirmation of BNI-enzyme interactions will be an important next step. Moving forward, extending these findings to field-scale systems will be essential, combining CH_4 flux measurements with high-resolution microbial and transcriptomic analyses in BNI-rich environments such as rice paddies and wetlands. Incorporating BNI effects into process-based and Earth-system models will also be critical for evaluating their contribution to the global CH_4 budget. As BNI-based strategies continue to be developed for improving nitrogen-use efficiency and reducing N_2O emissions,

interdisciplinary studies linking agronomy, microbiology, and climate science offer a promising path to ensure that their broader impacts on GHG dynamics are fully understood.

Chapter 5 - Conclusion

Agricultural activities are the predominant source, responsible for over two-thirds of global anthropogenic N_2O emissions and one-third of total CH_4 emissions. And these systems are mostly controlled by microbial processes. To make a comprehensive understanding and control of both GHGs, we performed two different studies: 1) Building on the recognition of unquantified N_2O emissions from forages and control, 2) Impact of BNI on methanotrophs. Based on the mini-silo experiment and the Crop Production 2022 Summary of the United States Department of Agriculture National Agricultural Statistics Service, the total N_2O emission potential amounts to 5.3 MMT CO_2 eq. Mechanistic tests showed no evidence for a nitrification contribution (no effect of O_2 pulses or low-dose acetylene; no *amoA* transcripts) and instead identified denitrification as the dominant pathway: chlorate suppressed *narG* expression and cut N_2O by up to 99%, with effective mitigation even at 0.01% (w/w) and further improvement when paired with a modest external carbon source (acetate) to raise C/N. These results highlight a practical, cost-effective mitigation lever—judicious chlorate dosing (order-of-cents per ton DW) with carbon balancing—that can deliver large abatement relative to silage inoculant costs and yield substantial social-cost savings at scale. While extrapolation uncertainties remain (climate, storage type, management heterogeneity), the core findings are actionable: (i) incorporate forage-related N_2O into national inventories to close a major accounting gap; (ii) Lab-scale interventions that combine chlorate-based denitrification control with C/N management; and (iii) refine process attribution with expanded multi-omics and flux measurements across real silage systems. Measuring what matters enables management—quantifying this neglected source and demonstrating feasible controls provides an immediate pathway to meaningful N_2O reductions from a ubiquitous agricultural practice.

Second, this study also shows that plant-derived BNIs can unintentionally suppress CH_4 oxidation, revealing a key tradeoff in coupled N-C cycling: while BNIs curb nitrification and N_2O, they also diminish soil CH_4 sink strength. Across soil columns*, Brachiaria* reduced CH_4 consumption and selectively depleted more on Type I methanotrophs, a lineage-level pattern recapitulated in pure culture where *M. album* BG8 (Type I) was more sensitive than *M. trichosporium* OB3b (Type II). Kinetic assays and docking converge on an uncompetitive inhibition, pMMO-proximal mechanism in which diverse BNIs bind a hydrophobic pocket near the active-site entrance; MHPP acts largely pMMO-specifically, 1,9-D exhibits additional nonspecific cytotoxicity, and LA shows strong low-dose potency but limited maximal inhibition due to solubility. Comparative tests indicate methanotrophs are at least as sensitive per cell as ammonia oxidizers, implying BNIs can constrain both nitrification and methanotrophy. Together, these findings highlight that BNI-based agronomic strategies promising for nitrogen-use efficiency—must also account for potential weakening of the CH_4 sink, particularly in wetlands and rice systems, and motivate field-scale validation, structural confirmation of BNI–pMMO interactions, and integration of BNI effects into process and Earth-system models to more accurately predict GHG fluxes.

References

Aldy, J. E., Kotchen, M. J., Stavins, R. N., & Stock, J. H. (2021). Keep climate policy focused on the social cost of carbon. *Science*, *373*(6557), 850–852.

Amann, R. I., Binder, B. J., Olson, R. J., Chisholm, S. W., Devereux, R., & Stahl, D. A. (1990). oligonucleotide probes with flow cytometry for analyzing mixed microbial populations. Combination of 16S rRNA-Targeted Oligonucleotide Probes with Flow Cytometry for Analyzing Mixed Microbial Populations. *Appl Environ Microbiol*, *56*(6), 1919–1925.

Andrianarisoa, K. S., Zeller, B., Poly, F., Siegenfuhr, H., Bienaimé, S., Ranger, J., & Dambrine, E. (2010). Control of Nitrification by Tree Species in a Common-Garden Experiment. *Ecosystems*, *13*(8), 1171–1187. https://doi.org/10.1007/s10021-010-9390-x

Antony, C. P., Kumaresan, D., Ferrando, L., Boden, R., Moussard, H., Scavino, A. F., Shouche, Y. S., & Murrell, J. C. (2010). Active methylotrophs in the sediments of Lonar Lake, a saline and alkaline ecosystem formed by meteor impact. *ISME Journal*, *4*(11), 1470–1480. https://doi.org/10.1038/ismej.2010.70

Arp, D. J., Chain, P. S. G., & Klotz, M. G. (2007). The impact of genome analyses on our understanding of ammonia-oxidizing bacteria. In *Annual Review of Microbiology* (Vol. 61, pp. 503–528). https://doi.org/10.1146/annurev.micro.61.080706.093449

Ávila, C. L. S., & Carvalho, B. F. (2020). Silage fermentation—updates focusing on the performance of micro-organisms. In *Journal of Applied Microbiology* (Vol. 128, Issue 4, pp. 966–984). John Wiley and Sons Inc. https://doi.org/10.1111/jam.14450

Barnard, R., Leadley, P. W., & Hungate, B. A. (2005). Global change, nitrification, and denitrification: A review. In *Global Biogeochemical Cycles* (Vol. 19, Issue 1, pp. 1–13). American Geophysical Union. https://doi.org/10.1029/2004GB002282

Barnes, R. F., Nelson, C. J., Collins, M., & Moore, K. J. (2003). *Forages, An Introduction to Grassland Agriculture* (6th ed.). Wiley.

Bédard, C., & Knowles, R. (1989). Physiology, biochemistry, and specific inhibitors of CH_4, NH_4^+, and CO oxidation by methanotrophs and nitrifiers. *Microbiological Reviews*, *53*(1), 68–84. https://doi.org/10.1128/mr.53.1.68-84.1989

Berg, P. E. R., Klemedtsson, L., & Rosswall, T. (1982). Inhibitory effect of low partial pressures of acetylene on nitrification. *Soil Biology and Biochemistry*, *14*(3), 301–303.

Braker, G., Fesefeldt, A., & Witzel, K.-P. (1998). Development of PCR primer systems for amplification of nitrite reductase genes (*nirK* and *nirS*) to detect denitrifying bacteria in environmental samples. *Applied and Environmental Microbiology*, *64*(10), 3769–3775.

Braker, G., & Tiedje, J. M. (2003). Nitric oxide reductase (*norB*) genes from pure cultures and environmental samples. *Applied and Environmental Microbiology*, *69*(6), 3476–3483. https://doi.org/10.1128/AEM.69.6.3476-3483.2003

Brooks, B. R., Brooks, C. L., Mackerell, A. D., Nilsson, L., Petrella, R. J., Roux, B., Won, Y., Archontis, G., Bartels, C., Boresch, S., Caflisch, A., Caves, L., Cui, Q., Dinner, A. R., Feig, M., Fischer, S., Gao, J., Hodoscek, M., Im, W., … Karplus, M. (2009). CHARMM: The biomolecular simulation program. *Journal of Computational Chemistry*, *30*(10), 1545–1614. https://doi.org/10.1002/jcc.21287

Bru, D., Sarr, A., & Philippot, L. (2007). Relative abundances of proteobacterial membrane-bound and periplasmic nitrate reductases in selected environments. *Applied and*

Environmental Microbiology, *73*(18), 5971–5974. https://doi.org/10.1128/AEM.00643-07

Bueno, A. V. I., Vigne, G. L. D., Novinski, C. O., Bayer, C., Jobim, C. C., & Schmidt, P. (2020a). Natamycin as a potential silage additive: A lab trial using sugarcane to assess greenhouse gas emissions. *Revista Brasileira de Zootecnia*, *49*(2012). https://doi.org/10.37496/RBZ4920200017

Bueno, A. V. I., Vigne, G. L. D., Novinski, C. O., Bayer, C., Jobim, C. C., & Schmidt, P. (2020b). Natamycin as a potential silage additive: A lab trial using sugarcane to assess greenhouse gas emissions. *Revista Brasileira de Zootecnia*, *49*. https://doi.org/10.37496/RBZ4920200017

Butterbach-Bahl, K., Baggs, E. M., Dannenmann, M., Kiese, R., & Zechmeister-Boltenstern, S. (2013a). Nitrous oxide emissions from soils: How well do we understand the processes and their controls? *Philosophical Transactions of the Royal Society B: Biological Sciences*, *368*(1621). https://doi.org/10.1098/rstb.2013.0122

Butterbach-Bahl, K., Baggs, E. M., Dannenmann, M., Kiese, R., & Zechmeister-Boltenstern, S. (2013b). Nitrous oxide emissions from soils: How well do we understand the processes and their controls? In *Philosophical Transactions of the Royal Society B: Biological Sciences* (Vol. 368, Issue 1621). https://doi.org/10.1098/rstb.2013.0122

Byrnes, R. C., Nùñez, J., Arenas, L., Rao, I., Trujillo, C., Alvarez, C., Arango, J., Rasche, F., & Chirinda, N. (2017). Biological nitrification inhibition by *Brachiaria* grasses mitigates soil nitrous oxide emissions from bovine urine patches. *Soil Biology and Biochemistry*, *107*, 156–163. https://doi.org/10.1016/j.soilbio.2016.12.029

Callaway, T. R., Anderson, R. C., Genovese, K. J., Poole, T. L., Anderson, T. J., Byrd, J. A., Kubena, L. F., & Nisbet, D. J. (2002). Sodium chlorate supplementation reduces *E. coli* O157:H7 populations in cattle 1. In *J. Anim. Sci* (Vol. 80). https://academic.oup.com/jas/article/80/6/1683/4789577

Calvo Buendia, E., Tanabe, K., Kranjc, A., Baasansuren, J., Fukuda, M., Ngarize, S., Osako, A., Pyrozhenko, Y., Shermanau, P., & Federici, S. (2019). *2019 Refinement to the 2006 IPCC Guidelines for National Greenhouse Gas Inventories*.

Cassman, K. G., Dobermann, A., & Walters, D. T. (2002). Agroecosystems, Nitrogen-use Efficiency, and Nitrogen Management. *AMBIO: A Journal of the Human Environment*, *31*(2), 132–140. https://doi.org/10.1579/0044-7447-31.2.132

Chee-Sanford, J. C., Connor, L., Krichels, A., Yang, W. H., & Sanford, R. A. (2020). Hierarchical detection of diverse Clade II (atypical) *nosZ* genes using new primer sets for classical- and multiplex PCR array applications. *Journal of Microbiological Methods*, *172*. https://doi.org/10.1016/j.mimet.2020.105908

Choi, D. W., Kunz, R. C., Boyd, E. S., Semrau, J. D., Antholine, W. E., Han, J. I., Zahn, J. A., Boyd, J. M., De la Mora, A. M., & DiSpirito, A. A. (2003). The membrane-associated methane monooxygenase (pMMO) and pMMO-NADH:Quinone oxidoreductase complex from Methylococcus capsulatus bath. *Journal of Bacteriology*, *185*(19), 5755–5764. https://doi.org/10.1128/JB.185.19.5755-5764.2003

Chuan Wang, L., & Burris, R. H. (n.d.). *TOXIC GASES IN SILAGE Mass Spectrometric Study of Nitrogenous Gases Produced by Silage The time course of production of nitrogenous gases from laboratory-scale and full-scale*. https://pubs.acs.org/sharingguidelines

Colin Murrell, J., & Jetten, M. S. M. (2009). The microbial methane cycle. In *Environmental Microbiology Reports* (Vol. 1, Issue 5, pp. 279–284). https://doi.org/10.1111/j.1758-2229.2009.00089.x

Collins, M., & Owens, V. N. (2003). *Preservation of forage as hay and silage. U: Barnes RF, Nelson CJ, Collins M., Moore KJ (eds). Forages: an introduction to grassland agriculture*. Iowa State Press, Ames.

Conrad, R. (2009). The global methane cycle: Recent advances in understanding the microbial processes involved. *Environmental Microbiology Reports*, *1*(5), 285–292. https://doi.org/10.1111/j.1758-2229.2009.00038.x

Conrad, R., Klose, M., Claus, P., & Enrich-Prast, A. (n.d.). *Methanogenic pathway, 13 C isotope fractionation, and archaeal community composition in the sediment of two clear-water lakes of Amazonia*.

Contreras-Govea, F. E., Muck, R. E., Mertens, D. R., & Weimer, P. J. (2011). Microbial inoculant effects on silage and in vitro ruminal fermentation, and microbial biomass estimation for alfalfa, bmr corn, and corn silages. *Animal Feed Science and Technology*, *163*(1), 2–10.

Core Writing Team, P. (2014). Climate change 2014: synthesis report. *Contribution of Working Groups I, II and III to the Fifth Assessment Report of the Intergovernmental Panel on Climate Change*, *151*.

Cornish-Bowden, Athel. (1979). *Fundamentals of enzyme kinetics*. Butterworths.

Coskun, D., Britto, D. T., Shi, W., & Kronzucker, H. J. (2017). Nitrogen transformations in modern agriculture and the role of biological nitrification inhibition. *Nature Plants*, *3*(June), 1–10. https://doi.org/10.1038/nplants.2017.74

Crombie, A. T., & Murrell, J. C. (2014). Trace-gas metabolic versatility of the facultative methanotroph *Methylocella silvestris*. *Nature*, *510*(7503), 148–151. https://doi.org/10.1038/nature13192

Daims, H., Lebedeva, E. v., Pjevac, P., Han, P., Herbold, C., Albertsen, M., Jehmlich, N., Palatinszky, M., Vierheilig, J., Bulaev, A., Kirkegaard, R. H., von Bergen, M., Rattei, T., Bendinger, B., Nielsen, P. H., & Wagner, M. (2015). Complete nitrification by *Nitrospira* bacteria. *Nature*, *528*(7583), 504–509. https://doi.org/10.1038/nature16461

Darby, D. E., & Jofriet, J. C. (1993). Density of silage in horizontal silos. *Canadian Agricultural Engineering*, *35*(4), 275.

Davidson, E. A., & Kanter, D. (2014a). Inventories and scenarios of nitrous oxide emissions. *Environmental Research Letters*, *9*(10). https://doi.org/10.1088/1748-9326/9/10/105012

Davidson, E. A., & Kanter, D. (2014b). Inventories and scenarios of nitrous oxide emissions. *Environmental Research Letters*, *9*(10). https://doi.org/10.1088/1748-9326/9/10/105012

Dedysh, S. N., & Dunfield, P. F. (2011). Facultative and obligate methanotrophs: How to identify and differentiate Them. In *Methods in Enzymology* (Vol. 495, pp. 31–44). Academic Press Inc. https://doi.org/10.1016/B978-0-12-386905-0.00003-6

Denman, K. L., Brasseur USA, G., Ramachandran, S., Leite da Silva Dias, P., Wofsy, S. C., Brasseur, G., Chidthaisong, A., Ciais, P., Cox, P., Dickinson, R., Hauglustaine, D., Heinze, C., Holland, E., Jacob, D., Lohmann, U., Ramachandran, S., da Silva Dias, P., Wofsy, S., Zhang, X., … Averyt, K. (n.d.). *7 Couplings Between Changes in the*

Climate System and Biogeochemistry Coordinating Lead Authors: This chapter should be cited as.
Dent, K. C., Stephen, J. R., & Finch-Savage, W. E. (2004). Molecular profiling of microbial communities associated with seeds of Beta vulgaris subsp. vulgaris (sugar beet). *Journal of Microbiological Methods*, *56*(1), 17–26.
Eberhardt, J., Santos-Martins, D., Tillack, A. F., & Forli, S. (2021). AutoDock Vina 1.2.0: New docking methods, expanded force field, and python bindings. *Journal of Chemical Information and Modeling*, *61*(8), 3891–3898. https://doi.org/10.1021/acs.jcim.1c00203
Fang, X., Pyle, J. A., Chipperfield, M. P., Daniel, J. S., Park, S., & Prinn, R. G. (2019a). Challenges for the recovery of the ozone layer. *Nature Geoscience*, *12*(8), 592–596. https://doi.org/10.1038/s41561-019-0422-7
Fang, X., Pyle, J. A., Chipperfield, M. P., Daniel, J. S., Park, S., & Prinn, R. G. (2019b). Challenges for the recovery of the ozone layer. *Nature Geoscience*, *12*(8), 592–596.
Ferris, M. J., Muyzer, G., & Ward, D. M. (1996). Denaturing gradient gel electrophoresis profiles of 16S rRNA-defined populations inhabiting a hot spring microbial mat community. *Applied and Environmental Microbiology*, *62*(2), 340–346. https://doi.org/10.1128/aem.62.2.340-346.1996
Finch, H. J. S., Samuel, A. M., & Lane, G. P. F. (2014a). Conservation of grass and forage crops. *Lockhart & Wiseman's Crop Husbandry Including Grassland*, 513–526. https://doi.org/10.1533/9781782423928.4.513
Finch, H. J. S., Samuel, A. M., & Lane, G. P. F. (2014b). Conservation of grass and forage crops. *Lockhart & Wiseman's Crop Husbandry Including Grassland*, 513–526. https://doi.org/10.1533/9781782423928.4.513
Francis, C. A., Roberts, K. J., Beman, J. M., Santoro, A. E., & Oakley, B. B. (2005). Ubiquity and diversity of ammonia-oxidizing archaea in water columns and sediments of the ocean. *Proceedings of the National Academy of Sciences of the United States of America*, *102*(41), 14683–14688. https://doi.org/10.1073/pnas.0506625102
Fu, X., Hou, R., Yang, P., Qian, S., Feng, Z., Chen, Z., Wang, F., Yuan, R., Chen, H., & Zhou, B. (2022). Application of external carbon source in heterotrophic denitrification of domestic sewage: A review. *Science of the Total Environment*, *817*, 153061.
Ghatak, A., Chaturvedi, P., Waldherr, S., Subbarao, G. V., & Weckwerth, W. (2023). PANOMICS at the interface of root–soil microbiome and BNI. *Trends in Plant Science*, *28*(1), 106–122. https://doi.org/10.1016/j.tplants.2022.08.016
Gidden, M. J., Gasser, T., Grassi, G., Forsell, N., Janssens, I., Lamb, W. F., Minx, J., Nicholls, Z., Steinhauser, J., & Riahi, K. (2023). Aligning climate scenarios to emissions inventories shifts global benchmarks. *Nature*, *624*(7990), 102–108.
Grossi, G., Goglio, P., Vitali, A., & Williams, A. G. (2019a). Livestock and climate change: Impact of livestock on climate and mitigation strategies. *Animal Frontiers*, *9*(1), 69–76. https://doi.org/10.1093/af/vfy034
Grossi, G., Goglio, P., Vitali, A., & Williams, A. G. (2019b). Livestock and climate change: Impact of livestock on climate and mitigation strategies. *Animal Frontiers*, *9*(1), 69–76. https://doi.org/10.1093/af/vfy034
Hafner, S. D., Howard, C., Muck, R. E., Franco, R. B., Montes, F., Green, P. G., Mitloehner, F., Trabue, S. L., & Rotz, C. A. (2013). Emission of volatile organic

compounds from silage: Compounds, sources, and implications. In *Atmospheric Environment* (Vol. 77, pp. 827–839). https://doi.org/10.1016/j.atmosenv.2013.04.076

Hakemian, A. S., & Rosenzweig, A. C. (2007). The biochemistry of methane oxidation. In *Annual Review of Biochemistry* (Vol. 76, pp. 223–241). https://doi.org/10.1146/annurev.biochem.76.061505.175355

Hall, B. D., Dutton, G. S., & Elkins, J. W. (2007). The NOAA nitrous oxide standard scale for atmospheric observations. *Journal of Geophysical Research Atmospheres*, *112*(9). https://doi.org/10.1029/2006JD007954

Hanson, R. S., & Hanson, T. E. (1996). Methanotrophic bacteria. *Microbiological Reviews*, *60*(2), 439–471. https://doi.org/

Henry, S., Bru, D., Stres, B., Hallet, S., & Philippot, L. (2006). Quantitative detection of the *nosZ* gene, encoding nitrous oxide reductase, and comparison of the abundances of 16S rRNA, *narG, nirK, and nosZ* genes in soils. *Applied and Environmental Microbiology*, *72*(8), 5181–5189. https://doi.org/10.1128/AEM.00231-06

Henry, S., Texier, S., Hallet, S., Bru, D., Dambreville, C., Chèneby, D., Bizouard, F., Germon, J. C., & Philippot, L. (2008). Disentangling the rhizosphere effect on nitrate reducers and denitrifiers: Insight into the role of root exudates. *Environmental Microbiology*, *10*(11), 3082–3092. https://doi.org/10.1111/j.1462-2920.2008.01599.x

Holmes, A. J., Costello, A., Lidstrom, M. E., & Murrell, J. C. (1995). Evidence that particulate methane monooxygenase and ammonia monooxygenase may be evolutionarily related. *FEMS Microbiology Letters*, *132*, 203–208. https://doi.org/10.1111/j.1574-6968.1995.tb07834.x

Holmes, A. J., Costello, A., Lidstrom, M. E., & Murrell, J. C. (2006). Evidence that participate methane monooxygenase and ammonia monooxygenase may be evolutionarily related. *FEMS Microbiology Letters*, *132*(3), 203–208. https://doi.org/10.1111/j.1574-6968.1995.tb07834.x

Hu, H. W., Chen, D., & He, J. Z. (2015a). Microbial regulation of terrestrial nitrous oxide formation: Understanding the biological pathways for prediction of emission rates. In *FEMS Microbiology Reviews* (Vol. 39, Issue 5, pp. 729–749). Oxford University Press. https://doi.org/10.1093/femsre/fuv021

Hu, H. W., Chen, D., & He, J. Z. (2015b). Microbial regulation of terrestrial nitrous oxide formation: Understanding the biological pathways for prediction of emission rates. *FEMS Microbiology Reviews*, *39*(5), 729–749. https://doi.org/10.1093/femsre/fuv021

Hu, H. W., Chen, D., & He, J. Z. (2015c). Microbial regulation of terrestrial nitrous oxide formation: Understanding the biological pathways for prediction of emission rates. In *FEMS Microbiology Reviews* (Vol. 39, Issue 5, pp. 729–749). Oxford University Press. https://doi.org/10.1093/femsre/fuv021

Hubley, J. H., Thomson, A. W., & Wilkinson, J. F. (1975). Specific inhibitors of methane oxidation in Methylosinus trichosporium. *Arch. Microbiol*, *102*, 199–202.

Ikeda, S., Kaneko, T., Okubo, T., Rallos, L. E. E., Eda, S., Mitsui, H., Sato, S., Nakamura, Y., Tabata, S., & Minamisawa, K. (2009). Development of a bacterial cell enrichment method and its application to the community analysis in soybean stems. *Microbial Ecology*, *58*, 703–714.

Itokawa, H., Hanaki, K., & Matsuo, T. (2001). Nitrous oxide production in high-loading biological nitrogen removal process under low COD/N ratio condition. *Water Research*, *35*(3), 657–664.

Iyer, G., Ledna, C., Clarke, L., Edmonds, J., McJeon, H., Kyle, P., & Williams, J. H. (2017). Measuring progress from nationally determined contributions to mid-century strategies. *Nature Climate Change*, *7*(12), 871–874.

Jia, Z., & Conrad, R. (2009). Bacteria rather than Archaea dominate microbial ammonia oxidation in an agricultural soil. *Environmental Microbiology*, *11*(7), 1658–1671. https://doi.org/10.1111/j.1462-2920.2009.01891.x

Jumper, J., Evans, R., Pritzel, A., Green, T., Figurnov, M., Ronneberger, O., Tunyasuvunakool, K., Bates, R., Žídek, A., Potapenko, A., Bridgland, A., Meyer, C., Kohl, S. A. A., Ballard, A. J., Cowie, A., Romera-Paredes, B., Nikolov, S., Jain, R., Adler, J., … Hassabis, D. (2021). Highly accurate protein structure prediction with AlphaFold. *Nature*, *596*(7873), 583–589. https://doi.org/10.1038/s41586-021-03819-2

Kampschreur, M. J., Temmink, H., Kleerebezem, R., Jetten, M. S. M., & van Loosdrecht, M. C. M. (2009). Nitrous oxide emission during wastewater treatment. In *Water Research* (Vol. 43, Issue 17, pp. 4093–4103). Elsevier Ltd. https://doi.org/10.1016/j.watres.2009.03.001

Kanter, D. R., Wagner-Riddle, C., Groffman, P. M., Davidson, E. A., Galloway, J. N., Gourevitch, J. D., van Grinsven, H. J. M., Houlton, B. Z., Keeler, B. L., & Ogle, S. M. (2021). Improving the social cost of nitrous oxide. *Nature Climate Change*, *11*(12), 1008–1010.

Keltjens, J. T., Pol, A., Reimann, J., & Op Den Camp, H. J. M. (2014). PQQ-dependent methanol dehydrogenases: Rare-earth elements make a difference. In *Applied Microbiology and Biotechnology* (Vol. 98, Issue 14, pp. 6163–6183). Springer Verlag. https://doi.org/10.1007/s00253-014-5766-8

Klimasmith, I. M., & Kent, A. D. (2022a). Micromanaging the nitrogen cycle in agroecosystems. In *Trends in Microbiology* (Vol. 30, Issue 11, pp. 1045–1055). Elsevier Ltd. https://doi.org/10.1016/j.tim.2022.04.006

Klimasmith, I. M., & Kent, A. D. (2022b). Micromanaging the nitrogen cycle in agroecosystems. *Trends in Microbiology*, *30*(11), 1045–1055. https://doi.org/10.1016/j.tim.2022.04.006

Klimasmith, I. M., & Kent, A. D. (2022c). Micromanaging the nitrogen cycle in agroecosystems. In *Trends in Microbiology* (Vol. 30, Issue 11, pp. 1045–1055). Elsevier Ltd. https://doi.org/10.1016/j.tim.2022.04.006

Knapp, C. W., Fowle, D. A., Kulczycki, E., Roberts, J. A., & Graham, D. W. (2007). *Sciences of the USA 12040-12045 PNAS* (Vol. 104, Issue 29).

Knief, C. (2015a). Diversity and habitat preferences of cultivated and uncultivated aerobic methanotrophic bacteria evaluated based on pmoA as molecular marker. In *Frontiers in Microbiology* (Vol. 6, Issue DEC). Frontiers Media S.A. https://doi.org/10.3389/fmicb.2015.01346

Knief, C. (2015b). Diversity and habitat preferences of cultivated and uncultivated aerobic methanotrophic bacteria evaluated based on pmoA as molecular marker. In *Frontiers in Microbiology* (Vol. 6, Issue DEC). Frontiers Media S.A. https://doi.org/10.3389/fmicb.2015.01346

Knowles, R. (1996). Denitrification: microbiology and ecology. *Life Support & Biosphere Science*, *3*(1–2), 31–34.

Kokkonen, P., Beier, A., Mazurenko, S., Damborsky, J., Bednar, D., & Prokop, Z. (2021). Substrate inhibition by the blockage of product release and its control by tunnel

engineering. *RSC Chemical Biology*, *2*(2), 645–655. https://doi.org/10.1039/d0cb00171f

Koo, C. W., Tucci, F. J., He, Y., & Rosenzweig, A. C. (2022). Recovery of particulate methane monooxygenase structure and activity in a lipid bilayer. *Science*, *375*(6586), 1287–1291. https://doi.org/10.1126/science.abm3282

Kozlowski, J. A., Dimitri Kits, K., & Stein, L. Y. (2016a). Comparison of nitrogen oxide metabolism among diverse ammonia-oxidizing bacteria. *Frontiers in Microbiology*, *7*(JUL). https://doi.org/10.3389/fmicb.2016.01090

Kozlowski, J. A., Dimitri Kits, K., & Stein, L. Y. (2016b). Comparison of nitrogen oxide metabolism among diverse ammonia-oxidizing bacteria. *Frontiers in Microbiology*, *7*(JUL). https://doi.org/10.3389/fmicb.2016.01090

Krommweh, M. S., Schmithausen, A. J., Deeken, H. F., Büscher, W., & Maack, G. C. (2020a). A new experimental setup for measuring greenhouse gas and volatile organic compound emissions of silage during the aerobic storage period in a special silage respiration chamber. *Environmental Pollution*, *267*. https://doi.org/10.1016/j.envpol.2020.115513

Krommweh, M. S., Schmithausen, A. J., Deeken, H. F., Büscher, W., & Maack, G. C. (2020b). A new experimental setup for measuring greenhouse gas and volatile organic compound emissions of silage during the aerobic storage period in a special silage respiration chamber. *Environmental Pollution*, *267*. https://doi.org/10.1016/j.envpol.2020.115513

Kučera, I. (2006). Interference of chlorate and chlorite with nitrate reduction in resting cells of Paracoccus denitrificans. *Microbiology*, *152*(12), 3529–3534. https://doi.org/10.1099/mic.0.29276-0

Kuypers, M. M. M., Marchant, H. K., & Kartal, B. (2018a). The microbial nitrogen-cycling network. In *Nature Reviews Microbiology* (Vol. 16, Issue 5, pp. 263–276). Nature Publishing Group. https://doi.org/10.1038/nrmicro.2018.9

Kuypers, M. M. M., Marchant, H. K., & Kartal, B. (2018b). The microbial nitrogen-cycling network. *Nature Reviews Microbiology*, *16*(5), 263–276.

Lacerda, M. J. R., Freitas, K. R., & Silva, J. W. da. (2009). *Determining forage dry matter using microwave oven and conventional method.*

Ladha, J. K., Pathak, H., Krupnik, T. J., Six, J., & van Kessel, C. (2005). Efficiency of Fertilizer Nitrogen in Cereal Production: Retrospects and Prospects. *Advances in Agronomy*, *87*(05), 85–156. https://doi.org/10.1016/S0065-2113(05)87003-8

Laffite, A., Florio, A., Andrianarisoa, K. S., Creuze des Chatelliers, C., Schloter-Hai, B., Ndaw, S. M., Periot, C., Schloter, M., Zeller, B., Poly, F., & le Roux, X. (2020). Biological inhibition of soil nitrification by forest tree species affects Nitrobacter populations. *Environmental Microbiology*, *22*(3), 1141–1153. https://doi.org/10.1111/1462-2920.14905

Lee, S. W., Keeney, D. R., Lim, D. H., Dispirito, A. A., & Semrau, J. D. (2006). Mixed pollutant degradation by Methylosinus trichosporium OB3b expressing either soluble or particulate methane monooxygenase: Can the tortoise beat the hare. *Applied and Environmental Microbiology*, *72*(12), 7503–7509. https://doi.org/10.1128/AEM.01604-06

Li, D., Ni, K., Zhang, Y., Lin, Y., & Yang, F. (2019). Fermentation characteristics, chemical composition and microbial community of tropical forage silage under

different temperatures. *Asian-Australasian Journal of Animal Sciences*, *32*(5), 665–674. https://doi.org/10.5713/ajas.18.0085

Lieberman, R. L., & Rosenzweig, A. C. (2004). Biological methane oxidation: Regulation, biochemistry, and active site structure of particulate methane monooxygenase. In *Critical Reviews in Biochemistry and Molecular Biology* (Vol. 39, Issue 3, pp. 147–164). https://doi.org/10.1080/10409230490475507

Liebner, S., & Svenning, M. M. (2013). Environmental transcription of mmoX by methane-oxidizing Proteobacteria in a subarctic palsa peatland. *Applied and Environmental Microbiology*, *79*(2), 701–706. https://doi.org/10.1128/AEM.02292-12

Liu, R., Hu, H., Suter, H., Hayden, H. L., He, J., Mele, P., & Chen, D. (2016). Nitrification is a primary driver of nitrous oxide production in laboratory microcosms from different land-use soils. *Frontiers in Microbiology*, *7*(SEP), 1–10. https://doi.org/10.3389/fmicb.2016.01373

Liu, S., Han, P., Hink, L., Prosser, J. I., Wagner, M., & Brüggemann, N. (2017a). Abiotic conversion of extracellular NH2OH contributes to N2O emission during ammonia oxidation. *Environmental Science and Technology*, *51*(22), 13122–13132. https://doi.org/10.1021/acs.est.7b02360

Liu, S., Han, P., Hink, L., Prosser, J. I., Wagner, M., & Brüggemann, N. (2017b). Abiotic Conversion of Extracellular NH2OH Contributes to N2O Emission during Ammonia Oxidation. *Environmental Science and Technology*, *51*(22), 13122–13132. https://doi.org/10.1021/acs.est.7b02360

Lontoh, S., & Semrau, J. D. (1998). Methane and Trichloroethylene Degradation by Methylosinus trichosporium OB3b Expressing Particulate Methane Monooxygenase. In *APPLIED AND ENVIRONMENTAL MICROBIOLOGY* (Vol. 64, Issue 3). https://journals.asm.org/journal/aem

Maw, S. J., Johnson, C. L., Lewis, a C., & Mcquaid, J. B. (2002). A Note on the Emission of Nitrogen Oxides from Silage in Opened Bunker Silos. *Environ Monit Assess*, *74*, 209–215. https://doi.org/10.1023/A:1014227504369

McDonald, I. R., Bodrossy, L., Chen, Y., & Murrell, J. C. (2008). Molecular ecology techniques for the study of aerobic methanotrophs. In *Applied and Environmental Microbiology* (Vol. 74, Issue 5, pp. 1305–1315). https://doi.org/10.1128/AEM.02233-07

Morgan, M. E., & Pereira, R. L. (1962). Volatile Constituents of Grass and Corn Silage. II. Gas-entrained Aroma. *Journal of Dairy Science*, *45*(4), 467–471. https://doi.org/10.3168/jds.S0022-0302(62)89428-4

Muck, R. E., Nadeau, E. M. G., McAllister, T. A., Contreras-Govea, F. E., Santos, M. C., & Kung, L. (2018a). Silage review: Recent advances and future uses of silage additives. *Journal of Dairy Science*, *101*(5), 3980–4000. https://doi.org/10.3168/jds.2017-13839

Muck, R. E., Nadeau, E. M. G., McAllister, T. A., Contreras-Govea, F. E., Santos, M. C., & Kung, L. (2018b). Silage review: Recent advances and future uses of silage additives. In *Journal of Dairy Science* (Vol. 101, Issue 5, pp. 3980–4000). Elsevier Inc. https://doi.org/10.3168/jds.2017-13839

Müller, C. E. (2005). Fermentation patterns of small-bale silage and haylage produced as a feed for horses. *Grass and Forage Science*, *60*(2), 109–118. https://doi.org/10.1111/j.1365-2494.2005.00457.x

Müller, C. E., Pauly, T. M., & Udén, P. (2007). Storage of small bale silage and haylage - Influence of storage period on fermentation variables and microbial composition. *Grass and Forage Science*, *62*(3), 274–283. https://doi.org/10.1111/j.1365-2494.2007.00580.x

Müller, C. E., von Rosen, D., & Udén, P. (2008a). Effect of forage conservation method on microbial flora and fermentation pattern in forage and in equine colon and faeces. *Livestock Science*, *119*(1–3), 116–128. https://doi.org/10.1016/j.livsci.2008.03.007

Müller, C. E., von Rosen, D., & Udén, P. (2008b). Effect of forage conservation method on microbial flora and fermentation pattern in forage and in equine colon and faeces. *Livestock Science*, *119*(1–3), 116–128. https://doi.org/10.1016/j.livsci.2008.03.007

Müller, C. E., von Rosen, D., & Udén, P. (2008c). Effect of forage conservation method on microbial flora and fermentation pattern in forage and in equine colon and faeces. *Livestock Science*, *119*(1–3), 116–128. https://doi.org/10.1016/j.livsci.2008.03.007

Murphy, L. S., & Smith, G. E. (1967). Nitrate Accumulations in Forage Crops 1. *Agronomy Journal*, *59*(2), 171–174.

Nardi, P., Laanbroek, H. J., Nicol, G. W., Renella, G., Cardinale, M., Pietramellara, G., Weckwerth, W., Trinchera, A., Ghatak, A., & Nannipieri, P. (2020). Biological nitrification inhibition in the rhizosphere: Determining interactions and impact on microbially mediated processes and potential applications. In *FEMS Microbiology Reviews* (Vol. 44, Issue 6, pp. 874–908). Oxford University Press. https://doi.org/10.1093/femsre/fuaa037

Nichol, T., Murrell, J. C., & Smith, T. J. (2019). Biochemistry and molecular biology of methane monooxygenase. *Aerobic Utilization of Hydrocarbons, Oils, and Lipids*, 99–115.

Norton, J. M., & Stark, J. M. (2011). Regulation and measurement of nitrification in terrestrial systems. *Methods in Enzymology*, *486*, 343–368.

Oremland, R. S., & Capone, D. G. (1988). Use of "specific" inhibitors in biogeochemistry and microbial ecology. In *Advances in microbial ecology* (pp. 285–383). Springer.

Orschler, L., Agrawal, S., & Lackner, S. (2019). On resolving ambiguities in microbial community analysis of partial nitritation anammox reactors. *Scientific Reports*, *9*(1). https://doi.org/10.1038/s41598-019-42882-8

O'Sullivan, C. A., Fillery, I. R. P. P., Roper, M. M., & Richards, R. A. (2016a). Identification of several wheat landraces with biological nitrification inhibition capacity. *Plant and Soil*, *404*(1–2), 61–74. https://doi.org/10.1007/s11104-016-2822-4

O'Sullivan, C. A., Fillery, I. R. P., Roper, M. M., & Richards, R. A. (2016b). Identification of several wheat landraces with biological nitrification inhibition capacity. *Plant and Soil*, *404*(1–2), 61–74. https://doi.org/10.1007/s11104-016-2822-4

Owens, M. C. and V. N. (2003a). Preservation of Forage as Hay and Silage. In R. F. Barnes, C. J. Nelson, M. Collins, & K. J. Moore (Eds.), *Forages. An Introduction to Grassland Agriculture. Vol. 1* (6th Editio, Vol. 56, Issue 6, p. 673). Wiley-Blackwell. https://doi.org/10.2307/4003946

Owens, M. C. and V. N. (2003b). Preservation of Forage as Hay and Silage. In R. F. Barnes, C. J. Nelson, M. Collins, & K. J. Moore (Eds.), *Forages. An Introduction to Grassland Agriculture. Vol. 1* (6th Editio, Vol. 56, Issue 6, p. 673). Wiley-Blackwell. https://doi.org/10.2307/4003946

Pariasca Tanaka, J., Nardi, P., & Wissuwa, M. (2010). Nitrification inhibition activity, a novel trait in root exudates of rice. *AoB PLANTS*, *2010*(3), 1–11. https://doi.org/10.1093/aobpla/plq014

Peters, M., Rao, I., Fisher, M. J., Subbaraoa, G. v., Martens, S. D., Herrero, M., Hoek, R. van der, Schultze-Kraft, R., Miles, J. W., Castro, A., Graefe, S., Tiemann, T. T., Ayarza, M. A., & Glenn Hyman. (2013). Tropical forage-based systems to mitigate greenhouse gas emissions. In *Eco-Efficiency: From Vision to Reality* (pp. 172–184).

Phillips, J. C., Hardy, D. J., Maia, J. D. C., Stone, J. E., Ribeiro, J. V., Bernardi, R. C., Buch, R., Fiorin, G., Hénin, J., Jiang, W., McGreevy, R., Melo, M. C. R., Radak, B. K., Skeel, R. D., Singharoy, A., Wang, Y., Roux, B., Aksimentiev, A., Luthey-Schulten, Z., … Tajkhorshid, E. (2020). Scalable molecular dynamics on CPU and GPU architectures with NAMD. *Journal of Chemical Physics*, *153*(4). https://doi.org/10.1063/5.0014475

Pusede, S. E., & Cohen, R. C. (2012). On the observed response of ozone to NOx and VOC reactivity reductions in San Joaquin Valley California 1995-present. *Atmospheric Chemistry and Physics*, *12*(18), 8323–8339. https://doi.org/10.5194/acp-12-8323-2012

Ravishankara, A. R., Daniel, J. S., & Portmann, R. W. (2009a). Nitrous oxide (N2O): The dominant ozone-depleting substance emitted in the 21st century. *Science*, *326*(5949), 123–125. https://doi.org/10.1126/science.1176985

Ravishankara, A. R., Daniel, J. S., & Portmann, R. W. (2009b). Nitrous oxide (N2O): The dominant ozone-depleting substance emitted in the 21st century. *Science*, *326*(5949), 123–125. https://doi.org/10.1126/science.1176985

Reay, D. S., Davidson, E. A., Smith, K. A., Smith, P., Melillo, J. M., Dentener, F., & Crutzen, P. J. (2012a). Global agriculture and nitrous oxide emissions. In *Nature Climate Change* (Vol. 2, Issue 6, pp. 410–416). Nature Publishing Group. https://doi.org/10.1038/nclimate1458

Reay, D. S., Davidson, E. A., Smith, K. A., Smith, P., Melillo, J. M., Dentener, F., & Crutzen, P. J. (2012b). Global agriculture and nitrous oxide emissions. *Nature Climate Change*, *2*(6), 410–416. https://doi.org/10.1038/nclimate1458

Rennert, K., Errickson, F., Prest, B. C., Rennels, L., Newell, R. G., Pizer, W., Kingdon, C., Wingenroth, J., Cooke, R., & Parthum, B. (2022). Comprehensive evidence implies a higher social cost of CO2. *Nature*, *610*(7933), 687–692.

Ross, M. O., & Rosenzweig, A. C. (2017). A tale of two methane monooxygenases. In *Journal of Biological Inorganic Chemistry* (Vol. 22, Issues 2–3, pp. 307–319). Springer Verlag. https://doi.org/10.1007/s00775-016-1419-y

Rotthauwe, J. H., Witzel, K. P., & Liesack, W. (1997). The ammonia monooxygenase structural gene amoa as a functional marker: Molecular fine-scale analysis of natural ammonia-oxidizing populations. *Applied and Environmental Microbiology*, *63*(12), 4704–4712. https://doi.org/10.1128/aem.63.12.4704-4712.1997

Saunois, M., R. Stavert, A., Poulter, B., Bousquet, P., G. Canadell, J., B. Jackson, R., A. Raymond, P., J. Dlugokencky, E., Houweling, S., K. Patra, P., Ciais, P., K. Arora, V., Bastviken, D., Bergamaschi, P., R. Blake, D., Brailsford, G., Bruhwiler, L., M. Carlson, K., Carrol, M., … Zhuang, Q. (2020). The global methane budget 2000-2017. *Earth System Science Data*, *12*(3), 1561–1623. https://doi.org/10.5194/essd-12-1561-2020

Sayavedra-Soto, L. A., Hamamura, N., Liu, C. W., Kimbrel, J. A., Chang, J. H., & Arp, D. J. (2011). The membrane-associated monooxygenase in the butane-oxidizing Gram-positive bacterium Nocardioides sp. strain CF8 is a novel member of the AMO/PMO family. *Environmental Microbiology Reports*, *3*(3), 390–396. https://doi.org/10.1111/j.1758-2229.2010.00239.x

Schinner, F., Öhlinger, R., Kandeler, E., & Margesin, R. (1996). Nitrification and denitrification. In *Methods in soil biology* (pp. 144–161). Springer.

Schmithausen, A. J., Deeken, H. F., Gerlach, K., Trimborn, M., Weiß, K., Büscher, W., & Maack, G. C. (2022). Greenhouse gas formation during the ensiling process of grass and lucerne silage. *Journal of Environmental Management*, *304*. https://doi.org/10.1016/j.jenvman.2021.114142

Semrau, J. D., Dispirito, A. A., Obulisamy, P. K., & Kang-Yun, C. S. (2020). Methanobactin from methanotrophs: Genetics, structure, function and potential applications. In *FEMS Microbiology Letters* (Vol. 367, Issue 5). Oxford University Press. https://doi.org/10.1093/femsle/fnaa045

Semrau, J. D., DiSpirito, A. A., & Yoon, S. (2010). Methanotrophs and copper. *FEMS Microbiology Reviews*, *34*(4), 496–531. https://doi.org/10.1111/j.1574-6976.2010.00212.x

Semrau, J. D., Jagadevan, S., Dispirito, A. A., Khalifa, A., Scanlan, J., Bergman, B. H., Freemeier, B. C., Baral, B. S., Bandow, N. L., Vorobev, A., Haft, D. H., Vuilleumier, S., & Murrell, C. J. (2013). Methanobactin and MmoD work in concert to act as the "copper-switch" in methanotrophs. *Environmental Microbiology*, *15*(11), 3077–3086. https://doi.org/10.1111/1462-2920.12150

Soundharrajan, I., Kim, D. H., Srisesharam, S., Kuppusamy, P., Park, H. S., Yoon, Y. H., Kim, W. H., Song, Y. G., & Choi, K. C. (2017a). Application of customised bacterial inoculants for grass haylage production and its effectiveness on nutrient composition and fermentation quality of haylage. *3 Biotech*, *7*(5), 1–9. https://doi.org/10.1007/s13205-017-0965-5

Stein, L. Y. (2023). Ending the era of Haber–Bosch. In *Environmental Microbiology* (Vol. 25, Issue 1, pp. 102–104). John Wiley and Sons Inc. https://doi.org/10.1111/1462-2920.16220

Subbarao, G. v., Arango, J., Masahiro, K., Hooper, A. M., Yoshihashi, T., Ando, Y., Nakahara, K., Deshpande, S., Ortiz-Monasterio, I., Ishitani, M., Peters, M., Chirinda, N., Wollenberg, L., Lata, J. C., Gerard, B., Tobita, S., Rao, I. M., Braun, H. J., Kommerell, V., … Iwanaga, M. (2017). Genetic mitigation strategies to tackle agricultural GHG emissions: The case for biological nitrification inhibition technology. *Plant Science*, *262*(May), 165–168. https://doi.org/10.1016/j.plantsci.2017.05.004

Subbarao, G. V., Ishikawa, T., Ito, O., Nakahara, K., Wang, H. Y., & Berry, W. L. (2006). A bioluminescence assay to detect nitrification inhibitors released from plant roots: A case study with *Brachiaria humidicola*. *Plant and Soil*, *288*(1–2), 101–112. https://doi.org/10.1007/s11104-006-9094-3

Subbarao, G. v., Ito, O., Sahrawat, K. L., Berry, W. L., Nakahara, K., Ishikawa, T., Watanabe, T., Suenaga, K., Rondon, M., & Rao, I. M. (2006). Scope and strategies for regulation of nitrification in agricultural systems—Challenges and opportunities. *Critical Reviews in Plant Sciences*, *25*(4), 303–335. https://doi.org/10.1080/07352680600794232

Subbarao, G. V., Kishii, M., Bozal-Leorri, A., Ortiz-Monasterio, I., Gao, X., Ibba, M. I., Karwat, H., Gonzalez-Moro, M. B., Gonzalez-Murua, C., Yoshihashi, T., Tobita, S., Kommerell, V., Braun, H.-J., & Iwanaga, M. (2021). Enlisting wild grass genes to combat nitrification in wheat farming: A nature-based solution. *Proceedings of the National Academy of Sciences*, *118*(35), 2106595118. https://doi.org/10.1073/pnas.2106595118

Subbarao, G. V, Nakahara, K., Hurtado, M. P., Ono, H., Moreta, D. E., Salcedo, A. F., Yoshihashi, A. T., Ishikawa, T., Ishitani, M., Ohnishi-Kameyama, M., Yoshida, M., Rondon, M., Rao, I. M., Lascano, C. E., Berry, W. L., & Ito, O. (2009a). Evidence for biological nitrification inhibition in *Brachiaria* pastures. *Proceedings of the National Academy of Sciences of the United States of America*, *106*(41), 17302–17307. https://doi.org/10.1073/pnas.0903694106

Subbarao, G. v, Nakahara, K., Hurtado, M. P., Ono, H., Moreta, D. E., Salcedo, A. F., Yoshihashi, A. T., Ishikawa, T., Ishitani, M., Ohnishi-Kameyama, M., Yoshida, M., Rondon, M., Rao, I. M., Lascano, C. E., Berry, W. L., & Ito, O. (2009b). Evidence for biological nitrification inhibition in *Brachiaria* pastures. *Proceedings of the National Academy of Sciences of the United States of America*, *106*(41), 17302–17307. https://doi.org/10.1073/pnas.0903694106

Subbarao, G. V., Nakahara, K., Ishikawa, T., Yoshihashi, T., Ito, O., Ono, H., Ohnishi-Kameyama, M., Yoshida, M., Kawano, N., & Berry, W. L. (2008). Free fatty acids from the pasture grass *Brachiaria humidicola* and one of their methyl esters as inhibitors of nitrification. *Plant and Soil*, *313*(1–2), 89–99. https://doi.org/10.1007/s11104-008-9682-5

Subbarao, G. V., Rondon, M., Ito, O., Ishikawa, T., Rao, I. M., Nakahara, K., Lascano, C., & Berry, W. L. (2007a). Biological nitrification inhibition (BNI) - Is it a widespread phenomenon? *Plant and Soil*, *294*(1–2), 5–18. https://doi.org/10.1007/s11104-006-9159-3

Subbarao, G. v., Rondon, M., Ito, O., Ishikawa, T., Rao, I. M., Nakahara, K., Lascano, C., & Berry, W. L. (2007b). Biological nitrification inhibition (BNI) - Is it a widespread phenomenon? *Plant and Soil*, *294*(1–2), 5–18. https://doi.org/10.1007/s11104-006-9159-3

Subbarao, G. v., Sahrawat, K. L., Nakahara, K., Rao, I. M., Ishitani, M., Hash, C. T., Kishii, M., Bonnett, D. G., Berry, W. L., & Lata, J. C. (2013). A paradigm shift towards low-nitrifying production systems: The role of biological nitrification inhibition (BNI). *Annals of Botany*, *112*(2), 297–316. https://doi.org/10.1093/aob/mcs230

Subbarao, G. V., & Searchinger, T. D. (2021). A "more ammonium solution" to mitigate nitrogen pollution and boost crop yields. *Proceedings of the National Academy of Sciences*, *118*(22), 2107576118. https://doi.org/10.1073/pnas.2107576118

Sun, L., Lu, Y., Yu, F., Kronzucker, H. J., & Shi, W. (2016a). Biological nitrification inhibition by rice root exudates and its relationship with nitrogen-use efficiency. *New Phytologist*, *212*(3), 646–656. https://doi.org/10.1111/nph.14057

Sun, L., Lu, Y., Yu, F., Kronzucker, H. J., & Shi, W. (2016b). Biological nitrification inhibition by rice root exudates and its relationship with nitrogen-use efficiency. *New Phytologist*, *212*(3), 646–656. https://doi.org/10.1111/nph.14057

Teng, F., Darveekaran Nair, S. S., Zhu, P., Li, S., Huang, S., Li, X., Xu, J., & Yang, F. (2018). Impact of DNA extraction method and targeted 16S-rRNA hypervariable

region on oral microbiota profiling. *Scientific Reports*, *8*(1), 1–12. https://doi.org/10.1038/s41598-018-34294-x

Tesfamariam, T., Yoshinaga, H., Deshpande, S. P., Srinivasa Rao, P., Sahrawat, K. L., Ando, Y., Nakahara, K., Hash, C. T., & Subbarao, G. v. (2014). Biological nitrification inhibition in sorghum: The role of sorgoleone production. *Plant and Soil*, *379*(1–2), 325–335. https://doi.org/10.1007/s11104-014-2075-z

Thomson, a. J., Giannopoulos, G., Pretty, J., Baggs, E. M., & Richardson, D. J. (2012). Biological sources and sinks of nitrous oxide and strategies to mitigate emissions. *Philosophical Transactions of the Royal Society B: Biological Sciences*, *367*(1593), 1157–1168. https://doi.org/10.1098/rstb.2011.0415

Thomson, A. J., Giannopoulos, G., Pretty, J., Baggs, E. M., & Richardson, D. J. (2012). Biological sources and sinks of nitrous oxide and strategies to mitigate emissions. In *Philosophical Transactions of the Royal Society B: Biological Sciences* (Vol. 367, Issue 1593, pp. 1157–1168). Royal Society. https://doi.org/10.1098/rstb.2011.0415

Tian, H., Xu, R., Canadell, J. G., Thompson, R. L., Winiwarter, W., Suntharalingam, P., Davidson, E. A., Ciais, P., Jackson, R. B., & Janssens-Maenhout, G. (2020). A comprehensive quantification of global nitrous oxide sources and sinks. *Nature*, *586*(7828), 248–256.

Tian, H., Xu, R., Canadell, J. G., Thompson, R. L., Winiwarter, W., Suntharalingam, P., Davidson, E. A., Ciais, P., Jackson, R. B., Janssens-Maenhout, G., Prather, M. J., Regnier, P., Pan, N., Pan, S., Peters, G. P., Shi, H., Tubiello, F. N., Zaehle, S., Zhou, F., … Yao, Y. (2020a). A comprehensive quantification of global nitrous oxide sources and sinks. *Nature*, *586*(7828), 248–256. https://doi.org/10.1038/s41586-020-2780-0

Tian, H., Xu, R., Canadell, J. G., Thompson, R. L., Winiwarter, W., Suntharalingam, P., Davidson, E. A., Ciais, P., Jackson, R. B., Janssens-Maenhout, G., Prather, M. J., Regnier, P., Pan, N., Pan, S., Peters, G. P., Shi, H., Tubiello, F. N., Zaehle, S., Zhou, F., … Yao, Y. (2020b). A comprehensive quantification of global nitrous oxide sources and sinks. *Nature*, *586*(7828), 248–256. https://doi.org/10.1038/s41586-020-2780-0

Topp, E., & Knowles, R. (1984). Effects of nitrapyrin [2-chloro-6-(trichloromethyl) pyridine] on the obligate methanotroph Methylosinus trichosporium OB3b. *Applied and Environmental Microbiology*, *47*(2), 258–262. https://doi.org/10.1128/aem.47.2.258-262.1984

Trotsenko, Y. A., & Murrell, J. C. (2008). Metabolic Aspects of Aerobic Obligate Methanotrophy{star, open}. In *Advances in Applied Microbiology* (Vol. 63, pp. 183–229). https://doi.org/10.1016/S0065-2164(07)00005-6

U.S. EPA. (2018). Inventory of U.S. Greenhouse Gas Emissions and Sinks. In *EPA* (Vol. 106, Issue 11). https://doi.org/EPA 430-T-18-003

USDA. (2023a). *Crop Production 2022 Summary*. https://downloads.usda.library.cornell.edu/usda-esmis/files/k3569432s/9306v916d/wm119139b/cropan23.pdf

USDA. (2023b). *Crop production 2022 summary*. www.nass.usda.gov

USEPA. (2019). *Inventory of U.S. Greenhouse Gas Emissions and Sinks*. https://doi.org/10.1017/CBO9781107415324.004

USEPA. (2023). *Inventory of U.S. Greenhouse Gas Emissions and Sinks: 1990-2021 – Main Report*. https://www.epa.gov/ghgemissions/inventory-us-greenhouse-gas-emissions-and-

van Kessel, M. A. H. J., Speth, D. R., Albertsen, M., Nielsen, P. H., Op Den Camp, H. J. M., Kartal, B., Jetten, M. S. M., & Lücker, S. (2015). Complete nitrification by a single microorganism. *Nature*, *528*(7583), 555–559. https://doi.org/10.1038/nature16459

Vorholt, J. A. (2012). Microbial life in the phyllosphere. *Nature Reviews Microbiology*, *10*(12), 828–840. https://doi.org/10.1038/nrmicro2910

Wahlen M. (1993). The Global methane cycle. *Annual Review of Earth and Planetary Sciences, 21(1):407–426.* https://doi.org/https://doi.org/10.1146/annurev.earth.21.1.407

Wang, J., Huang, Q., Li, Y., Tu, X., Chen, Z., Elrys, A. S., Cheng, Y., & Ma, L. (2023). A shift from nitrification to denitrification-dominated N2O emission in an acidic soil following organic amendment. *Biology and Fertility of Soils*, *59*(1), 117–122.

Wang, X., Bai, J., Xie, T., Wang, W., Zhang, G., Yin, S., & Wang, D. (2021). Effects of biological nitrification inhibitors on nitrogen use efficiency and greenhouse gas emissions in agricultural soils: A review. *Ecotoxicology and Environmental Safety*, *220*, 112338. https://doi.org/10.1016/j.ecoenv.2021.112338

Wei, W., Isobe, K., Nishizawa, T., Zhu, L., Shiratori, Y., Ohte, N., Koba, K., Otsuka, S., & Senoo, K. (2015). Higher diversity and abundance of denitrifying microorganisms in environments than considered previously. *ISME Journal*, *9*(9), 1954–1965. https://doi.org/10.1038/ismej.2015.9

Wrage, N., Velthof, G. L., van Beusichem, M. L., & Oenema, O. (2001). Role of nitrifier denitrification in the production of nitrous oxide. *Soil Biology and Biochemistry*, *33*(12–13), 1723–1732. https://doi.org/10.1016/S0038-0717(01)00096-7

Wrage, N., Velthof, G. L., Van Beusichem, M. L., & Oenema, O. (2001). Role of nitrifier denitrification in the production of nitrous oxide. *Soil Biology and Biochemistry*, *33*(12–13), 1723–1732.

Wrage-Mönnig, N., Horn, M. A., Well, R., Müller, C., Velthof, G., & Oenema, O. (2018a). The role of nitrifier denitrification in the production of nitrous oxide revisited. In *Soil Biology and Biochemistry* (Vol. 123, pp. A3–A16). Elsevier Ltd. https://doi.org/10.1016/j.soilbio.2018.03.020

Wrage-Mönnig, N., Horn, M. A., Well, R., Müller, C., Velthof, G., & Oenema, O. (2018b). The role of nitrifier denitrification in the production of nitrous oxide revisited. In *Soil Biology and Biochemistry* (Vol. 123, pp. A3–A16). Elsevier Ltd. https://doi.org/10.1016/j.soilbio.2018.03.020

Xu, J., Zhang, Z., Wu, Y., Liu, B., Xia, X., & Chen, Y. (2024). Effects of C/N ratio on N2O emissions and nitrogen functional genes during vegetable waste composting. *Environmental Science and Pollution Research*, 1–15.

Yang, J., Feng, L., Pi, S., Cui, D., Ma, F., Zhao, H. ping, & Li, A. (2020a). A critical review of aerobic denitrification: Insights into the intracellular electron transfer. In *Science of the Total Environment* (Vol. 731). Elsevier B.V. https://doi.org/10.1016/j.scitotenv.2020.139080

Yang, J., Feng, L., Pi, S., Cui, D., Ma, F., Zhao, H. ping, & Li, A. (2020b). A critical review of aerobic denitrification: Insights into the intracellular electron transfer. In *Science of*

the Total Environment (Vol. 731). Elsevier B.V. https://doi.org/10.1016/j.scitotenv.2020.139080

Yang, S., Lee, J., Mahmood, M., Min, D., & Im, J. (2023). Evaluation and optimization of lysis method for microbial DNA extraction from epiphytic phyllosphere samples. *Journal of Microbiological Methods*, *206*, 106677.

Yang, S., Mahmood, M., Baral, R., Wu, H., Almloff, M., Stanton, L. E., Min, D., Smiley, B. K., Iiams, J. C., & Yu, J. (2024). Forage conservation is a neglected nitrous oxide source. *PNAS Nexus*, *3*(9), pgae373.

Yoshinari, T., Hynes, R., & Knowles, R. (1977). Acetylene inhibition of nitrous oxide reduction and measurement of denitrification and nitrogen fixation in soil. *Soil Biology and Biochemistry*, *9*(3), 177–183.

Zakir, H. A. K. M., Subbarao, G. V., Pearse, S. J., Gopalakrishnan, S., Ito, O., Ishikawa, T., Kawano, N., Nakahara, K., Yoshihashi, T., Ono, H., & Yoshida, M. (2008a). Detection, isolation and characterization of a root-exuded compound, methyl 3-(4-hydroxyphenyl) propionate, responsible for biological nitrification inhibition by sorghum (Sorghum bicolor). *New Phytologist*, *180*(2), 442–451. https://doi.org/10.1111/j.1469-8137.2008.02576.x

Zakir, H. A. K. M., Subbarao, G. V., Pearse, S. J., Gopalakrishnan, S., Ito, O., Ishikawa, T., Kawano, N., Nakahara, K., Yoshihashi, T., Ono, H., & Yoshida, M. (2008b). Detection, isolation and characterization of a root-exuded compound, methyl 3-(4-hydroxyphenyl) propionate, responsible for biological nitrification inhibition by sorghum (Sorghum bicolor). *New Phytologist*, *180*(2), 442–451. https://doi.org/10.1111/j.1469-8137.2008.02576.x

Zhou, B., Duan, J., Xue, L., Zhang, J., & Yang, L. (2019). Effect of plant-based carbon source supplements on denitrification of synthetic wastewater: focus on the microbiology. *Environmental Science and Pollution Research*, *26*, 24683–24694.

Zhou, W., Jones, D. L., Hu, R., Clark, I. M., & Chadwick, D. R. (2020). Crop residue carbon-to-nitrogen ratio regulates denitrifier N 2 O production post flooding. *Biology and Fertility of Soils*, *56*, 825–838.